MAGNONS IN FERROMAGNETIC FILMS

A Dissertation

by

GANG LI

Submitted to the Office of Graduate and Professional Studies of
Texas A&M University
in partial fulfillment of the requirements for the degree of

DOCTOR OF PHILOSOPHY

Chair of Committee,	Valery L. Pokrovsky
Committee Members,	Artem G. Abanov
	Donald Naugle
	Stephen A. Fulling
Head of Department,	Grigory V. Rogachev

December 2020

Major Subject: Physics

ABSTRACT

The theory of magnons in ferromagnetic films has important applications to real magnets and a rather long history. In this dissertation, we first present a new version of the asymptotically exact theory of the spectrum and transverse distribution of magnetization in long-wave magnons. It is based on the exact analytical solution of the linearized Landau-Lifshitz equation in a film. We also studied and used symmetry of the Hamiltonian. Our new method simplifies all calculations and provides analytical results for the range of parameters most important for experiment. The quantization of the transverse wave vector and the role of evanescent waves at different values of parameters are studied. Another important motivation of this work was its application to the problem of Bose-Einstein condensation (BEC) and superfluidity of magnons. We use a classical modification of the Holstein-Primakoff transformation to solve the Landau-Lifshitz equation, the exact phase diagram for magnon condensate in Yttrium Iron Garnet Film is studied. We also collaborated with an experimental group that provides direct experimental evidence that magnons in a condensate exhibit a repulsive interaction resulting in condensate stabilization. We propose a mechanism, which is responsible for the interaction inversion. This mechanism supports their conclusions by the theoretical model based on the Gross-Pitaevskii equation.

DEDICATION

To my parents and my younger brother.

ACKNOWLEDGMENTS

First I would like to thank my advisor, Professor Valery Pokrovsky who gave me so much support and guidance throughout my research with patience and dedication. I appreciate him for his patience and for leading me through the difficulties during research. He gave the best guidance I ever had with his endless enthusiasm and immense knowledge. His enthusiasm for understanding new things has always been impressive and encouraged me. His deep insights and wide knowledge of physics have benefited me very much and will continue to benefit me in the future.

I would like to thank my committee members, Professors Artem Abanov, Donald Naugle, and Stephen A. Fulling, especially to Dr. Artem Abanov for his guidance during my early Ph.D. life. My thanks also go to Dr. Thomas Nattermann. Collaborating with and learning from him benefited me greatly.

I also thank all my friends here. Among them, I would like to express my sincere gratitude to my former colleague in Prof. Pokrovsky's group, Dr. Chen Sun, who gave me much help and many valuable suggestions throughout my research.

CONTRIBUTORS AND FUNDING SOURCES

Contributors

This work was supervised by a dissertation committee consisting of Professor Valery L. Pokrovsky (advisor) and Professors Artem G. Abanov and Donald Naugle of the Department of Physics and Astronomy, and Professor Stephen A. Fulling of the Department of Mathematics.

All work for the dissertation was completed by the student, primarily under the guidance of Professor Valery L. Pokrovsky, and partially by Dr. Thomas Nattermann from the University of Cologne.

Funding Sources

This work was financially supported by research assistantship from my advisor Dr. Valery Pokrovsky under the auspices of 02-512992 William R Thurman '58 Chair Physics, and partially by teaching assistantship from the department of Physics and Astronomy at Texas A&M University.

NOMENCLATURE

BEC	Bose-Einstein condensation
LLE	Landau-Lifshitz equation
TDM	distribution of magnetization in direction transverse to the film
BLS	Brillioun light scattering
EOM	equation of motion
YIG	yttrium iron garnet
1D	one dimension/one-dimensional
2D	two dimension/two-dimensional
3D	three dimension/three-dimensional

TABLE OF CONTENTS

Page

LIST OF FIGURES

FIGURE Page

LIST OF TABLES

TABLE Page

1. INTRODUCTION*

The theory of magnons in ferromagnetic films has important applications to real magnets and a rather long history. The first exact result was obtained by Damon and Eshbach [6] for purely dipolar interaction. Gann [7] was the first who indicated the possibility of the exact solution of this problem including exchange and dipolar interactions. De Wames and Wolfram obtained such an exact solution [8, 9], reducing a system of Landau-Lifshitz and magnetostatic equations for magnetization and fields generated by spin wave to an ordinary linear differential equation of 6-th order for the distribution of magnetization in the direction transverse to the film (TDM). Arias [10] extended the de Wames-Wolfram solution to the case of the magnetic field tilted to the film. Kalinikos [11] found an integral-differential equation for the TDM. Kalinikos and Slavin [12] applied a truncated expansion of the solution into a Fourier-series over a complete set of eigenfunctions of the Hamiltonian with exchange interaction and diagonalized the real Hamiltonian projected onto a finite-dimensional space. In principle, such a procedure gives the solution with any desirable precision at increasing dimensionality of the space. Their numerical results agreed well with another numerical calculation using the same model by Kreisel *et al.* [1] for a thick film. In the latter work, the authors have found numerically the spectrum of the linearized and discretized Landau-Lifshitz equation as eigenvalues of a large matrix representing this equation.

Rezende [13] assumed that magnetization does not depend on the transverse coordinate x and exactly diagonalized the resulting Hamiltonian. Though such assumption is qualitatively justified for the spin wave mode with the lowest energy, it is obviously invalid for higher modes. In a recent work Sonin [14] has found the magnon spectrum and shape of the TDM for spin waves propagating along the direction of magnetic field and magnetization. His solution is a particular case of the Wolfram and de Wames work [9] but he obtained an explicit analytical expression for the transverse wave vector quantization in the limit of thick films $d \gg \ell$ and $1/d \ll |k_z| \ll 1/\ell$, ℓ

*Part of this chapter uses material with permission from "Long-wave magnons in a ferromagnetic film" by Gang Li, Chen Sun, Thomas Nattermann and Valery L. Pokrovsky, 2018, PHYSICAL REVIEW B, 98, 014436, Copyright 2018 by APS

is the dipolar length of the film and d is the thickness of the film. More complete bibliography of the subject that includes different approximate methods can be found in reference [12] and newer references in [1].

In this dissertation we propose a combined approach: we solve the differential equation and then select those solutions that satisfy the integral equation. This approach strongly simplifies calculations since magnetostatic boundary conditions (MBC) are satisfied automatically and there is no need to find the magnetic field outside the film. Further simplification is obtained by employing symmetry of the spin-wave solution. These simplifications allow us to find analytically the magnons spectra and the TDM in a broad range of parameters for thick films and analyze in some details the case of thin films $d \lesssim \ell$ which is very important for applications to nanodevices. Thin films are of special interest since bilayers of a magnetic insulator and a heavy metal can be used for transfer of information by magnons[15, 16]. This is a prospective way to avoid ohmic losses that appear in electronic systems on the nano-scale. We show that formally the spectrum of magnons in a film has the same analytical form as in the bulk, but quantization of the transverse wave vector and TDM depend on the thickness of the film d and other variables in a highly non-trivial way. In contrast to standard semiclassical approximation that becomes valid when the number of transverse modes n is a large number, in thick ferromagnetic films there exist several different asymptotics that depend on values of dimensionless parameters $k_\parallel \ell$, $k_\parallel d$ and angle of propagation. Here $k_\parallel = \sqrt{k_y^2 + k_z^2}$. At all values of parameters and fixed frequency, the TDM consists of one oscillating mode and two evanescent modes. Due to the fact that the Hamiltonian of this problem is invariant with respect to two discrete transformations: reflection in the central plane of the film combined with time reversal and reflection in the (x, z)-plane combined with time reversal, magnon spectrum is divided into two infinite series. In the simplest situation they correspond to even and odd transverse distribution of magnetization, "even" n-th mode has $2n$ nodes between boundaries, while "odd" one has $2n + 1$ nodes $(n = 0, ...\infty)$. Evanescent waves can be neglected in the exchange-dominated range of wave vectors $k_\parallel \gg 1/\ell$, they can be neglected in the bulk, but they allow to satisfy boundary conditions. Otherwise evanescent waves must be taken

into account. Specifically, they play an important role in the case of thin films $d \lesssim \ell$. Our method can be extended to include anisotropy (spin-orbit interaction), tilted external magnetic field and other shapes of the sample.

Another important motivation of this disseration was its application to the problem of Bose-Einstein condensation(BEC) and superfluidity of magnons [17]. The condensation is non-linear phenomenon depending on interaction. Usual microscopic approach based on Holstein-Primakoff representation requires knowledge of spectra at large wave vectors and their interaction amplitudes for thermal renormalization. The Landau-Lifshitz equation reduces the complex renormalization procedure to one experimentally measurable value: spontaneous magnetization as function of temperature. Several authors [18, 1, 5] additionally employed the Rezende approximation [13] which assumes the transverse distribution of magnetization for magnons to be constant. This assumption is wrong just at wave vectors $\pm\mathbf{Q}$ corresponding to absolute minimum of magnon energy [14] .

The study presented in this dissertation have been published in [19] and [20].

The outline of this dissertation is as follows:

In Chapter 2, we give a brief review of Bose-Einstein condensation and magnons.

In Chapter 3, we present a new, simplified asymptotically exact theory of the spectrum and transverse distribution of magnetization in long-wave-length magnons propagating in a ferromagnetic film. The theory is based on the exact solution of the linearized Landau-Lifshitz equation (LLE). In Sections 3.6 of this chapter, we present the results of our common work with the group of experimenters from University of Muenster (Germany) that provides experimental evidence of repulsion of magnons at permanent pumping instead of attraction found theoretically in the absence of pumping (see the references in the text of section 3.6). We proposed a theoretical model that explains experimentally observed repulsion, this model is based on the Gross-Pitaevskii equation.

In Chapter 4, we develop the amplitude representation of the Landau-Lifshitz-Gilbert theory of ferromagnets to study magnon BEC. It is a classical modification of the Holstein-Primakoff transformation. Using this representation, we calculated the relaxation of condensed magnons due to three-magnon processes. We also studied the exact phase diagram for magnon condensate in

Yttrium Iron Garnet Film.

Chapter 5 contains a cumulative list of our results and prospects of further research.

2. BOSE-EINSTEIN CONDENSATION AND MAGNONS

The phenomena of Bose-Einstein condensation was first predicted in 1925 by Einstein [21] following a paper by Satyendra Nath Bose in which he derived the Planck law for black-body radiation by using new statistics. According to this prediction, a large fraction of identical particles would occupy the same quantum state (the lowest energy state) under some conditions.

The well-known formula for condensation temperature for ideal Bose-gas:

$$T_c = \frac{3.31\hbar^2 n^{2/3}}{m} \tag{2.1}$$

There are two kinds of BEC, the first one is the BEC for real particles. the second is the BEC for quasiparticles. The first example of BEC of real particles is the transition of liquid ^{4}He to the superfluid state discovered in 1938 by Kapitza [22] and Allen and Misener [23]. The viscosity of ^{4}He vanishes at temperature 2.17 K and normal pressure. Fritz London was the first to propose the BEC as a mechanism for superfluidity in ^{4}He [24]. Since the mass here is the mass of an atom or molecule, not an electron, the value T_c for He atoms at rather high density $n = 10^{24}$ is calculated according to ideal gas formula 2.1 , the transition occurs about 3 K. It is the correct order of magnitude. However numerous attempts to find the condensate by the method of inelastic scattering of neutrons were not conclusive. They have shown only that the condensate density at $T = 0K$ does not exceed 5-7 $\%$ of total density. This is the result of strong interaction. Since a superfluid ^{4}He is a strongly interacting system that is far from an ideal gas, so that it was not straightforward at all to connect the two concepts of BEC and superfluidity. Only the experiments with cooled dilute gases of alkali atoms convincingly proved the existence of condensate.

It took nearly 70 years before the pure BEC system was realized. In 1995 Wieman, Cornell and Ketterle discovered two other systems displaying BEC, both of them being laser-cooled gases of alkali atoms (potassium and sodium) [25, 26]. They condensed at temperatures of a few hundred nanokelvins. This discovery was considered definitive proof of superfluidity.

On the other side, the BEC of quasiparticles were observed from the beginning of this century, specifically: i) magnons in a ferrite film [27]; ii) excitons-polaritons in quantum dots [28]; iii) photons in a microcavity filled by a gas of dye molecules [29]. In the cases i) and iii) BEC are observed at room temperature. Since the mass of a quasiparticle is usually much smaller than that of real particles and the density of the quasiparticle system can be easily increased by external pumping without worrying about the formation of molecules, the transition temperature of BEC is relatively higher than that of real particles. However, the lifetime of a quasiparticle is much smaller than that of real particles. This means that the BEC of quasiparticles is not a real equilibrium state, just a quasi-equilibrium state. What we are interested in is the magnon BEC, that was studied in a macroscopic film. It provides a good platform for studying transport properties related to BEC.

Spin waves, first predicted by F. Bloch [30] in 1929, are propagating disturbances in the ordering of magnetic materials. The quanta of spin waves are called magnons, magnons can be treated as bosonic quasiparticles and carry a fixed amount of energy and lattice momentum. The simplest way of understanding magnon is to consider its Hamiltonian. There are several kinds of interactions in magnetic materials, e.g. the exchange interaction, the Zeeman interaction, and the dipolar interaction.

The Hamiltonian of magnons in magnetic materials includes the nearest-neighbor exchange, Zeeman and dipolar interactions:

$$H = H_{ex} + H_Z + H_d, \tag{2.2}$$

$$H_{ex} = -J \sum_{\langle i,j \rangle} \mathbf{S}_i \cdot \mathbf{S}_j, , \tag{2.3}$$

$$H_Z = -g\mu_B \sum_i \mathbf{S}_i \cdot \mathbf{H}, \tag{2.4}$$

$$H_d = -\frac{1}{2}(g\mu_B)^2 \sum_{i \neq j} \frac{3(\mathbf{S}_i \cdot \hat{\mathbf{r}}_{ij})(\mathbf{S}_j \cdot \hat{\mathbf{r}}_{ij}) - \mathbf{S}_i \cdot \mathbf{S}_j}{r_{ij}^3}, \tag{2.5}$$

where $\langle i, j \rangle$ denotes summation over nearest-neighbor sites only. There are two cases: $J > 0$ and $J < 0$. For $J > 0$, the exchange interaction is called ferromagetic, in which case the ground

state spin configurations have all spins pointing in the same direction. For $J < 0$, the exchange interaction is called antiferromagetic. Neighboring spins would favor antiparallel configuration. g is the Landé g-factor, μ_B is the Bohr magneton, and $\mathbf{H}$ is a uniform external magnetic field.

In continuos approximation the Hamiltonian eq.(2.2-2.5):

$$H = \int_V d^3r \left[\frac{D}{2} \left(\nabla_\alpha \mathbf{M} \right)^2 - \mathbf{H} \cdot \mathbf{M} + \frac{1}{2} \left(\mathbf{M} \cdot \boldsymbol{\nabla} \right) \int_V d^3r' \left(\mathbf{M}' \cdot \boldsymbol{\nabla}' \right) \frac{1}{|\mathbf{r} - \mathbf{r}'|} \right] \tag{2.6}$$

The local magnetization vector $\mathbf{M}(\mathbf{r}) = g\mu_B \hat{\mathbf{S}}(\mathbf{r})/v_0$ where $\hat{\mathbf{S}}(\mathbf{r})$ is the local spin averaged over the sphere with the center in the point $\mathbf{r}$ and the radius R much larger than the lattice constant, but much smaller than the wavelength of the magnon and thickness of the film; v_0 is the volume of primitive cell., D is the exchange energy divided by $M^2 a$, where a is the lattice constant. V stands for volume and prime denotes dependence on the coordinate $\mathbf{r}'$. Note that the coefficient D has a dimensionality of the square of the length. The value $\ell = \sqrt{D}$ is called dipolar length.

3. LONG-WAVE MAGNONS IN A FERROMAGNETIC FILM*

In this chapter we present a new, simplified asymptotically exact theory of the spectrum and transverse distribution of magnetization in long-wave-length magnons propagating in a ferromagnetic film. Theory is based on exact solution of linearized Landau-Lifshitz equation (LLE). To avoid complications we assume the film to be isotropic in the film plane, and external magnetic field H and the spontaneous magnetization M to be oriented in plane, see Fig.3.1. Their direction is accepted for $z-$axis, whereas the $x-$axis is directed perpendicular to the film that occupies the volume between parallel planes $x = \pm\frac{d}{2}$. The Hamiltonian $\mathcal{H}$ coincides with eq. (2.6). Since this Hamiltonian is a key element for calculation of spectrum we repeat it here and remind the notations:

$$\mathcal{H} = \int_V d^3r \left[\frac{D}{2} \left(\nabla_\alpha \mathbf{M}\right)^2 - \mathbf{H}\cdot\mathbf{M} + \frac{1}{2}\left(\mathbf{M}\cdot\boldsymbol{\nabla}\right) \int_V d^3r' \left(\mathbf{M}'\cdot\boldsymbol{\nabla}'\right) \frac{1}{|\mathbf{r}-\mathbf{r}'|} \right] \tag{3.1}$$

Here $\mathbf{M}(\mathbf{r})$ is the local magnetization vector, D is the exchange energy divided by $M^2 a$, where a is the lattice constant. V stands for volume and prime denotes dependence on the coordinate $\mathbf{r}'$. Note that the coefficient D has dimensionality of square of length. The value $\ell = \sqrt{D}$ is called dipolar length. This is the scale of distance at which dipolar and exchange interactions become of the same order of magnitude. Typically it is about 10-30 nm.

3.1 Equations of motion and magnon solutions

A weak excitation of the equilibrium state is described by the transverse components of magnetization $\mathbf{M} \equiv (M_x, M_y)$. They obey the linearized LLE:

$$\dot{\mathbf{M}} \;=\; \gamma\left[\left(H - MD\Delta\right)\mathbf{M} + M\mathbf{h}\right]\times\hat{z}, \tag{3.2}$$

*Part of this chapter uses material with permission from "Long-wave magnons in a ferromagnetic film" by Gang Li, Chen Sun, Thomas Nattermann and Valery L. Pokrovsky, 2018, PHYSICAL REVIEW B, 98, 014436, Copyright 2018 by APS; and from "Direct evidence of spatial stability of Bose-Einstein condensate of magnons" by Borisenko, I V and Divinskiy, B and Demidov, V E and Li, G and Nattermann, T and Pokrovsky, V L and Demokritov, S O, 2020, Nature Communications, 11, 1691, Copyright 2020 by Nature Publishing Group

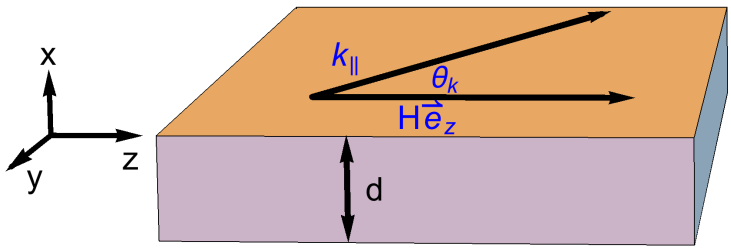

Figure 3.1: The coordinate system for a ferromagnetic film of thickness d: $z-$axis is chosen along the common direction of the magnetic field and static magnetization, $x-$axis is perpendicular to the film, θ_k is the angle between the magnon wave vector and magnetic field.

$\hat{z}$ is the unit vector in z-direction and $\Delta \equiv \boldsymbol{\nabla}^2$;

$$\mathbf{h} = \boldsymbol{\nabla}_{\perp}\phi \tag{3.3}$$

denotes the dipolar field induced by magnetization inside and outside the film, with $\boldsymbol{\nabla}_{\perp} \equiv \left(\partial_x, \partial_y\right)^{\top}$ and

$$\phi\left(\mathbf{r}\right) = -\boldsymbol{\nabla}_{\perp} \cdot \int d^3r' \mathbf{M}' \left|\mathbf{r} - \mathbf{r}'\right|^{-1}. \tag{3.4}$$

The number of parameters of the present problem can be reduced by the scale transformations

$$t \to \omega_H^{-1} t, \qquad \mathbf{r} \to \sqrt{\frac{\chi}{4\pi}}\, \ell\, \mathbf{r}, \qquad \mathbf{M} \to M\mathbf{M}. \tag{3.5}$$

Here $\omega_H \equiv \gamma H$ denotes the Larmor frequency and $\chi \equiv 4\pi M/H$ is the static magnetic susceptibility (we absorb a factor 4π in its definition to simplify final expressions). In rescaled units equation of motion simplifies to

$$\dot{\mathbf{M}} = \left[\left(1 - \Delta\right)\mathbf{M} + \frac{\chi}{4\pi}\mathbf{h}\right] \times \hat{z}. \tag{3.6}$$

Table 3.1: Values of parameters for YIG and Permalloy at room temperature, and dimensionless values $\chi = 4\pi M/H$ and $d_r = \sqrt{H/M}d/\ell$ at external magnetic field $H = 1$ kOe, for films with different thickness d.

quantity	symbol (unit)	YIG	Permalloy
magnetization	M (kOe)	0.139	0.860
Curie temperature	T_C (K)	560	872
dipolar length	ℓ (nm)	37.8	28.7
χ	χ	1.75	10.8
d_r at $d = 5$ μm	d_r	355	188
d_r at $d = 0.1$ μm	d_r	7.09	3.76

The equations (3.3) and (3.4) remain unchanged. The remaining parameters of the problem are susceptibility χ and the sample width d in new units. Table 1 shows the values of characteristic parameters and reduced values for YIG films and Permalloy.

Applying Laplacian Δ to eq. (3.6) and using magnetostatic equation

$$\Delta\phi = 4\pi\boldsymbol{\nabla}_\perp \cdot \mathbf{M}, \tag{3.7}$$

one gets the equation for $\mathbf{M}$:

$$\Delta\dot{\mathbf{M}} = [(1-\Delta)\Delta\mathbf{M} + \chi\boldsymbol{\nabla}_\perp(\boldsymbol{\nabla}_\perp\cdot\mathbf{M})]\times\hat{z}. \tag{3.8}$$

It must be solved with standard magnetostatic boundary conditions (MBC) that requires continuity of tangential components of magnetic field $\mathbf{h}$ and normal component of magnetic induction $\mathbf{b} = \mathbf{h} + 4\pi\mathbf{M}$ at two surfaces of the film. Another set of boundary conditions originates from variation of magnetization (spins) on surfaces if they are free. It leads to equations:

$$\partial_x\mathbf{M}\big|_{x=\pm d/2} = 0. \tag{3.9}$$

We call them exchange boundary conditions (EBC). More general EBC $\partial_x\mathbf{M} + \hat{\lambda}\mathbf{M}\big|_{x=\pm d/2} = 0$

corresponding to spin-orbital anisotropy can also be considered by our method.

In a propagating wave with in-plane wave vector $\mathbf{k}_\parallel = k_y\hat{y} + k_z\hat{z}$, the oscillating components of magnetization can be written as

$$\mathbf{M} = \begin{pmatrix} m_x(x)\cos\left(\mathbf{k}_\parallel \cdot \mathbf{r} - \omega t\right) \\ m_y(x)\sin\left(\mathbf{k}_\parallel \cdot \mathbf{r} - \omega t\right) \end{pmatrix}. \tag{3.10}$$

The Ansatz (3.10) implies a similar presentation for components of magnetic field: $h_x(\mathbf{r}) = h_x(x)\cos\left(\mathbf{k}_\parallel \cdot \mathbf{r} - \omega t\right)$, $h_y(\mathbf{r}) = h_y(x)\sin\left(\mathbf{k}_\parallel \cdot \mathbf{r} - \omega t\right)$. Thus, this Ansatz turns initial equations (3.2) into a system of ordinary differential equations for vectors fields $\mathbf{m}(x) = \begin{pmatrix} m_x(x) \\ m_y(x) \end{pmatrix}$ and $\mathbf{h}(x) = \begin{pmatrix} h_x(x) \\ h_y(x) \end{pmatrix}$ into a following system:

$$\omega\mathbf{m} - (1 + k_\parallel^2 - d_x^2)\sigma_1\mathbf{m} - \frac{\chi}{4\pi}\sigma_1\mathbf{h} = 0 \tag{3.11}$$

where d_x denotes differentiation over x and σ_1 is the first Pauli matrix. The equations (3.3), (3.4) and (3.11) can be considered as a closed system of integral-differential equations for vector field $\mathbf{m}(x)$ which describes the transverse distribution of magnetization. The same ansatz turns eq. (3.8) into a system of ordinary linear homogeneous differential equations with constant coefficients for the vector field $\mathbf{m} \equiv (m_x, m_y)^\top$. General solution of such a system is a superposition of basic exponential solutions $\mathbf{m}(x) = \mathbf{m}_0 e^{ik_x x}$. After division by $k^2 = k_\parallel^2 + k_x^2$ equation for $\mathbf{m}_0$ reads

$$\left(\Omega - iB\sigma_3\right)\mathbf{m}_0 = 0, \qquad \Omega = \begin{pmatrix} \omega & -A_y \\ -A_x & \omega \end{pmatrix}. \tag{3.12}$$

Here $A_\alpha = 1 + k^2 + \chi\hat{k}_\alpha^2$, and $B = \chi\hat{k}_x\hat{k}_y$. $\hat{k}_\alpha = k_\alpha/k$ denotes the cosine of direction and σ_3 is the third Pauli matrix. The solvability condition of eq. (3.12), $\omega^2 + B^2 - A_xA_y = 0$, delivers the

magnon dispersion relation:

$$\omega^2 = \left(1 + k^2\right)\left(1 + \chi + k^2 - \chi\hat{k}_z^2\right). \tag{3.13}$$

It does not depend on the sample thickness and has therefore the same form as in the bulk. Boundary conditions, will, however restrict possible $\mathbf{k}$-vectors, as it will be shown below. The dispersion relation (3.13) can be treated as a cubic equation for k^2, assuming that ω and k_z are given. Its three solutions can be written as $k_i^2 = k_{x,i}^2 + k_\parallel^2$. Thus $k_{x,i}$ is a function of ω and $\mathbf{k}_\parallel$. Close investigation shows that all 3 roots of cubic equation for k^2 are real, one of them k_1^2 is positive, two others k_2^2 and k_3^2 are negative in the entire physically available range of parameters (see Appendix 1 for details). Positive root k_1^2 corresponds to oscillating transverse mode, two negative roots correspond to evanescent waves.

Equation (3.12) and boundary conditions are invariant under operation $x \to -x, k_y \to -k_y$. It means that all eigenvalues ω are at least double degenerate and the eigenfunctions with the same ω and opposite signs of k_y are connected with a simple relation:

$$m_{x,y}(x; k_y) = m_{x,y}(-x; -k_y). \tag{3.14}$$

The value k_z enters in equations only as k_z^2. Therefore, the solution does not change at transformation $k_z \to -k_z$. These properties can be obtained from invariance of the Hamiltonian with respect to two discrete transformations: reflection in the central plane of the film combined with time reversal and reflection in the (x, z)-plane combined with time reversal. Time reversal in addition to reflection is necessary to keep pseudo-vector of spontaneous magnetization invariant.

The transverse distribution of magnetization $\mathbf{m}(x)$ must be a real vector field. Therefore for any mode it can be written as follows:

$$\mathbf{m}(x) = \mathbf{a}_i \cos k_{x,i}x + \mathbf{b}_i \sin k_{x,i}x, \tag{3.15}$$

where $\mathbf{a}_i$ are real constant 2-component vectors as well as $\mathbf{b}_1$. The vectors $\mathbf{b}_2$ and $\mathbf{b}_3$ are purely imaginary. According to (3.12), vectors $\mathbf{a}_i, \mathbf{b}_i$ obey equation $\Omega \cdot \mathbf{a}_i - B\sigma_3 \mathbf{b}_i = 0$ which implies the amplitude relation

$$\mathbf{b}_i = \Lambda(\mathbf{k}, \omega) \cdot \mathbf{a}_i, \qquad \Lambda = \sigma_3 \Omega / B. \tag{3.16}$$

Symmetry discussed above retains invariant coefficients $\mathbf{a}_i$ and changes sign of coefficients $\mathbf{b}_i$ ($i = 1, 2, 3$).

3.2 Boundary conditions and consistency requirement

The EBC (3.18) include 4 equations, two on each surface. They can not be satisfied with a single-mode solution (3.15) associated with one of three possible values of k_x^2. Indeed, according to eq. (3.16) such a solution depends only on two independent parameters, for example a_x, a_y. Only a proper superposition of three solutions can satisfy the EBC and CE simultaneously. Such a general solution of the equation (3.12) represents the vector $\mathbf{m}(x)$ as a superposition:

$$\mathbf{m}(x) = \sum_{i=1}^{3} \left(\mathbf{a}_i \cos k_{ix} x + \mathbf{b}_i \sin k_{ix} x \right), \tag{3.17}$$

where k_{ix} denotes the x-component of the wave vector corresponding to $i-$th solution of cubic equation (it is purely imaginary for evanescent waves) and $\mathbf{a}_i, \mathbf{b}_i$ are the vector amplitudes of $i-$th mode. Using eq. (3.17), the EBC equations can be rewritten in terms of 12 independent coordinates of vectors $\mathbf{a}_i, \mathbf{b}_i$; $i = 1, 2, 3$:

$$\sum_{i=1}^{3} \mathbf{a}_i k_{ix} \sin \alpha_i = 0; \;\; \sum_{i=1}^{3} \mathbf{b}_i k_{ix} \cos \alpha_i = 0; \;\; \alpha_i = \frac{k_{ix} d}{2}. \tag{3.18}$$

The MBC are satisfied automatically for any distribution of magnetization if magnetic potential obeys the integral relation (3.4). In particular, it will be satisfied for magnetization represented by superposition (3.17). We have proved that any solution of equation of motions must be such a superposition. However, the inverse statement that any such a superposition is solution of equations of motions (3.6) is wrong. It happens because equations of motion contain not only differential,

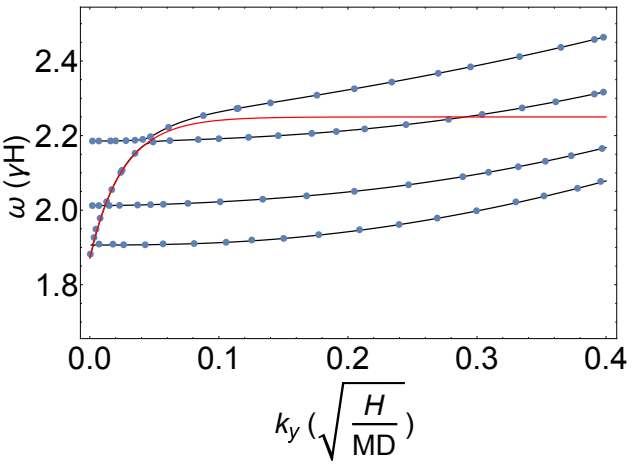

(a)

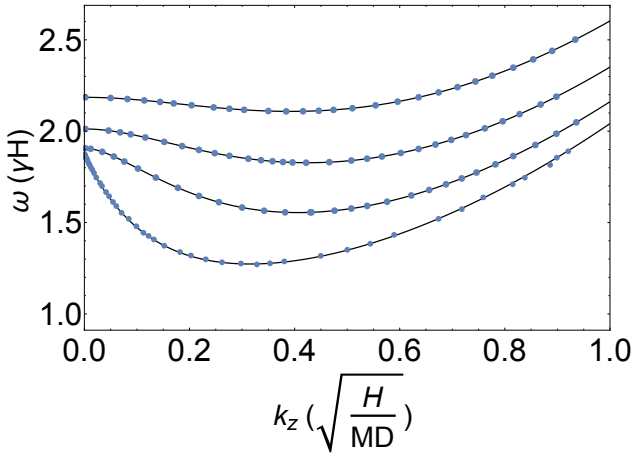

(b)

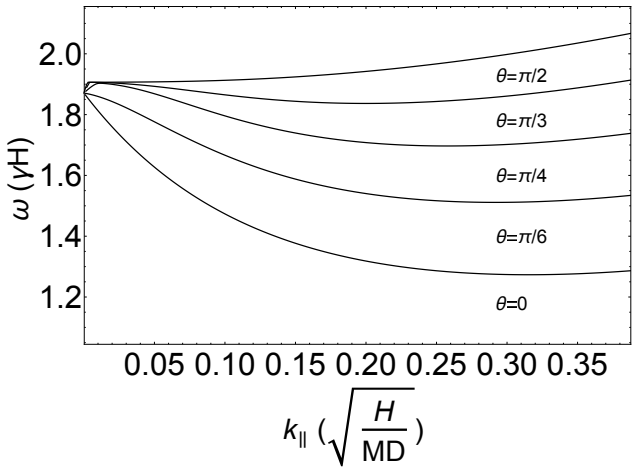

(c)

Figure 3.2: Results of numerical calculations for the case $d = 18.2$ and $\chi = 2.5$. (a) The spectra of first four quantized modes for direction of propagation perpendicular to magnetization. (b) Spectra of the first four modes for direction of propagation parallel to magnetization. (c) Spectra of the first transverse modes for $\theta = 0, \frac{\pi}{6}, \frac{\pi}{4}, \frac{\pi}{3}, \frac{\pi}{2}$. Black solid curves correspond to our numerical calculations, red solid line is the Damon-Eshbach surface mode, points are adapted from numerical calculations by Kreisel *et al.*. [1]

but also integral terms. The choice of valid solutions is realized by *condition of consistency*. It requires magnetic potential ϕ to be a superposition of exponents $e^{\pm ik_{ix}x}$ where $k_i^2 = k_{ix}^2 + k_\parallel^2$ are solutions of the cubic equation discussed earlier. We will see that integrals in $\phi(x)$ eq. (3.4) generate extra exponents of the type $e^{\pm k_\parallel x}$ that are not allowed by cubic equation. Consistency requires coefficients at them to be zero. Below we display an explicit form of these consistency equations (CE).

Integration over longitudinal coordinates y, z in eq. (3.4) can be performed explicitly with the result:

$$\phi = -4\pi\left(d_x\eta_x + k_y\eta_y\right); \;\; \eta_j = \frac{1}{2k_\parallel}\int_{-\frac{d}{2}}^{\frac{d}{2}} e^{-k_\parallel|x-x'|}m_j(x')dx'. \tag{3.19}$$

The basic integrals that enter $\eta_j(x)$, $j = x, y$ are:

$$\begin{aligned}&\int_{-\frac{d}{2}}^{\frac{d}{2}} dx' \frac{e^{-k_\parallel|x-x'|}}{2k_\parallel}\begin{pmatrix}\cos k_{ix}x'\\ \sin k_{ix}x'\end{pmatrix}\\ =&\frac{1}{k_i^2}\begin{pmatrix}\cos k_{ix}x\\ \sin k_{ix}x\end{pmatrix} - \frac{e^{-\frac{k_\parallel d}{2}}}{k_\parallel k_i^2}\begin{pmatrix}f_{ic}\cosh k_\parallel x\\ f_{is}\sinh k_\parallel x\end{pmatrix}.\end{aligned} \tag{3.20}$$

Here $k_i^2 = k_\parallel^2 + k_{ix}^2$ and we denote $f_{ic} = k_\parallel\cos\alpha_i - k_{ix}\sin\alpha_i$, $f_{is} = k_\parallel\sin\alpha_i + k_{ix}\cos\alpha_i$ with $\alpha_i = k_{ix}d/2$. Eq. (3.20) visibly demonstrates the appearance in the magnetic potential of exponents $\exp\left(\pm k_\parallel x\right)$ forbidden by secular cubic equations for k^2 since it corresponds to $k^2 = 0$. It vanishes in ϕ only due to superposition. The consistency equations require coefficients at $\cosh k_\parallel x$ and $\sinh k_\parallel x$ to be zero. The corresponding equations can be written as follows:

$$\begin{aligned}&\sum_{i=1}^{3}\frac{1}{k_i^2}\left(k_\parallel a_{ix}f_{ic} + k_y b_{iy}f_{is}\right) = 0\\ &\sum_{i=1}^{3}\frac{1}{k_i^2}\left(k_\parallel b_{ix}f_{is} + k_y a_{iy}f_{ic}\right) = 0.\end{aligned} \tag{3.21}$$

In order to turn CE together with the EBC (3.18) into a closed system of 6 equations for 6 independent amplitudes a_{ix}, b_{ix} it is possible to use relations between a_{iy}, b_{iy} and a_{ix}, b_{ix} following

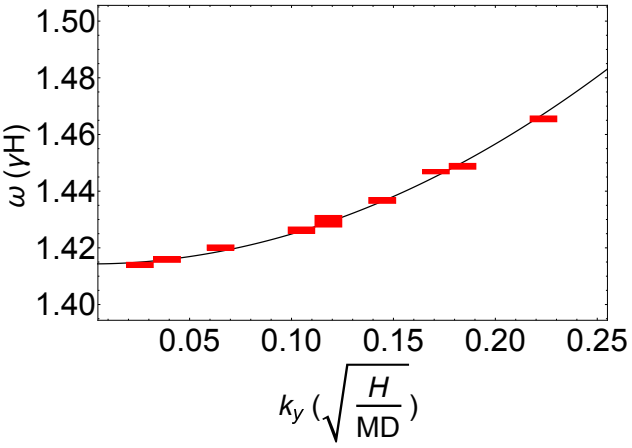

(a)

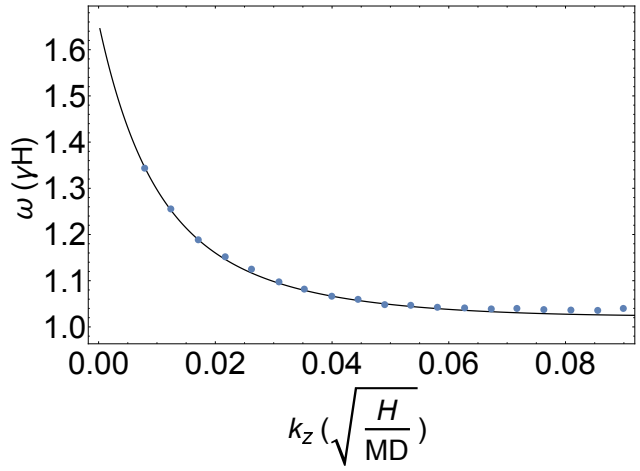

(b)

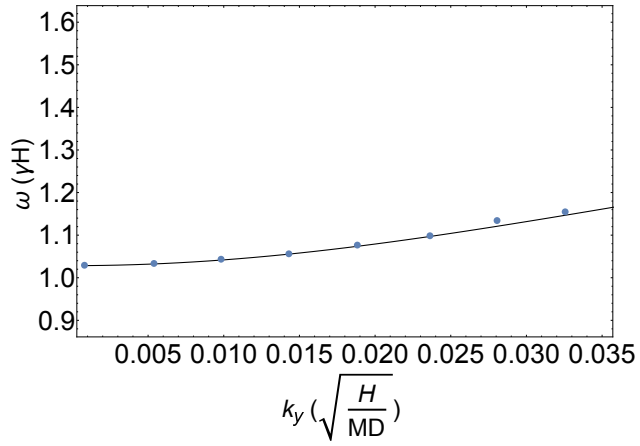

(c)

Figure 3.3: Comparison of theoretical spectrum with experiments. In experiments Brillouin light scattering spectroscopy was used.(a) Comparison with A. A. Serga *et al.*[2] $d = 5\ \mu m$, H=1750 Oe . (b) Comparison with V. E. Demidov *et al.*[3] $d = 5.1\ \mu m$, H=1000 Oe for direction of propagation parallel to magnetization. (c) Comparison with V. E. Demidov *et al.*[3] $d = 5.1\ \mu m$, H=1000 Oe. for fixed $k_z = 3.4 \times 10^4 cm^{-1}$.

from the equations of motion in the form (3.12):

$$a_{iy} = \frac{\omega}{A_{iy}} a_{ix} - \frac{B_i}{A_{iy}} b_{ix}; \;\; b_{iy} = \frac{B_i}{A_{iy}} a_{ix} + \frac{\omega}{A_{iy}} b_{ix}, \tag{3.22}$$

where $A_{iy} = 1 + k_i^2 + \frac{\chi k_y^2}{k_i^2}$ and $B_i = \frac{\chi k_{ix} k_y}{k_i^2}$. Besides that it is necessary to eliminate values k_i^2 and k_{ix} with $i = 2, 3$. As it follows from the ubic equation for $z = k^2$, if the first (positive) root $z_1 = k_1^2$ is fixed, two others can be found from the equation:

$$k_{2,3}^2 = -1 - \frac{\chi}{2} - \frac{k_1^2}{2} \pm \sqrt{\left(1 + \frac{\chi}{2} + \frac{k_1^2}{2}\right)^2 - \frac{\chi k_z^2}{k_1^2}}. \tag{3.23}$$

In this way all k_i^2 and k_{ix} with $i = 2, 3$ are determined through the single positive wave vector k_{1x}.

The system of 4 EBC (3.18) and 2 CE equations considered as 6 linear homogeneous equations for a_{ix}, b_{ix} has non-zero solutions only if its determinant is equal to zero. This requirement determines discrete set of k_{1x}, i.e. transverse quantization of wave vector. This equation is exact in the framework of the model considered. In Fig. 3.2 we show results of numerical calculations of quantized spectra from requirements of zero determinant for $d = 18.2$, and $\chi = 2.5$ for direction of propagation perpendicular and parallel to magnetization and spectra of the first transverse modes for a few different directions of propagation specified by the angle $\theta = \arctan \frac{k_y}{k_z}$.

The spectra for parallel and perpendicular direction of propagation (Fig. 3.2 (a) and 3.2 (b)) display excellent agreement with the numerical calculations of the work [1] based on diagonalization of a big matrix. We have found also the excellent agreement with similar calculations of the same work made from a film of YIG with thickness 5 μm.

Comparison of the theoretical spectrum with experiment [2, 3] is given in Fig.3.3. The experiment used Brillouin scattering spectroscopy. Its precision is not sufficient for resolution of excited states. Dramatic increase of precision was achieved recently by the experimental group led by J. Ketterson [4]. His method employs direct excitation of magnons by microwave from a specially invented antenna. It consists of periodically repeated emitters fed by an adjustable frequency generator. The distance between emitters determines the excited magnon wave-length. The

magnon frequency at this wave vector is determined as a position of the resonant singularity on the intensity vs. frequency characteristic or the maximum absorption of microwave radiation. The enhanced resolution allowed observation of several (up to 9) modes of magnons. This is the first time that different transverse modes of magnons were observed experimentally. Comparison of the theoretical spectrum with their experimental results [4] is given in Fig.3.4. The agreement between theory and experiment is excellent.

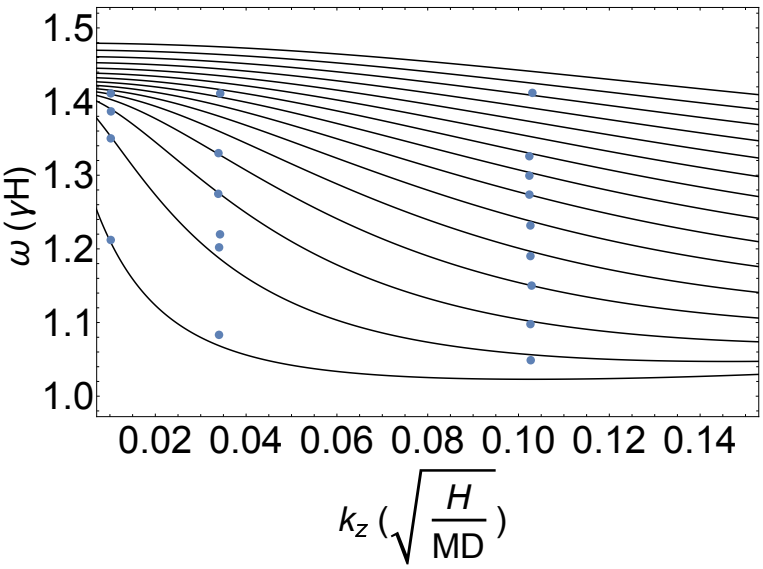

Figure 3.4: Comparison of theoretical spectrum with experiment. Solid curves are our calculations of the first 15 transverse modes for the YIG film of thickness 5μm, 4πM= 1940 Oe and H= 1960 Oe . Points on them are frequencies measured by J. Lim *et al.* [4] at three fixed wavelengths for different transverse mode.

To give a more visible idea on the origin of these results, we consider 6 EBC-CE equations in some detail. Only $\cos k_{1x}d/2$ and $\sin k_{1x}d/2$ are oscillating functions of their arguments. The functions f_{1c}, f_{1s} are linear functions of $\cos\alpha_1,\ \sin\alpha_1$ and therefore also oscillate. Other functions containing $\cos\alpha_{2,3},\ \sin\alpha_{2,3}$ are hyperbolic functions and change monotonically with k_{1x}. In the 6×6 matrix C of the EBC-CE equations the first two columns are linear combinations of $\sin\alpha_1,\ \cos\alpha_1$, the rest are monotonic functions. Therefore, the determinant has a form $\det C = \mathcal{K}\sin^2\alpha_1 + 2\mathcal{L}\sin\alpha_1\cos\alpha_1 + \mathcal{M}\cos^2\alpha_1$, where $\mathcal{K}, \mathcal{L}, \mathcal{M}$ are monotonic functions of

k_{1x} or α_1. Equation $\det C = 0$ can be rewritten as $\mathcal{K}\tan^2\alpha_1 + 2\mathcal{L}\tan\alpha_1 + \mathcal{M} = 0$ with formal solution:

$$\tan\alpha_1 = \frac{-\mathcal{L} \pm \sqrt{\mathcal{L}^2 - \mathcal{K}\mathcal{M}}}{\mathcal{K}}. \tag{3.24}$$

This is an implicit equation for k_{1x}. It shows that the consequent quantized values k_{1x} are located between points $n\pi/d$ and that these quantized values form two series corresponding to two signs in front of the square root in previous equation.

Thus, the quantized values of k_{1x} can be enumerated by an index ν taking two values $+$ and $-$ and by an integer number n taking values from 0 to ∞. We will denote these quantized values as $k_{x,\nu,n}$. For large n the main part of $k_{x,\nu,n}$ is $2\pi n/d$. An approximate formula for the quantized values reads:

$$k_{x,\nu,n} = \frac{2\pi n}{d} + \frac{2}{d}\arctan\frac{-\mathcal{L} \pm \sqrt{\mathcal{L}^2 - \mathcal{K}\mathcal{M}}}{\mathcal{K}}. \tag{3.25}$$

In the argument of $\arctan k_{1x}$ must be replaced by $2\pi n/d$. The expressions for the coefficients $\mathcal{K}, \mathcal{L}, \mathcal{M}$ are too long to be placed here. In real numerical calculations we found numerically the zeros of the 6-th order determinant.

3.3 General properties of magnon spectra in thick films

In thick films $d \gg 1$ comparatively simple analytical formulae for the magnon spectrum and ratio of amplitudes can be found. In what follows we assume that $k_{1x} \ll k_\parallel$. Since the minimal k_{1x} is of the order of $1/d$, this inequality implies that $k_\parallel \gg 1/d$. Most of the experiments with magnon Bose-condensation [27, 31, 32], hybridization of magnons and phonons [33, 34], and many others satisfied these conditions. However, experiments with magnetic resonance require very small $|k_z|$. The region of rather small $k_\parallel \lesssim 1/d$ will be considered in section 3.4. At a fixed k_1^2 two negative roots of cubic equation are:

$$k_{2,3}^2 \approx -\left(1 + \frac{\chi}{2} + \frac{k_1^2}{2}\right) \pm \sqrt{\left(1 + \frac{\chi}{2} + \frac{k_1^2}{2}\right)^2 - \chi\frac{k_\parallel^2\cos^2\theta}{k_1^2}} \tag{3.26}$$

For 2 positive numbers a and b such that $a^2 > b$ the following inequality is correct $-a + \sqrt{a^2 - b} < -\frac{b}{2a} < 0$. Therefore $k_2^2 < 0$ and $k_{2x}^2 = k_2^2 - k_\parallel^2 < -k_\parallel^2$. Thus, $|k_{2x}| > k_\parallel \gg k_{1x}$. This inequality is valid even more for $|k_{3x}|$ since $k_3^2 \approx -(2 + \chi)$. Then the EBC together with the linear relations between pairs a_{iy}, b_{iy} and a_{ix}, b_{ix} (3.22) show that the moduli of values $c_{i\alpha} \equiv e^{(|k_{ix}|d/2)} a_{i\alpha}$ and $d_{i\alpha} \equiv \exp\{|k_{ix}|d/2\} b_{i\alpha}$ with $i = 2, 3$ and $\alpha = x, y$ are much less than moduli of $a_{1\alpha}$, $b_{1\alpha}$ by a small factor not larger by an order of magnitude than $k_{1x}/k_\parallel$. Therefore, the contribution of evanescent waves to the CE is relatively small and only the contribution of oscillating transverse waves must be taken into account. The equation of quantization (3.24) can be written more explicitly:

$$\begin{aligned} &\tan\frac{k_x d}{2} = \frac{k_\parallel - k_x R}{k_\parallel R + k_x};\ R = \Gamma \mp \sqrt{\Gamma^2 + 1}; \\ &\Gamma = \frac{1}{2B}\left(\frac{k_\parallel A_y}{k_y} - \frac{k_y A_x}{k_\parallel}\right); \end{aligned} \tag{3.27}$$

In this equation we omitted subscript 1 everywhere since evanescent waves do not enter the quantization condition. At $k_y = 0$, $\Gamma = \infty$ and $R = 0$ for the sign $-$ and $R = \infty$ for the sign $+$. In the first case, the quantization condition turns into $\tan\frac{k_x d}{2} = \frac{|k_z|}{k_x}$. This quantization condition was first found by Damon and Eshbach [6] and reproduced by Sonin [14]. It corresponds to even modes. The second case corresponds to odd modes, the quantization condition is $\tan\frac{k_x d}{2} = -\frac{k_x}{|k_z|}$. The quantized values of k_x at $n \ll |k_z|d$ are $k_{x,-,n} \approx (2n+1)\frac{\pi}{d}$ and $k_{x,+,n} \approx 2(n+1)\frac{\pi}{d}$ $(n = 0, 1...)$.

For general direction of propagation and at $1 \ll n \ll k_\parallel d$, in the r.-h. side of the quantization equation (3.27), k_x must be replaced by $2\pi n/d$. Thus, the equation for k_x becomes explicit. Its solution reads $k_{x,\nu,n} = \frac{2\pi n}{d} + \mu_{\nu,n}$, where $\mu_{\nu,n} = \frac{2}{d}\arctan\frac{k_\parallel - 2\pi n R_\nu/d}{k_\parallel R_\nu + 2\pi n/d}$, where $R_\nu = \Gamma + \nu\sqrt{\Gamma^2+1}$ and Γ is given by the last eq. (3.27) in which k_x in B and A_x is replaced by $2\pi n/d$. Thus, $\mu_{-,n}$ decreases slowly from π/d at $n = 0$ to $\frac{\pi}{2d}$ at $n \sim \sqrt{k_\parallel}d$. In entire the above defined range of parameters the phases μ for two series of modes are connected by relation:

$$\mu_{+,n} = \mu_{-,n} + \pi/d$$

The ratio of of amplitudes b_x/a_x is a slow function of n, but this function is different for different ν:

$$\frac{b_{x,\nu,n}}{a_{x,\nu,n}} = -\frac{k_\parallel A_y}{k_y \omega} R_\nu - \frac{B}{\omega} \tag{3.28}$$

At fixed direction of propagation given by $\theta = \text{const}$, the frequency $\omega_{\nu,n}$ of a mode ν, n with $n \ll k_\parallel d$ as function of $k_\parallel$ has a minimum at the non-zero value

$$k_{\parallel 0} \approx \left(\frac{\chi \cos^2 \theta}{2 + \chi \sin^2 \theta} \right)^{1/4} k_{x,\nu,n}^{1/2}. \tag{3.29}$$

According to this equation, $k_{\parallel 0} \gg k_{x,\nu,n}$. The limitation to n ensures that $k_{x,\nu,n} \ll 1$ and as a consequence $k_{\parallel 0} \ll 1$. The frequency at the minimum is $\omega_{min} = 1 + O(k_{\parallel 0}^2)$. A more general equation for the position of the minimum that is valid also at $1/d \ll k$ reads:

$$k_{\parallel 0}^2 = \frac{2 + \chi \sin^2 \theta}{2} u \left(\frac{4\chi \cos^2 \theta k_x^2}{(2 + \chi \sin^2 \theta)^3} \right), \tag{3.30}$$

where the function $u(x)$ is defined as the positive solution of cubic equation $u^3 + u^2 - x = 0$. A rather good approximation for it is given by expression $u(x) \approx \frac{\sqrt{x}}{(1+\sqrt{x})^{1/3}}$. Plot of the function $u(x)$ and an approximation to it is given by Fig. 3.5. At not very large n and fixed θ, the wave

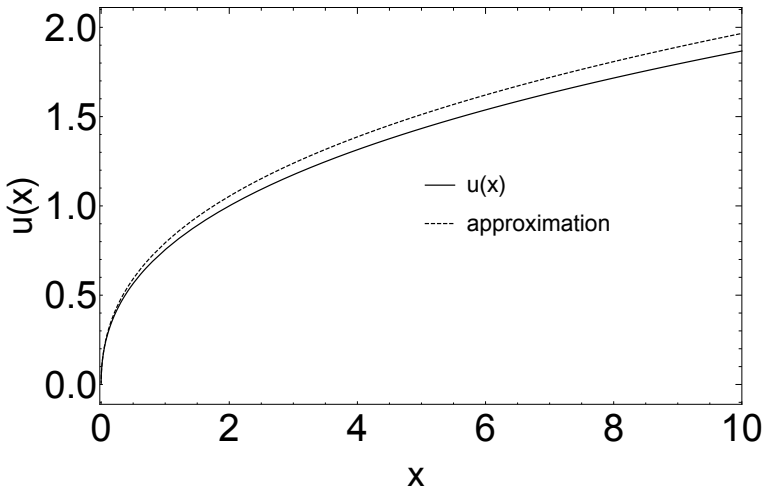

Figure 3.5: Plot of function $u(x)$ and approximation to it.

vector at minimum $k_{\|0}$ grows with n or equivalently with $k_x \approx 2\pi n/d$. However, it can not grow at very big $n \gg d$ or equivalently at $k_x \gg 1$ since at such big values of k_x the exchange interaction dominates. Therefore, the frequency with high precision obeys equation $\omega = 1 + k^2$ and has the only minimum at $k_\| = 0$ independently on the direction of propagation. Thus, we conclude that the wave vector $k_{\|0}$ at minimum of frequency reaches its maximum at some value of the transverse wave vector $k_x \sim 1$ and then decreases to zero value at another value of transverse wave vector of the order of unity. Our equation (3.27) strictly speaking is not valid at $k_x \gtrsim k_\|$, but we will show that it can serve as interpolation between exact results in the regions of small $k_x \ll k_\|$ and large k_x in the exchange dominance range. Indeed, if exchange dominates and the dipolar interaction can be neglected, the Landau-Lifshitz equation (3.11) implies $m_x(x) = m_y(x)$ i.e. $a_{1y} = a_{1x}$ and $b_{1y} = b_{1x}$. On the other hand, the linear relations (3.22) between $x-$ and $y-$components of vectors $\mathbf{a}_1$ and $\mathbf{b}_1$ in the range $k_1^2 \gg 1$ give $a_{1y} = a_{1x} + o(k_1^{-2})b_{1x}$ and $b_{1y} = b_{1x} + o(k_1^{-2})a_{1x}$. These relations show that indeed the contribution of the dipolar interaction and associated evanescent waves in the exchange dominant region of variables is negligibly small. Therefore, eq.(3.27) is asymptotically exact in the exchange range and thus is a reasonable interpolation matching two limiting ranges of the ratio $k_x/k_\|$. Employing this equation, we find that $k_{\|0}$ reaches its maximum value $\left(k_{\|0}\right)_{max} = \sqrt{k_1^2 - k_x^2}$;

$$k_1^2 = \frac{\sqrt{(2 + \chi \sin^2\theta)^2 + 6\chi\cos^2\theta} - (2 + \chi\sin^2\theta)}{6}$$

at $k_x^2 = \frac{2+\chi}{3\chi}\tan^2\theta k_1^4 + \frac{1}{3}k_1^2$. At larger k_x, the value $k_{\|0}$ decreases and at $k_x = \frac{1}{2}\left(\sqrt{(2 + \chi\sin^2\theta)^2 + 8\chi\cos^2\theta} - 2 - \chi\sin^2\theta\right)^{1/2}$ becomes equal to zero. Let denote the corresponding number of that mode $n_0(\theta)$.

At fixed n and θ increasing, $k_{\|0}$ decreases. At $\theta = \pi/2$ minimum and maximum coalesce. The point $k_y = 0$ is the only minimum of frequency in the spectrum of any magnon mode propagating perpendicularly to the permanent magnetization ($\cos\theta = 0$). The reader is referred to Appendix 2 for derivation of all relations concerning the motion of the frequency minimum at changing $\mathbf{k}_\|$ and

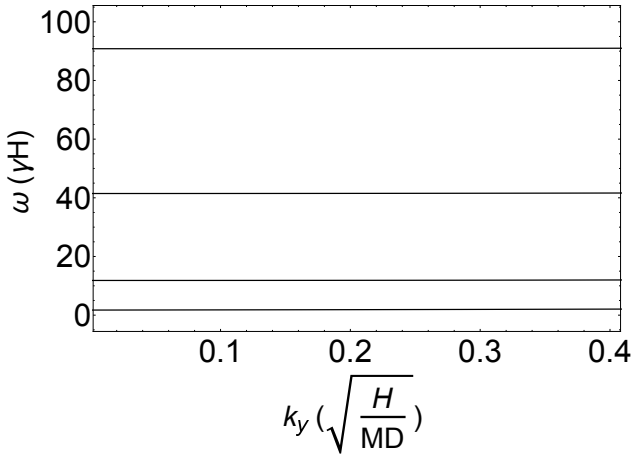

(a)

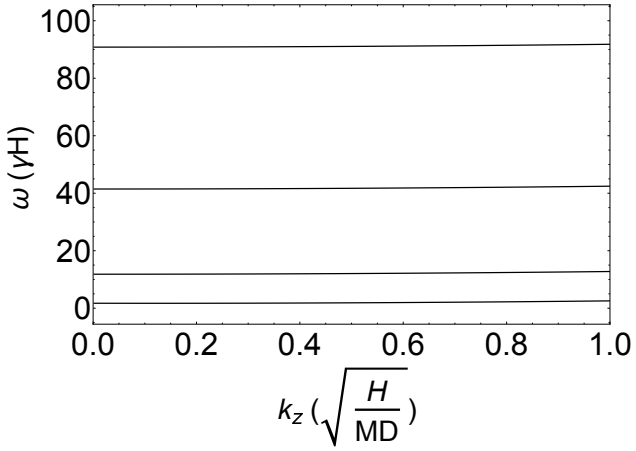

(b)

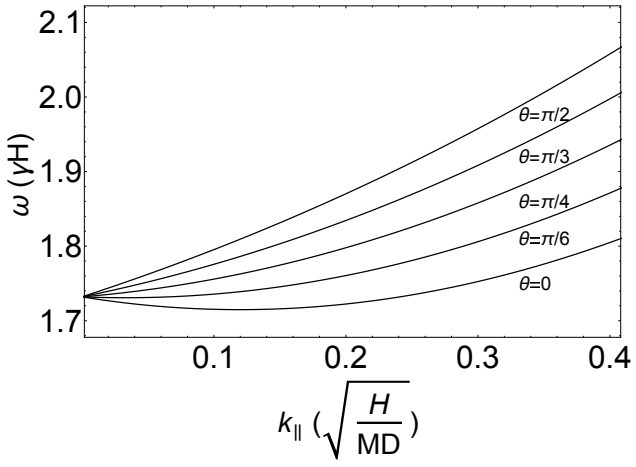

(c)

Figure 3.6: Results of numerical calculations for a thin film $d = 1$ and $\chi = 2$. (a) The spectra of first four quantized modes for direction of propagation perpendicular to magnetization. (b) Spectra of the first four modes for direction of propagation parallel to magnetization. (c) Spectra of the first transverse modes for $\theta = 0, \frac{\pi}{6}, \frac{\pi}{4}, \frac{\pi}{3}, \frac{\pi}{2}$. Note the difference of scales in fig.b and c.

the number n of mode, and to Appendix 3 for peculiarities of quantization and TDM for magnons propagating perpendicularly to the spontaneous magnetization ($k_z = 0$). A local maximum of frequency for a fixed number of mode $n < n_0(\theta)$ at any fixed θ except of $\theta = \pi/2$ is located at $k_\parallel = 0$. The value of frequency at the maximum is equal to $\omega_{max} = \sqrt{(1+k_x^2)(1+\chi+k_x^2)}$. For the mode with minimal frequency and excited modes with $n \ll d$ it simplifies to $\omega = \sqrt{1+\chi}$, frequency of the ferromagnetic resonance. Such a value of frequency right of the right minimum is reached at $k_\parallel = \left(\sqrt{1+\chi+\chi^2\sin^2\theta/2} - 1 - \chi^2\sin^2\theta/2\right)^{1/2}$, much larger than the parallel wave vector at the absolute minimum $k_\parallel \sim 1/\sqrt{d}$ [14]. This result shows a rather strong asymmetry of the spectral curve with respect to its minimum generated by dipolar forces. This asymmetry is very important for different applications. The presence of two minima is definitive in structure of magnon Bose-condensation and possible superfluidity[17]. The strong asymmetry of the minimum means that the quadratic approximation for the energy near minimum becomes invalid at relatively small deviation of the wave vector from minimum. As a result two condensates subject to the action of a pulsed magnetic field acquire different velocities.

The TDM in each mode is described by a superposition of one oscillating and two evanescent modes. The oscillating mode is a sum of the type $a\cos k_x x + b\sin k_x x$. At any direction of propagation except $\theta = 0$, both a and b are not zero. The mode becomes even or odd only at $\theta = 0$ and asymptotically at large $k_\parallel \gg 1$ when the exchange interaction dominates. The EBC in this case are satisfied by either even or odd TDM.The admixture of alternative parity has order of magnitude k^{-2}.

In conclusion we establish the correspondence between the commonly used names of different spin waves and our classification of magnons. The backward volume spin waves (BVSW) are magnons with the wave vectors in the range between two frequency minima, whereas forward volume waves have wave vectors outside of this interval. The volume magnetic standing wave (VMSW) is the same as our lowest transverse mode. Sometimes in the literature it is treated as this mode at small $k_\parallel$ and k_x, i.e. in the range of dominant dipolar interaction. Finally, the term perpendicular standing spin waves (PSSW) is the same as our higher magnon modes, i.e.

$\nu = -$, $n \geq 1$ and $\nu = +$, any n.

3.4 Spectral properties of thin films

The film is considered as thin if its thickness is of the order or less than 1, i.e. ℓ in dimensional units. Since characteristic value of ℓ is between a few nanometers (in YIG) to a few tens of nanometers, experimental realization of ultrathin films of YIG with $d \ll 1$ seems rather unrealistic. It may be realized in ferromagnetic films of few monolayers thick. In a thin film with $d \sim 1$, transverse modes with large n have $k_{1x} \approx 2\pi n/d \gg 1$ in the exchange dominance region. Therefore, only a few modes with lowest possible frequencies are of experimental and theoretical interest. In these modes evanescent waves penetrate the film on a depth comparable with its film thickness. Therefore their contribution to spectral properties and TDM is not less important than the contribution of the oscillating wave. A compact analytic expression has been found only for frequency as function of wave vector see eq. 3.13. The quantization of the transverse wave vector and frequency is determined by the general equation (3.24). Examples of spectra in thin films plotted in Fig. 3.6 show that qualitatively they are similar to the spectra in thick films. Each mode fixed by numbers ν, n at not very large n also has a minimum of frequency at some $k_\parallel \neq 0$, but it does not obey equation $\frac{\partial \omega^2}{\partial k_\parallel^2} = 0$ since k_{1x} also depends on $k_\parallel$. The graphs of position of minima and the value of frequency in minimum for the lowest mode vs d for thin films are shown in Fig.3.7 (a) and Fig.3.7 (b). In the same figures 3.7 (a) and 3.7 (b), we compared our results with calculations of the same values by Kreisel *et al.* [1]. Finally, the graphs of k_{1x} for the lowest mode vs d at fixed $k_\parallel$ and $\theta = 0$ are shown in Fig. 3.7 (c). An example of TDM for the lowest mode and the first excited mode in thin films is shown in Fig. 3.8. Fig. 3.6 (a) and Fig. 3.6 (b) show that at $d = 1$, the energy of the transverse excitation weakly depends on k_z, a feature that could be expected for ultrathin films $d \ll 1$. Fig.3.6 (c) shows that the energy of transverse ground state at fixed $k_\parallel$ monotonically grows with the angle of propagation θ.

All ground state spectra cross at the point $k_\parallel = 0, \omega \approx \sqrt{1+\chi}$ ($\sqrt{3} \approx 1.73$ for $\chi = 2$), exactly the same result as for the thick film. This is manifestation of a general property of films with arbitrary thickness: at $\mathbf{k}_\parallel = 0$, the transverse wave vector of the lowest transverse mode is

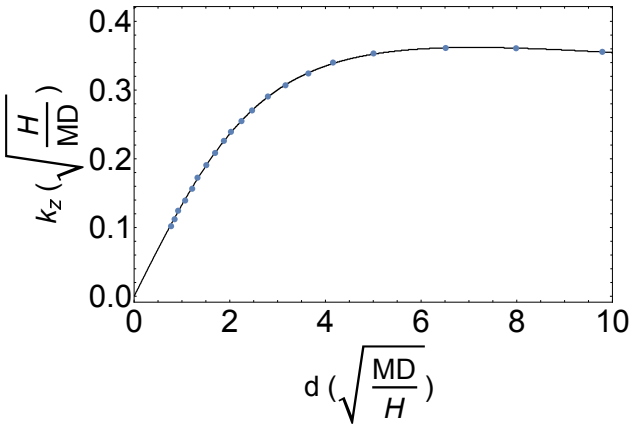

(a)

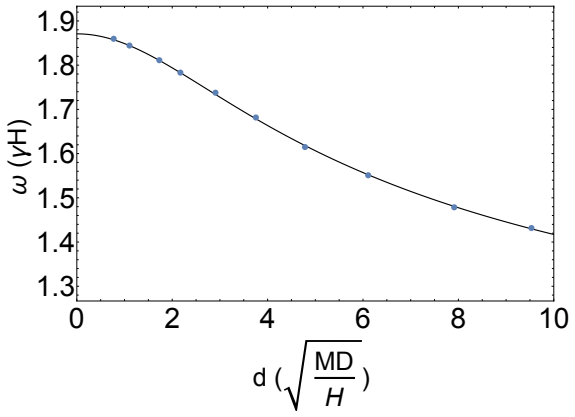

(b)

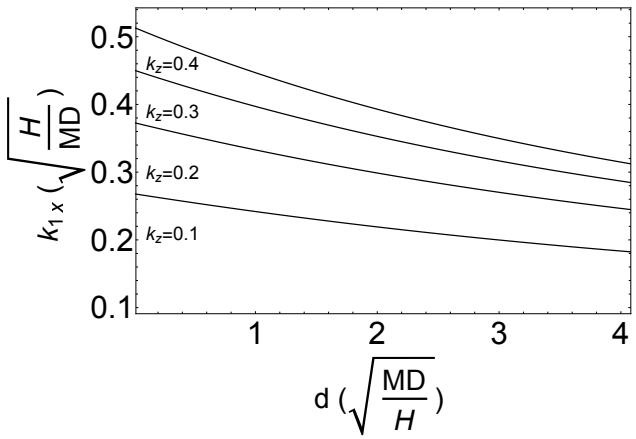

(c)

Figure 3.7: Results of numerical calculations for the case $\chi = 2.5$ and $\theta = 0$. (a) Position of minima for the lowest mode vs d for thin films. (b) The value of frequency at the minimum for the lowest mode vs d for thin films. (c) k_{1x} for the lowest mode vs d at fixed $k_z = 0.1, 0.2, 0.3, 0.4$. Black solid curves correspond to our numerical calculations, points are adapted from numerical calculations by Kreisel *et al.*. [1]

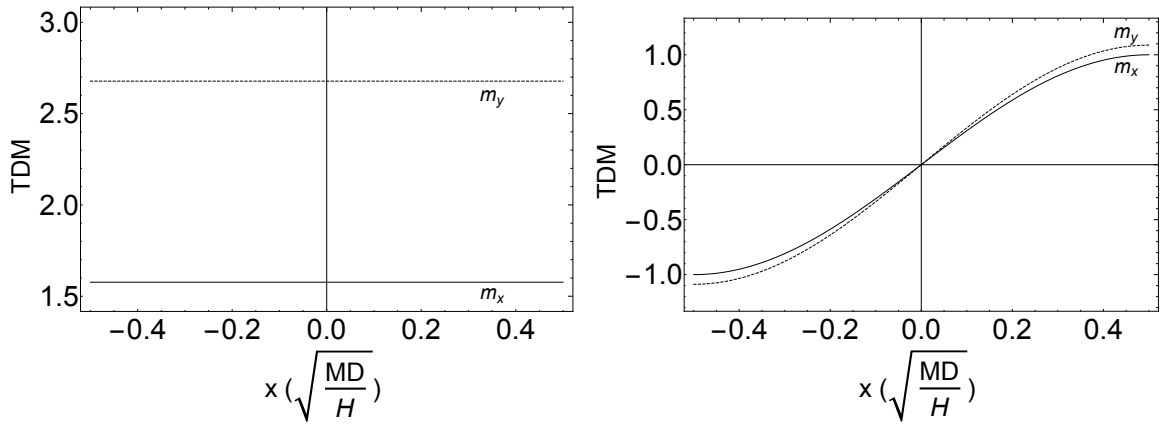

(a) (b)

Figure 3.8: For the case $\chi = 2$ and $\theta = 0$ (a) TDM for the lowest mode at $k_\parallel = 0.1$ and $a_{1x} = 1$. (b) TDM for the first excited mode at $k_\parallel = 0.1$ and $b_{1x} = 1$.

also equal to zero. The frequency of the lowest mode is equal to $\omega_0 = \sqrt{1+\chi}$ (ferromagnetic resonance frequency).

We postpone the proof of this general statement and consider first the limiting case of ultrathin films $d \to 0$ when $\theta = 0$. It will be shown that only wave vectors of the lowest transverse mode with $\nu = -, n = 0$ remains finite in this limit. All excited transverse state with other ν or n have wave vectors that go to infinity as $1/d$. To simplify calculations we consider only the simplest case of the waves propagating along the magnetization and magnetic field. Then the transverse modes have a definite parity. Non-zero amplitudes in such situation are $\mathbf{a}_i$ for even modes and $\mathbf{b}_i$ for odd ones. For finite wave vectors $\mathbf{k}_i$ in the considered limit $\sin k_{ix}d/2 \approx k_{ix}d/2$ and $\cos k_{ix}d/2 \approx 1$. This fact allows simplification of the EBC (3.18) and CE (3.21). The next simplification follows from the fact that relation between x and y components of vectors $\mathbf{a}_i$ and $\mathbf{b}_i$ (3.16) reduces to $a_{iy} = \frac{\omega}{1+k_i^2} a_{ix}$ and $b_{iy} = \frac{\omega}{1+k_i^2} b_{ix}$. After all these simplifications a following system of 3 equations with 3 independent amplitudes a_{ix} describes the quantization of an even mode:

$$\begin{cases} \sum_{i=1}^{3} k_{ix}^2 a_{ix} & = 0 \\ \sum_{i=1}^{3} \frac{k_{ix}^2}{1+k_i^2} a_{ix} & = 0 \\ \sum_{i=1}^{3} \frac{a_{ix}}{k_i^2} & = 0 \end{cases} \tag{3.31}$$

Zeros of the determinant of this system are quantized values of k_{1x}^2. To make this equation closed with respect to the variable k_{1x} or equivalently to variable $k_1 = \sqrt{k_{1x}^2 + k_z^2}$ it is necessary to use the dependence of k_2^2 and k_3^2 from k_1^2 given by eq. (3.23) and relations between k_{ix}^2 and k_i^2: $k_{ix}^2 = k_i^2 - k_z^2$. At small $k_z \ll 1$, the only positive root of this equation is

$$k_{1x} \approx \left(\frac{\chi}{2+\chi}\right)^{1/4} \sqrt{k_z} \tag{3.32}$$

At large k_z, k_{1x} asymptotically approaches a constant value $k_{1x} \approx \sqrt{\chi/2}$. Both these asymptotic

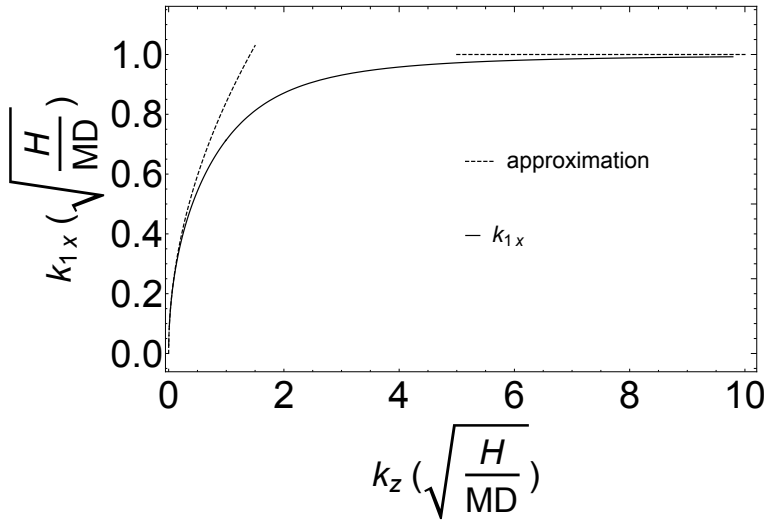

Figure 3.9: Plot of k_{1x} at $d \to 0$ and approximation to it when $\chi = 2$ and $\theta = 0$.

values are in excellent agreement with numerical calculations of the dependence of k_{1x} on k_z at $d \to 0$ (see Fig.3.9). Asymptotic of k_{1x} at small k_z confirms that indeed $k_{1x} = 0$ at $k_z = 0$. Thus, in the limit $d \to 0$ the value of frequency at $k_\parallel = 0$ is $\sqrt{1+\chi}$ as well as in the limit of large d. The comparison of the plots of k_{1x} vs. k_z at $d = 1$ and $d = 0$ is shown on Fig. 3.10.

Now we are in position to prove general statement that the frequency of the lowest mode at $\mathbf{k}_\parallel = 0$, is equal to $\sqrt{1+\chi}$ independently of thickness. Let us put $k_y = 0$ and consider $k_z \ll 1/d^2$. We will show that the first quantized value k_{1x} is determined by the same equation

(3.32), but the arguments must be modified. Anticipating the result (3.32), we assume that the first quantized value of k_{1x} is much smaller than 1, but much larger than k_z^2. Then eq. (3.23) implies that $k_{2x}^2 \approx -\chi k_z^2/\left[(2+\chi)\, k_{1x}^2\right]$ is also small by absolute value, whereas $k_{3x}^2 \approx -2-\chi$ remains of the order of unity by modulus. Let us first consider the EBC (3.18) that in considered situation take form

$$k_{1x}^2 a_{1x} + k_{2x}^2 a_{2x} - \sqrt{2+\chi}\frac{2\sinh\sqrt{2+\chi}d/2}{d} a_{3x} = 0 \tag{3.33}$$

$$k_{1x}^2 a_{1x} + k_{2x}^2 a_{2x} + \frac{2\sqrt{2+\chi}\sinh\sqrt{2+\chi}d/2}{(1+\chi)d} a_{3x} = 0 \tag{3.34}$$

These equations imply $a_{3x} = 0$. Then they become identical and define the ratio $a_{2x}/a_{1x} = -k_{1x}^2/k_{2x}^2$. Next consider the CE for a_{ix} that in the same limit has a form:

$$\frac{a_{1x}}{k_1^2} + \frac{a_{2x}}{k_2^2} = 0$$

Employing the ratio a_{1x}/a_{2x} found above, we again obtain eq. (3.32) for this more general situation. It shows that in the limit $k_z \to 0$, the limit of ratio k_z^2/k_{1x}^2 is also zero and the limiting value of ω is $\sqrt{1+\chi}$ independently on thickness. Note that in the limit $\mathbf{k}_\parallel = 0$ the magnetization in the lowest spin-wave mode does not depend on transverse coordinate.

In principle it could happen that the positive root k_1^2 would be less than $k_\parallel^2$. Then the value k_{1x}^2 is negative and all three waves participating in m_x, m_y are evanescent. Our numerical calculations did not discover such a solution in a wide range of parameters that presumably shows that the absence of purely evanescent waves in the films with free spins on boundaries. However, we do not have rigorous proof of this statement. Though thin films are more sensitive to the specific form of the EBC than thick ones, different versions of these conditions do not change the symmetry and general properties of solutions. An important problem is how the wave vector k_z corresponding to minimum of energy changes with thickness. For thick films it behaves as $1/\sqrt{d}$ [14] and grows when the film becomes thinner. However, in the range of ultrathin films it decreases with the thickness linearly. Therefore there exists a maximum of this wave vector. Numerical calculations

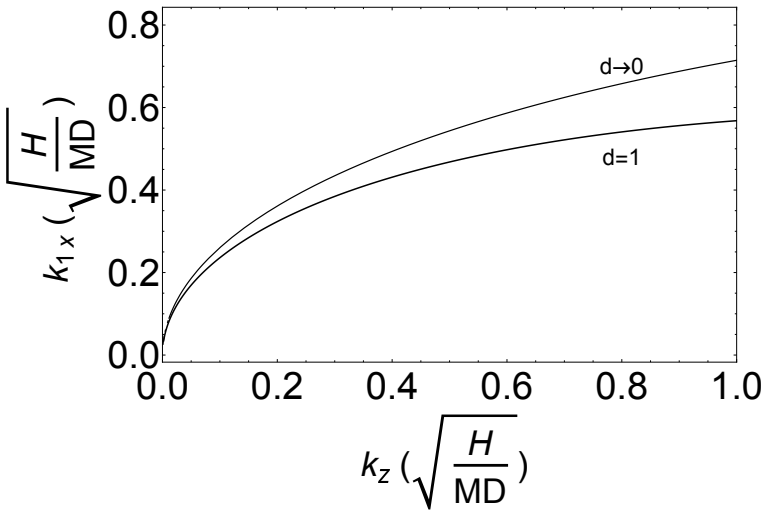

Figure 3.10: k_{1x} for the lowest mode at $d \to 0$ and $d = 1$ when $\chi = 2$ and $\theta = 0$.

illustrated by Fig. 3.7 (a) show that for $\chi = 2.5$, the maximum is reached at $d \approx 6$ and the maximal wave vector corresponding to the minimal frequency is about 0.3. The dimensionless k_z corresponding to the minimum of energy in the film of thickness $5\mu m$ is about 0.02. Thus the wave vector can be changed by a factor of about 15 by reducing thickness from $5\mu m$ to $15 - 30$nm. The minimal wavelength of a magnon gives an upper limit for the size of any soliton-like formation made from magnons that can be used for the transfer of information without dissipation or with very small dissipation[17].

3.5 Surface waves

Surface waves in ferromagnetic films were predicted by Damon and Eshbach [6] in the purely dipolar limit. For magnets with exchange and dipolar interaction this limit is valid for sufficiently small wave vectors $k_1 \ll 1$. At large $k_1 \gg 1$, the exchange forces become dominant and energy (frequency) of any mode of oscillation must be close to k^2. The meaning of the term "surface wave" for thick films $d \gg 1$ is that they are localized in a thin layer of the width $\sim 1 \ll d$. However, in thin films $d \lesssim 1$ these waves penetrate to the entire film. We will show that surface wave can be distinguished in thick films, but it is distributed between many modes of the complete Hamiltonian. In thin films the notion of surface wave is meaningless.

3.5.1 Spectrum in a magnet with purely dipolar interaction

Here we reproduce results by Damon and Eshbach employing our approach. The spectrum can be obtained from our equation (3.11) written for the case of zero exchange constant D. In this case there is no scale of length in the problem apart from the film thickness d, but it does not enter into equations of motion that for purely dipolar interaction are:

$$(\omega - \sigma_1)\,\mathbf{m} - \frac{\chi}{4\pi}\mathbf{h} = 0 \tag{3.35}$$

In components they are:

$$\begin{cases} \omega m_x - m_y + \frac{\chi}{4\pi} k_y \phi = 0 \\ -m_x + \omega m_y - \frac{\chi}{4\pi}\frac{d\phi}{dx} = 0 \end{cases} \tag{3.36}$$

The magnetic potential ϕ satisfies magnetostatic equation:

$$\frac{d^2\phi}{dx^2} - k_\parallel^2 \phi + 4\pi\left(\frac{dm_x}{dx} + k_y m_y\right) = 0 \tag{3.37}$$

Equations of motion can be solved with respect to components of $\mathbf{m}$ and substituted to eq. (3.37). The resulting differential equation for ϕ reads:

$$\left(1 - \frac{\chi}{\omega^2 - 1}\right)\frac{d^2\phi}{dx^2} - \left(k_\parallel^2 - \frac{\chi}{\omega^2 - 1}k_y^2\right)\phi = 0 \tag{3.38}$$

In contrast to the exchange case it is only of the second order. As any linear homogenous differential equation with constant coefficients, it has 2 independent exponential solutions of the form $e^{ik_x x}$. The values k_x are determined by equation:

$$k_x^2 = \frac{\omega^2 - 1}{1 + \chi - \omega^2}k_z^2 - k_y^2 \tag{3.39}$$

It also can be treated as equation for spectrum:

$$\omega = \sqrt{1 + \chi \frac{k_x^2 + k_y^2}{k^2}} \tag{3.40}$$

3.5.2 Surface wave propagating perpendicularly to magnetization

If a wave propagates perpendicularly to the magnetization and magnetic field, that implies $k_z = 0$. From equation (3.39) it follows that in this case $k_x = \pm i k_y$. It means that $k^2 = 0$ and the value of frequency determined by eq. (3.40) becomes uncertain. To find the spectrum, it is necessary to represent the solution $\mathbf{m}(x)$ in the form:

$$\mathbf{m}(x) = \mathbf{p}(x) \cosh k_y x + \mathbf{q}(x) \sinh k_y x \tag{3.41}$$

In contrast to the case of exchange and dipole interaction in pure dipole case there are no additional waves. According to eq. (52) of our Appendix 3, $\mathbf{q} = -\sigma_1 \mathbf{p}$, i.e. $q_x = -p_y$ and $q_y = -p_x$. There is no EBC, but the CE must be used. According to our eq. (58) in the same Appendix, they are reduced to the following system:

$$\begin{cases} \omega p_x - p_y + \chi e^{-\frac{|k_y| d}{2}} \sinh \frac{|k_y| d}{2} q_x = 0 \\ -p_x + \omega p_y + \chi e^{-\frac{|k_y| d}{2}} \cosh \frac{|k_y| d}{2} q_y = 0 \end{cases} \tag{3.42}$$

By employing the $p - q$ relation we find the closed system for components of vector $\mathbf{p}$:

$$\begin{cases} \omega p_x - p_y \left(1 + \chi e^{-\frac{|k_y| d}{2}} \sinh \frac{|k_y| d}{2}\right) = 0 \\ -p_x \left(1 + \chi e^{-\frac{|k_y| d}{2}} \cosh \frac{|k_y| d}{2}\right) + \omega p_y = 0 \end{cases} \tag{3.43}$$

By nullifying the determinant of this system, we get dispersion:

$$\omega = \sqrt{1 + \chi + \frac{\chi^2}{2} e^{-|k_y| d} \sinh |k_y| \, d} \tag{3.44}$$

This result coincides with eq. (23) of the cited Damon-Eshbach article. The frequency of the surface wave starts with $\omega = \sqrt{1+\chi}$ at $k_y = 0$ (the ferromagnetic resonance frequency) and reaches the saturation frequency $\omega = 1 + \frac{\chi}{2}$ at $|k_y| \to \infty$. As it is seen from the dependence of the frequency on k_y the transition between these two values proceeds in the interval $\Delta k_y \sim 1/d$, very short in thick films. If the exchange force is included, its influence becomes significant only at $k_y^2 \gtrsim \chi$. In all experiments χ was larger than 1.

3.5.3 Surface waves propagating at an arbitrary angle to the magnetization

We will use the representation (3.15) of the vector $\mathbf{m}(x) = \mathbf{a}\cos k_x x + \mathbf{b}\sin k_x x$ and 2 relations (3.22) between different components of the amplitude vectors. In the case of purely dipolar interaction, there are only 2 independent amplitudes, by our choice a_x and b_x. They must obey the CE (3.21). The condition of their solubility requires their determinant to be zero. It gives the following equation:

$$[k_\parallel^2 A_y^2 - k_y^2(\omega^2 + B^2)] f_c f_s - k_\parallel k_y A_y B(f_c^2 - f_s^2) = 0 \tag{3.45}$$

Here we used reduced coefficients $A_{x,y} = 1 + \frac{\chi k_{x,y}^2}{k^2}$; $B = \frac{\chi k_x k_y}{k^2}$ and the functions $f_c = k_\parallel \cos\alpha - k_y \sin\alpha$; , $f_s = k_\parallel \sin\alpha + k_y \cos\alpha$; $\alpha = \frac{k_x d}{2}$ defined in the section III below eq. (3.20). Employing the secular equation $\omega^2 = A_x A_y - B^2$, it is possible to transform eq. (3.45) to the following simplified form:

$$\frac{\tan\kappa_x}{\kappa_x} = -\frac{2\kappa_\parallel \kappa_z^2}{\kappa_z^2(\kappa_\parallel^2 - \kappa_x^2) + \chi\kappa^2\kappa_y^2} \tag{3.46}$$

where $\kappa_\alpha = k_\alpha d$, $(\alpha = x, y, z)$ and $\kappa_\parallel = \sqrt{\kappa_y^2 + \kappa_z^2}$. The surface wave should have imaginary k_x and consequently imaginary κ_x. Then the function in the l.-h. side of eq. (3.46) is positive and varies from 0 to 1. Thus, this equation has solution only if its r.-h. side is positive. The denominator in the r.-h. side of the this equation can be rewritten as $\left(\kappa_z^2 - \chi\kappa_y^2\right)|\kappa_x^2| + \kappa_\parallel^2\left(\kappa_z^2 + \chi\kappa_y^2\right)$. For

existence of solution this expression must be negative. This condition is satisfied only if

$$\tan\theta \equiv \frac{k_y}{k_z} \geq \frac{1}{\sqrt{\chi}} \tag{3.47}$$

Thus, at $\theta < \theta_c = \arctan\frac{1}{\sqrt{\chi}}$ the surface wave does not exist. In the interval $\theta_c \leq \theta \leq \frac{\pi}{2}$ the surface wave exists since the fraction in the r.-h. side of eq. (3.46) in this interval varies between 0 at $\kappa_x \to \infty$ and $-\infty$ at $|\kappa_x| = \kappa_\parallel\sqrt{\frac{\chi\tan^2\theta+1}{\chi\tan^2\theta-1}}$.

At a fixed θ and $\kappa_\parallel \to 0$, the solution of eq. (3.46) approaches zero as $|\kappa_x| \simeq \sqrt{\frac{2\kappa_\parallel}{\chi\tan^2\theta-1}}$. At $\kappa_\parallel \to \infty$, the solution asymptotically grows as $|\kappa_x| \simeq \kappa_\parallel\frac{\chi\tan^2\theta+1}{\chi\tan^2\theta-1}$. The corresponding values of frequency are $\omega = \sqrt{1+\chi}$ at $\kappa_\parallel = 0$, and $\omega = \sqrt{1+\chi+\frac{\cos^2\theta(\chi\tan^2\theta-1)^2}{4\tan^2\theta}}$ at $\kappa_\parallel = \infty$. At $\theta = \frac{\pi}{2}$, the frequency at large $\kappa_\parallel$ takes value $\omega = 1+\frac{\chi}{2}$. This result was already obtained in the previous subsection. In terms of the wave vector the transition from the long-wave to the short-wave asymptotics of the spectrum proceeds in the interval $\kappa_\parallel \sim 1/d$.

3.5.4 Surface waves with exchange interaction

In thick films $d \gg 1$, the exchange interaction is very small in comparison to dipolar interaction in the interval $\kappa_\parallel \sim 1/d$. Though in thick films the surface wave exists in a longer interval $\kappa_\parallel \ll 1$, it is difficult to distinguish its dispersion from that of a standard mode considered in section IV. Thus, the surface wave can be observed, but with some complications. As we know, the TDM for each mode is a superposition of three waves (see eq. (3.15)). Two of them are evanescent waves, but only one of the evanescent waves has a small imaginary k_x. The second one has all components of the wave vector of the order of unity. It is substantial for the EBC, but can be neglected in the CE. Apart of the evanescent waves, the wave with positive square of wave vector k_1^2 takes part in superposition. An analysis shows that $x-$component of this vector k_{1x} is also positive. This component is quantized by the set of EBC and CE. In the range of weak exchange interaction $\kappa_\parallel \ll 1$ and $\theta > \theta_c$, the dipolar interaction is dominant and the exchange interaction can be considered as a perturbation. Its influence is small everywhere except of vicinity of levels crossing, where the exchange interaction is responsible for the repulsion of purely dipolar levels.

Thus, at $\kappa_{\|} \ll 1$, each level of the complete Hamiltonian (with dipolar and exchange interaction included) consists of two or more pieces of different dipolar levels connected by pieces of the dipolar surface wave. Fig. 3.2 (a) demonstrates these combined levels. This peculiarity is clearly seen only at $\kappa_{\|} \sim 1/d$. The exchange interaction starting with $k \gtrsim 1$ becomes comparable or exceeding the dipolar one and makes the surface mode not distinguishable. In thin films $d \lesssim 1$ the exchange interaction is comparable with the dipolar or bigger than it already at $k \sim 1/d$. Therefore in a thin film no surface wave can be found.

3.6 Direct evidence of spatial stability of Bose-Einstein condensate of magnons

The discovery of the room-temperature magnon Bose-Einstein condensation (BEC) in yttrium-iron garnet (YIG) films driven by parametric pumping[27] has spurred intense experimental and theoretical studies of this phenomenon [35, 3, 36, 13, 37, 5, 38, 39, 31, 40, 41] and opened a new field in modern magnetism: room temperature quantum magnonics. The formation of magnon BEC is driven by the parametric pumping that has been experimentally confirmed by the observation of the spontaneous narrowing of the population function in the energy[27, 3, 39] and the phase space[36]. Moreover, the spontaneous coherence of this state has been proven by the observation of interference between two condensates in the real space, as well as by the observation of the formation of quantized vortices[31].

Despite of all these experimental observations, from the theoretical point of view, the possibility of magnon BEC is still questioned because of the issues associated with the condensate stability [18]. It is generally believed that the formation of a stable Bose-Einstein condensate is possible only if the particle scattering length a proportional to the inter-particle interaction coefficient g is positive (the so-called repulsive particle interaction) [42, 43]. Otherwise, the condensate is expected to collapse[44, 45]. However, the established theories of magnon-magnon interactions in unconfined ferromagnets [46, 47, 48, 49] with uniaxial anisotropy predict an attractive interaction between magnons, which was confirmed experimentally by numerous studies of magnetic solitons in films with weak in-plane [50, 51, 52] and strong out-of-plane [53, 54] anisotropy. The problem of interactions becomes particularly complex for magnons existing in in-plane magnetized films in

the vicinity of the lowest-energy state, where the BEC is formed, since the conventional interaction mechanisms originating from the dipolar shape anisotropy weaken strongly in this spectral part and other mechanisms, such as the interaction between condensed and non-condensed magnons [40, 55] can become dominant. Up to now, the clear understanding of these issues was missing resulting in a deep contradiction between the experiments demonstrating the possibility of stable magnon BEC and the theory predicting its collapse.

Here, the Demokritov' group provide a direct experimental evidence of stability of magnon BEC and the repulsive character of magnon-magnon interaction in the vicinity of the lowest-energy spectral state and its theoretical explanation are presented. By using a confining potential, they create a strong local disturbance of the condensate density and study the spatio-temporal dynamics of BEC. Their experimental data clearly show that, despite the artificially created strong local increase of the condensate density expected to stimulate the collapse process, no collapse occurs. On the contrary, the observed behaviors indicate that magnons forming the condensate experience repulsive interaction, which counteracts an accumulation of magnons in a particular spatial location. These conclusions are well supported by our calculations using a model based on the Gross-Pitaevskii equation. We also propose a mechanism, which is likely responsible for the observed repulsive interaction. We show that the effective magnon repulsion can be associated with the influence of additional dipolar magnetic fields appearing in response to any local increase of the condensate density. This interpretation is well supported by the quantitative analysis of the experimental data. Our findings resolve the long-standing question of stability of magnon condensates.

3.6.1 Studied system and experimental approach

The Demokritov' group studied the spatio-temporal dynamics of room-temperature magnon BEC in a YIG film using the experimental setup similar to that used in[40, 56]. The schematic of the experiment is illustrated in Fig. 3.11a, b. The condensate in YIG film with the thickness of 5.1 μm and the lateral dimensions of 2 $\times$ 2 mm is created by a microwave parametric pumping using a dielectric resonator with the resonant frequency of fp = 9.055 GHz. The pumping injects

primary magnons at the frequency of fp/2, which thermalize and create the BEC in the lowest-energy spectral state [27, 35]. The frequency of BEC is determined by the magnitude of the static magnetic field H_0, which was varied in the range 0.5-1.5 kOe. The representative data obtained at H_0 = 0.64 kOe corresponding to the BEC frequency of 1.9 GHz and the wavelength of about 1 μm. To study the spatial stability of the condensate, they use a confining potential, which is created by using an additional spatially inhomogeneous magnetic field ΔH induced by a dc electric flowing in a control strip line with the width of 10 μm (Fig. 3.11c). They study the condensate density n and, in particular, its spatial(Fig.3.12) and temporal (Fig.3.13) variation using microfocus Brillouin light scattering (BLS) technique. In stationary-regime experiments, both the pumping and the inhomogeneous field are applied continuously. Additionally, to investigate the temporal dynamics of the condensate, they perform experiments, where the pumping is applied in the form of pulses with the duration of 1 μs and the repetition period of 10 μs and the BLS signal was recorded as a function of the time delay with respect to the falling edge of the pumping pulse.

3.6.2 Theoretical description

If the interaction between magnons were attractive, the overall reduction of the condensate density would result in a spatial broadening of the density peak. In contrast, the data of Fig.3.13 show opposite behaviors: after the pumping is turned off, the density distribution $n(z)$ starts to narrow, thus the interaction is repulsive.

The BEC can be descried by the so called Gross-Pitaevskii equation.

$$i\hbar\frac{\partial\psi}{\partial t} = (-\frac{\hbar^2}{2m}\nabla^2 + u(x) + g|\psi|^2)\psi \tag{3.48}$$

Using the Madelung transform: $\psi = \sqrt{n}e^{i\phi}$, separating the real and the imaginary parts, we have

$$\frac{\partial n}{\partial t} = -\frac{\partial(nv)}{\partial z} \tag{3.49}$$

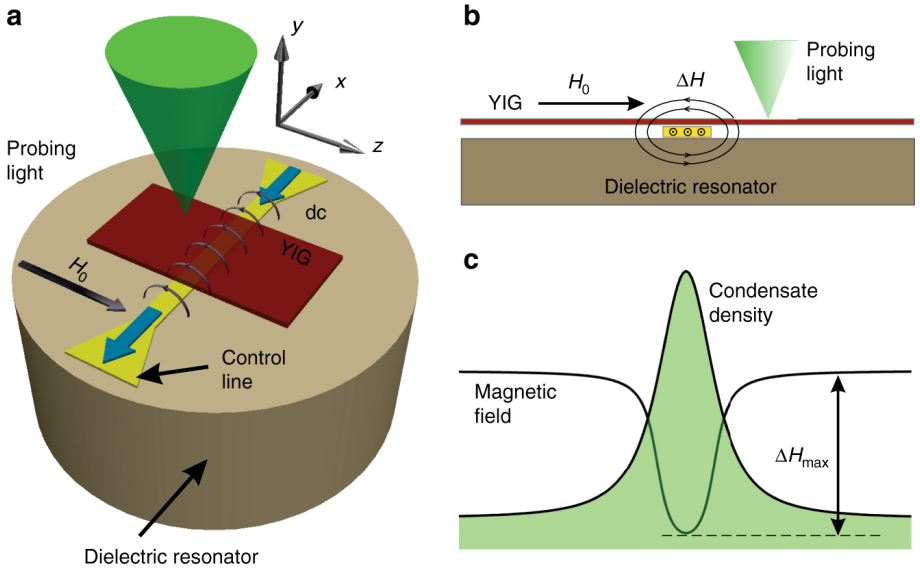

Figure 3.11: Schematic of the experiment.a General view of the experimental system. a) Dielectric resonator creates a microwave-frequency magnetic field, which parametrically excites primary magnons in the YIG film. After thermalization, the magnons form a BEC in the lowest-energy spectral state. DC electric current in the control line placed between the resonator and the YIG film, produces a non-uniform magnetic field, which adds to the uniform static field H_0. The local density of condensed magnons is recorded by BLS with the probing laser light focused onto the surface of the YIG film. b) Cross-section of the experimental system illustrating the field created by the control line. c) Spatial distribution of the horizontal component of the total magnetic field $H_0 + \Delta H$ and the corresponding spatial profile of the condensate density caused by the inhomogeneity of the field.

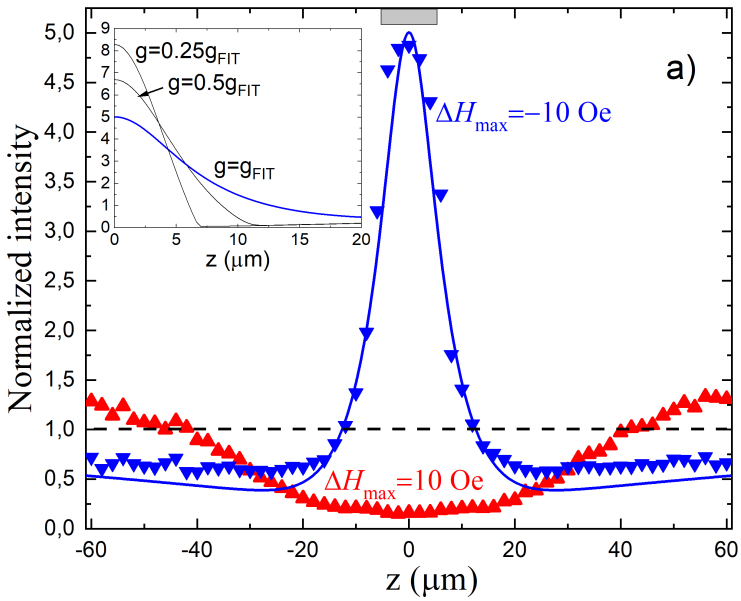

Figure 3.12: Representative profiles of the condensate density recorded by BLS for the case of a potential well (blue symbols) and a potential hill (red symbols) with the depth/height of 10 Oe. The shown profiles are normalized by the value of the density measured in the absence of the potential. The gray rectangle in the upper part marks the position of the control line creating the inhomogeneous field potential. Solid curves show the results obtained from the numerical solution of Eq. 3.49. Inset: Spatial profiles of the condensate density calculated for different magnitudes of the coefficient g describing the nonlinear magnon-magnon interaction with all other parameters fixed. The curve labeled gg = g_{FIT} is the same, as that in the main figure.

$$m\frac{dv}{dt} = -\frac{\partial}{\partial z}(u(x) + gn) \tag{3.50}$$

Taking into account pumping and decay of condensate magnons , eq. (3.49) becomes:

$$\frac{\partial n}{\partial t} = -\frac{\partial (nv)}{\partial z} - \frac{n - n_0}{\tau} \tag{3.51}$$

Taking into account dissipation. As usual for dissipative processes, one can write the connection between the effective potential $u + gn$ and drift velocity in the form:

$$v = -\eta\frac{\partial}{\partial z}(u(x) + gn) \tag{3.52}$$

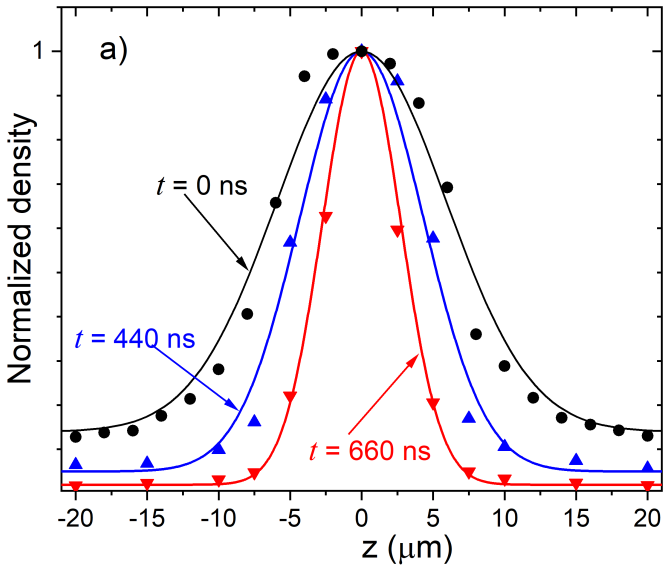

Figure 3.13: Time evolution of the condensate density in a potential well after turning the microwave pumping off. Normalized spatial profiles of the condensate density in a potential well with ΔH_{MAX}=-10 Oe recorded at different delays after the microwave pumping is turned off at t = 0. Solid lines are guides for the eye.

where η is the mobility of the condensate, defined by the momentum relaxation processes.

After substitution of Eq. (3.52) into Eq. (3.51), one obtains for the stationary case $\frac{\partial n}{\partial t} = 0$ the final non-linear second-order differential equation for the condensate density n:

$$\eta \nabla \left[n \nabla \left(u + gn \right) \right] = -\frac{n_0 - n}{\tau} \tag{3.53}$$

where $u = g_e \mu_B h$, using boundary conditions of n and shooting method, $g = 3 \times 10^{-39}$erg cm^3. Since g is positive, it means the interaction between magnons is repulsive.

If we use $u_{extra} = g_e \mu_B h_{extra}$ instead of gn.

$$h_{extra} = \nabla \phi; \ \phi \left(x, z \right) = \nabla_\perp \cdot \int_V dV' \frac{\mathbf{m}'}{|\mathbf{r} - \mathbf{r}'|} \tag{3.54}$$

Magnetization of extra magnons is associated with their density by relation:$\mathbf{m} = -g \mu_B n_{extra} \hat{\mathbf{z}}$

with $n_{extra} = n(z) - n_0$.

$$h_{extra} = 4\pi g_e \mu_B n_{extra}(z) - 2g\mu_B \int_{-\infty}^{\infty} \frac{d}{(z-z')^2 + \left(\frac{d}{2}\right)^2} n_{extra}(z')\, dz' \approx 4\pi g_e \mu_B n_{extra}(z) \tag{3.55}$$

Using $\mu_B = 9.3 \times 10^{-21}$ erg*G^{-1}, we get $u_{extra} = 4.3 * 10^{-39} * n_{extra} \approx gn$.
We conclude that the origin of this stability is the effective repulsive magnon-magnon interaction having a magneto-dipolar nature.

The concept of a resistive flow in a coherent condensate albeit being counter-intuitive inevitably follows from the experimental data supported by numerical calculations in the framework of simplified model. However, from this model it is not obvious what is the reason for gigantic enhancement or response. Here we issue estimates based on equations of motion and simple physical arguments that explains these reasons. Due to symmetry of problem it is obvious that density $n(z) = n_0\nu(z)$is the even function of z. Then eq. (3.49) in stationary regime shows that the current $j = n\nu$ is the odd function. Thus, $j = 0$ at$z = 0$, whereas $\frac{dj}{dz} = -\frac{n_0}{\tau}(\nu_{max} - 1)$. Since $\frac{dj}{dz}|_{z=0} < 0$ the current at $z > 0$ becomes negative and grows by absolute value. It reaches its minimal value j_{min} at a point with coordinate $z_1 \sim l$ ($1.16l$ in experimental curve) in which $\nu = 1$. It is possible to estimate the minimal current as $j_{min} = -\frac{n_0 z_1}{\tau}(0.66\nu_{max} - 1)$. Right of this point the derivative $\frac{dj}{dz}$ becomes positive and current eventually decreases by modulus and asymptotically vanishes. Parallel to this process $\nu(z)$ first decreases, reaches a positive minimum at some point $z_2 > z_1$ and asymptotically reaches value 1. Let assume that as even function, $1 - \nu(z)$ asymptotically behaves as $(\frac{l}{z})^2$. At sufficiently large $z = Z$, interaction amplitude that is of the order $-\mu_B^2(1-\nu)$ becomes comparable to intrinsic interaction amplitude $g_0 - \mu_B^2 \frac{\ell}{d}$, where d denotes the thickness of sample and ℓ is the correlation length in the homogeneous magnet equilibrium magnet (about 40 nm in YIG). This definition implies $Z \sim l^{3/2}/\ell^{1/2}$. However, this length is not sufficient for complete compensation of minimal current. The recovery length necessary to compensate it is $L_{rec} \sim \frac{|j_m in|}{Z - z_1} \int_{z_1}^{Z} (dj/dz)^{-1} dz$. This equation and previous estimates imply $L_{rec} \sim (0.66\nu_{max} - 1)\frac{l^2}{3\ell} \gg l$. With the experimental data it gives $L_{rec} \sim 15l = 150\mu m$. If

$L_{rec} < L$, where L is the length of condensate, this consideration does not give any lower limit for ν_{max}. In opposite situation such a lower boundary reads: $\nu_{max} \geq 1.5(\frac{3L\ell}{l^2} + 1)$ Note that this constraint contains only geometrical scales and therefore does not depend neither of the amplitude ΔH_{max} of nonuniform magnetic field nor of pumping intensity. It explains why it is much larger than $|\Delta H_{max}|/H_0$. It also explains why in the experiment saturates at further increase of ΔH_{max}. An alternative clue to the explanation of gigantic response is the fact that effective potential well in reality is very deep $|\Delta H_{max}| \gg \mu_B^2 n_0$. The extra magnons fills this potential well until their repulsion energy $4\mu_B^2 n_{extra}$ compensates their energy in potential well $2\mu_B \Delta H_{max}$. From this requirement we find $n_{extra} \sim n_0 |\Delta H_{max}|/(2\mu_B) \gg n_0$. This extremely intensive accumulation of magnons in the potential well explains gigantic response. No such accumulation proceedss in the case of potential barrier. In this case the density in minimum is exponentially small being controlled by quantum tunneling process. But outside of potential barrier the density relaxes to $\nu = 1$ on the scale $\sim l$.

In the geometry of this experiment, the reason for repulsion is the strong enhancement of magnon density inside the artificially prepared potential well for magnons. However, experiments show that even without this trap for magnons the homogeneous condensate in YIG subject to permanent pumping is stable. It means that in the stationary state under pumping the magnons repulse each other, whereas according to quasiequilibrium theory [5] they attract each other. Though this controversy is not yet completely resolved, the very fact of it shows that the quasiequilibrium state presumably is not realized. Just now we work on kinetic theory of stationary state to elucidate the reason of this phenomenon and to find what state is realized.

Another unexpected fact is extremely high mobility that was found as a fitting parameter from comparison of theoretical curve with experiment. this value of mobility corresponds to relaxation (decoherence) time $\tau \sim 1\mu$s, about 1000 times more than relaxation time for magnons inside the trap. We consider this very high value of relaxation time as a precursor of superfuidity. Indeed, the value of mobility is an average over a long interval of distance from the center of trap that is required to compensate initial very large dissipative current. On the overwhelming part of this

interval $L \gg w$, where w is the width of the trap,the density is close to the stationary homogeneous density n_0 . At homogenous $n = n_0$ the system is expected to be supefluid with infinite length and time of decoherence. Therefore, τ indeed should be rather high.

3.7 Conclusions

Our combined approach has simplified the exact solution of Landau-Lifshitz equations for geometry of an infinite film. As a result we have found many features of the solution that were not found earlier. We considered the group of symmetries for solutions that allows their classification. We studied not only the properties of thick, but also thin films which are most important for their possible technological applications. We also studied quantization of transverse motion for the ultrathin limit and have discovered that there is a big gap in the spectrum in this limit, and only the lowest mode has the transverse wave vector and frequency that do not depend on thickness. The motion of the minimum of frequency (energy) which is very important for the problem of Bose-Einstein-condensation and superfluidity of magnons was analyzed. In particular we have found the upper limit for the wave vector at the energy minimum reachable by reducing of the film thickness to 15-30 nm. The wavelength corresponding to this maximal wave vector limits the miniaturization of devices in which the information is transferred by non-linear localized magnetization waves.

Our theoretical model together with the experimental resultes the provide a direct evidence that the magnon BEC in YIG films is intrinsically stable with respect to the collapse in the real space. We show that the effective magnon repulsion can be associated with the influence of additional dipolar magnetic fields appearing in response to any local increase of the condensate density.

In the previous chapter, our main interest was focus on the energy spectrum and TDM of magnons. Now our interest transfers to other aspects of BEC, e.g. the coherence of two condensates and the relaxation time of condensed magnons.

In this chapter we use a classical representation for the Landau-Lifshitz equation, the energy spectrum of magnons is studied. Also, we apply this theory to get the exact phase diagram for different values of thickness d and magnetic field H and relaxation time of condensed magnons.

We assume the film to be isotropic in the film plane, and the external magnetic H and the spontaneous magnetization M to be oriented in-plane.

4.1 Hamiltonian formulation of the Landau-Lifshitz equation and amplitude representation

Landau-Lifshitz (LL) equation can be formulated as Hamilton equations for the magnetization $\mathbf{M}(\mathbf{r})$:

$$\frac{\partial \mathbf{M}}{\partial t} = \{H, \mathbf{M}\}, \tag{4.1}$$

where $\{A, B\}$ denotes Poisson brackets and H is the Hamiltonian containing exchange, dipolar and Zeeman energy:

$$H = H_{ex} + H_Z + H_d \tag{4.2}$$

$$H_{ex} = \frac{D}{2} \int (\nabla \mathbf{M})^2 \, dV \tag{4.3}$$

$$H_Z = -\mathcal{H} \int M_z \, dV \tag{4.4}$$

$$H_d = \frac{1}{2} \iint (\mathbf{M}\nabla)(\mathbf{M}'\nabla') \frac{1}{|\mathbf{r} - \mathbf{r}'|} dV dV' \tag{4.5}$$

In the last equation prime denotes dependence on $\mathbf{r}'$. The magnetization vector has the following Poisson brackets:

$$\{M_\alpha(\mathbf{r}), M_\beta(\mathbf{r}')\} = \gamma \delta(\mathbf{r} - \mathbf{r}') \epsilon_{\alpha\beta\gamma} M_\gamma(\mathbf{r}) \tag{4.6}$$

In eq. (4.6) $\gamma \equiv \frac{ge}{2mc}$ is classical gyromagnetic ratio.

LL equation is valid in the long-wave low-energy limit when spin-orbit, dipolar and Zeeman interactions are weak on the short length-scale compared to exchange interaction and when relaxation of the modulus of magnetization is much faster than the relaxation of transverse motion of magnetization. LL equation works under assumption that the modulus of magnetization M is conserved. It works well in the long-wave limit with precision controlled by small values a/λ and $\omega\tau_M$, where a is the lattice constant (1nm in YIG), λ is the magnon wavelength, ω is the magnon frequency and τ_M is the relaxation time of magnetization modulus. All phenomena in this limit are dominantly classical since the number of magnons in a volume with linear size of the order of λ is large and the quantization of their numbers can be neglected.

The amplitude function $\psi(\mathbf{r})$ is determined by the following relations:

$$M_z(\mathbf{r}) = M - \gamma\psi(\mathbf{r})\psi^*(\mathbf{r}) \tag{4.7}$$

$$M_+(\mathbf{r}) \equiv M_x(\mathbf{r}) + iM_y(\mathbf{r}) = \sqrt{\gamma}\psi(\mathbf{r})\sqrt{2M - \gamma\psi(\mathbf{r})\psi^*(\mathbf{r})} \tag{4.8}$$

This is a classical modification of the Holstein-Primakoff transformation. The Poisson brackets for amplitudes are:

$$\{\psi(\mathbf{r}), \psi^*(\mathbf{r}')\} = -i\delta(\mathbf{r} - \mathbf{r}') \tag{4.9}$$

Other Poisson brackets of the type $\{\psi(\mathbf{r}), \psi(\mathbf{r}')\}$ and $\{\psi^*(\mathbf{r}), \psi^*(\mathbf{r}')\}$ are equal to zero. As it follows from eq. (4.7), the square of the amplitude modulus $|\psi(\mathbf{r})|^2$ is the density of angular (spin) momentum carried by magnons. In the simplest situation it coincides with the density of magnons multiplied by Planck constant $\hbar$. Unlike in quantum mechanics the order of factors in terms is not substatantial. However, the Poisson brackets $\{A, B\}$ changes sign on permutation of values A and B.

In terms of amplitude the Hamiltonians (4.3,4.4,4.5) read:

$$H_{ex} = \frac{\gamma^2 D}{2} \int \left(\nabla \left(|\psi|^2\right)\right)^2 dV + \frac{\gamma D}{2} \int \left| \nabla \left(\psi \sqrt{2M - \gamma \left|\psi \left(\mathbf{r}\right)\right|^2} \right) \right|^2 dV \tag{4.10}$$

$$H_z = \gamma \mathcal{H} \int \left|\psi \left(\mathbf{r}\right)\right|^2 dV \tag{4.11}$$

$$H_d = \frac{1}{2} \iint \hat{\Omega} \left(\mathbf{r}\right) \hat{\Omega} \left(\mathbf{r}'\right) \frac{dV dV'}{\left|\mathbf{r} - \mathbf{r}'\right|} \tag{4.12}$$

where

$$\hat{\Omega} \left(\mathbf{r}\right) = \left(M - \gamma \left|\psi\right|^2\right) \partial_z + \frac{\sqrt{\gamma \left(2M - \gamma \left|\psi\right|^2\right)}}{2} \left(\psi \partial_- + \psi^* \partial_+\right)$$

In eq. (4.12) we omitted for brevity arguments in functions denoting $\psi \equiv \psi \left(\mathbf{r}\right)$, $\psi' \equiv \psi \left(\mathbf{r}'\right)$ and $\partial_\pm \equiv \partial_x \pm i\partial_y$; $\partial'_\pm \equiv \partial_{x'} \pm i\partial_{y'}$.

4.2 Quadratic Hamiltonian and its diagonalization

Quadratic in ψ and ψ^*part of the Hamiltonian is:

$$H_2 = H_{ex2} + H_{Z2} + H_{d2} \tag{4.13}$$

$$H_{ex2} = \gamma M D \int \left|\nabla \psi\right|^2 dV \tag{4.14}$$

$$H_{Z2} = \gamma \mathcal{H} \int \left|\psi\right|^2 dV \tag{4.15}$$

$$H_{dip2} = \frac{\gamma M}{4} \iint \frac{\left(\psi \partial_- + \psi^* \partial_+\right) \left(\psi' \partial'_- + \psi'^* \partial'_+\right)}{\left|\mathbf{r} - \mathbf{r}'\right|} dV dV' \tag{4.16}$$

The first step of diagonalization is the Fourier transformation with respect to in-plane variables y and z:

$$\psi \left(\mathbf{r}\right) = \sum_{\mathbf{q}} \chi_{\mathbf{q}} \left(x\right) \frac{e^{i\mathbf{q}\mathbf{r}}}{\sqrt{A}}, \tag{4.17}$$

where $\mathbf{q} = q_y\hat{y} + q_z\hat{z}$ is in-plane wave vector; x is a coordinate perpendicular to the plane of the film and A is the area of the plane surface. Inverse Fourier transformation reads:

$$\chi_{\mathbf{q}}(x) = \frac{1}{\sqrt{A}} \iint_{-\infty}^{\infty} \psi(\mathbf{r})\, e^{-i\mathbf{q}\mathbf{r}} dydz \tag{4.18}$$

Employing Poisson brackets for $\psi(\mathbf{r})$ eq. (4.9), it is straightforward to find Poisson brackets for amplitudes $\chi_{\mathbf{q}}(x)$:

$$\left\{\chi_{\mathbf{q}}(x), \chi^*_{\mathbf{q}'}(x')\right\} = -i\delta_{\mathbf{q}\mathbf{q}'}\delta(x - x') \tag{4.19}$$

In terms of variables $\chi_{\mathbf{q}}(x)$ the three parts of the Hamiltonian read:

$$H_{ex2} = \gamma M D \sum_{\mathbf{q}} \int_{-d/2}^{d/2} \left(\left| \frac{d\chi_{\mathbf{q}}}{dx} \right|^2 + \mathbf{q^2} \left|\chi_{\mathbf{q}}\right|^2 \right) dx \tag{4.20}$$

$$H_{Z2} = \gamma \mathcal{H} \sum_{\mathbf{q}} \int_{-d/2}^{d/2} |\chi_{\mathbf{q}}|^2 dx \tag{4.21}$$

$$\begin{aligned} H_{d2} \quad &= \pi M \gamma \sum_{\mathbf{q}} \iint_{-\frac{d}{2}}^{\frac{d}{2}} dx dx' \left[\chi_{\mathbf{q}}(d_x - q_y) + \chi^*_{-\mathbf{q}}(d_x + q_y)\right] \\ &\left[\chi'_{-\mathbf{q}}(d_{x'} + q_y) + \chi'^*_{\mathbf{q}}(d_{x'} - q_y)\right] G_q(x - x') \end{aligned} \tag{4.22}$$

In the last equation $G(x)$ is the Green function of 1d Helmholtz equation:

$$G_q(x) = \frac{e^{-q|x|}}{2q} \tag{4.23}$$

It obeys equation:

$$\left(d_x^2 - q^2\right) G_q(x) = -\delta(x) \tag{4.24}$$

The diagonalization of the Hamiltonian can be performed by Bogoliubov $u - v$ transformation.

Let define an eigen-vectors amplitudes:$\eta_{\mathbf{q}n}$ by the following canonical transformation:

$$\eta_{\mathbf{q}n} = \int\limits_{-d/2}^{d/2} \left[u_{\mathbf{q}n}(x)\, \chi_{\mathbf{q}}(x) + v_{\mathbf{q}n}(x)\, \chi^*_{-\mathbf{q}}(x) \right] dx \tag{4.25}$$

To be canonical this transformation must imply correct Poisson bracket for variables η:

$$\left\{ \eta_{\mathbf{q}n}, \eta^*_{\mathbf{q}'n'} \right\} = -i\delta_{\mathbf{q}\mathbf{q}'}\delta_{nn'} \tag{4.26}$$

Generalized canonicity (unitarity) condition for Bogoliubov transformation states:

$$\int\limits_{-d/2}^{d/2} \left[u_{\mathbf{q}n}(x)\, u^*_{\mathbf{q}n'}(x) - v_{\mathbf{q}n}(x)\, v^*_{\mathbf{q}n'}(x) \right] dx = \delta_{nn'} \tag{4.27}$$

Inverse transformation must have a form:

$$\chi_{\mathbf{q}}(x) = \sum_n \left(U_{\mathbf{q}n}(x)\, \eta_{\mathbf{q}n} + V_{\mathbf{q}n}(x)\, \eta^*_{-\mathbf{q}n} \right) \tag{4.28}$$

Replacing the amplitudes $\eta_{\mathbf{q}n}, \eta_{-\mathbf{q}n}$in eq. (4.28) by their Bogoliubov representation (4.25), we arrive at equations relating direct and inverse Bogolyubov transformations:

$$\begin{aligned} \sum_n \left(U_{\mathbf{q}n}(x)\, u_{\mathbf{q}n}(x') + V_{\mathbf{q}n}(x)\, v^*_{-\mathbf{q}n}(x') \right) &= \delta(x - x') \\ \sum_n \left(U_{\mathbf{q}n}(x)\, v_{\mathbf{q}n}(x') + V_{\mathbf{q}n}(x)\, u^*_{-\mathbf{q}n}(x') \right) &= 0 \end{aligned} \tag{4.29}$$

On the other hand the requirement of unitarity inverse Bogoliubov transformation reads:

$$\sum_n \left(U_{\mathbf{q}n}(x)\, U^*_{\mathbf{q}n}(x') - V_{\mathbf{q}n}(x)\, V^*_{\mathbf{q}n}(x') \right) = \delta(x - x') \tag{4.30}$$

Comparing this equation with the first eq. (4.29), we arrive at conclusion that $U_{\mathbf{q}n}(x) = u^*_{\mathbf{q}n}(x)$

and $V_{\mathbf{q}n}(x) = -v_{-\mathbf{q}n}(x)$. Thus, the inverse Bogolyubov transformation reads:

$$\chi_{\mathbf{q}}(x) = \sum_n \left(u^*_{\mathbf{q}n}(x)\, \eta_{\mathbf{q}n} - v_{-\mathbf{q}n}(x)\, \eta^*_{-\mathbf{q}n} \right) \tag{4.31}$$

In addition we find dual unitarity condition:

$$\sum_n \left(u^*_{\mathbf{q}n}(x)\, u_{\mathbf{q}n}(x') - v_{-\mathbf{q}n}(x)\, v^*_{-\mathbf{q}n}(x') \right) = \delta(x - x') \tag{4.32}$$

Amplitudes $\eta_{\mathbf{q}n}$ must be eigenvectors of the Hamiltonian, i.e.:

$$\{H, \eta_{\mathbf{q}n}\} = i\omega_{\mathbf{q}n}\eta_{\mathbf{q}n} \tag{4.33}$$

where frequencies $\omega_{\mathbf{q}n}$of corresponding modes are eigenvalues of this operator. Employing equations (4.13,4.20,4.21,4.22) for the Hamiltonian and Poisson brackets (4.19) for variables $\chi_{\mathbf{q}}(x)$, we arrive at following equations for the Bogoliubov transformation functions (we omit subscript n):

$$\begin{aligned}
\left[\omega - \gamma\left(\mathcal{H}{+}MD\left(q^2 - d_x^2\right)\right)\right] u_{\mathbf{q}}(x) &= 2\pi\gamma M\left[\left(q_y^2 - d_x^2\right)\zeta_u + \left(q_y - d_x\right)^2 \zeta_v\right], \\
\left[\omega + \gamma\left(\mathcal{H}{+}MD\left(q^2 - d_x^2\right)\right)\right] v_{\mathbf{q}}(x) &= -2\pi\gamma M\left[\left(q_y^2 - d_x^2\right)\zeta_v + \left(q_y + d_x\right)^2 \zeta_u\right].
\end{aligned} \tag{4.34}$$

Here the variables $\zeta_{u,v}$ are defined as integrals:

$$\begin{aligned}
\zeta_u(x) &= \int_{-d/2}^{d/2} G(x - x')\, u_{\mathbf{q}}(x')\, dx'; \\
\zeta_v(x) &= \int_{-d/2}^{d/2} G(x - x')\, v_{\mathbf{q}}(x')\, dx
\end{aligned} \tag{4.35}$$

Thus, Bogoliubov transformation functions obey a system (4.34) of integral-differential equations. However, due to relation (4.24) they can be reduced to a system of ordinary differential equations.

Indeed, application of the operator $q^2 - d_x^2$ to both parts of eqs. (4.34) turns them into linear homogeneous differential equations with constant coefficients. Therefore their solutions must be a superposition of exponents of the type $e^{i\kappa x}$ with κ being roots of the secular polynomial. To find this polynomial, it is convenient to introduce notation $k^2 \equiv q^2 + \kappa^2$ and vector $\mathbf{k}$ with components $k_x = |\kappa|$, $k_{y,z} = q_{y,z}$. In terms of these notations the ansatz $u_{\mathbf{q}}(x) = ue^{i\kappa x}$; $v_{\mathbf{q}}(x) = ve^{i\kappa x}$ together with application of the operator $q^2 - d_x^2$ to both parts of eqs. (4.34) turns them into the following system of linear equations for coefficients u and v:

$$\begin{aligned} &\left[\left(\omega - \gamma\left(\mathcal{H} + MDk^2\right)\right)k^2 - 2\pi\gamma M\left(k_x^2 + k_y^2\right)\right]u + 2\pi\gamma M\left(k_x + ik_y\right)^2 v = 0, \\ &-2\pi\gamma M\left(k_x - ik_y\right)^2 u + \left[\left(\omega + \gamma\left(\mathcal{H} + MDk^2\right)\right)k^2 + 2\pi\gamma M\left(k_x^2 + k_y^2\right)\right]v = 0. \end{aligned} \tag{4.36}$$

Condition of solvability for these equations reads:

$$\omega^2 k^2 = \gamma^2\left(\mathcal{H} + MDk^2\right)\left[\left(\mathcal{H} + MDk^2\right)k^2 + 4\pi M\left(k^2 - k_z^2\right)\right] \tag{4.37}$$

This equation can be interpreted as the dispersion relation for magnons:

$$\omega = \gamma\sqrt{\left(\mathcal{H} + MDk^2\right)\left(\mathcal{H} + MDk^2 + \frac{4\pi M\left(k_x^2 + k_y^2\right)}{k^2}\right)} \tag{4.38}$$

It does not depend of thickness of the film, i.e. it is the same as in the bulk. Thickness enters only in quantization of the wave vector of transverse mode k_x that will be discussed in the next section.

At fixed parameters D,M,$\mathcal{H}$ and frequency ω, eq. (4.37) is a qubic equation for the variable k^2. Note that it does not depend explicitly not only of thickness of the film d, but also of the value k_y. Inspection of coefficients of the qubic equation shows that the product of three roots is positive, whereas their sum is negative. Therefore, there are two opportunities: i) one root k^2 is positive and two others are negative or ii) one root is positive and two others are complex conjugated with negative real part. As Sonin has found [14] at $d \gg l \equiv \sqrt{D}$ and $kl \ll 1$, the variant i is realized.

An approximate equation for poistive root is

$$k^2 = k_z^2 \frac{4\pi\gamma^2 M\mathcal{H}}{\gamma^2\mathcal{H}\left(\mathcal{H}+4\pi M\right)-\omega^2} \tag{4.39}$$

Two others negative solutions $k^2 = -\lambda_{1,2}^2$ are determined by equation:

$$\lambda_{1,2}^2 \approx \left[2\pi + \frac{\mathcal{H}}{M} \pm \sqrt{4\pi^2 + \left(\frac{\omega}{\gamma M}\right)^2}\right] l^{-2} \tag{4.40}$$

Both values $\lambda_{1,2}^2$ are positive if $\omega^2 \leq \gamma^2\mathcal{H}\left(\mathcal{H}+4\pi M\right)$. Note that when frequency approaches the value $\omega = \gamma\sqrt{\mathcal{H}\left(\mathcal{H}+4\pi M\right)}$ at $k_z \neq 0$, approximation $kl \ll 1$ becomes invalid and qubic equation must be solved. At large $\omega \gg \gamma\sqrt{\mathcal{H}\left(\mathcal{H}+4\pi M\right)}$ the exchange term dominates and $\omega \approx \gamma M D k^2$. It corresponds to the region of wave vectors $kl \gg 1$. The 4 waves of type $e^{-\lambda_{1,2}\left(\frac{d}{2}\pm x\right)}$ corrsepond to four evanescent waves that are localized in a layer of the depth $\sim l$ near surfaces $x = \pm\frac{d}{2}$ limiting the film.

4.3 Self-consistency and boundary conditions: Quantization of transverse modes

We have proved that any propagating in-plane excitation is a superposition of several transverse modes. The transverse modes may be either superposition of $\cos k_x x$ and $\sin k_x x$ or evanescent waves. However, the inverse statement that any such superposition is a solution of equations of motion is wrong. This happens because the equations of motion are integral-differential. The system of ordinary differential equationswas obtained from them by application of additional differential operators. This operation introduces additional solutions of resulting system of equations that are not solutions of initial problem. Below we derive selection rules that leave only the solutions of initial integral-differential equations (4.34).

Equations for Bogoliubov transformation functions (4.34) allow real solution. Therefore the Bogoliubov functions can be searched in the form:

$$u_{\mathbf{q}}(x) = a\cos k_x x + b\sin k_x x + \sum_{m=1,2}\left(A_m\cosh\lambda_m x + B_m\sinh\lambda_m x\right) \tag{4.41}$$

$$v_{\mathbf{q}}(x) = c\cos k_x x + d\sin k_x x + \sum_{m=1,2}\left(C_m \cosh\lambda_m x + D_m \sinh\lambda_m x\right) \tag{4.42}$$

with all coefficients in eqs. (4.41,4.42) to be real numbers. They depend on $\mathbf{q}$ and some discrete variavles that will be determined later, but we do not show this dependence for brevity. Substitution of these expressions to integral-differential equations (4.34) result in appearance of an exponential function that do not belong to 6 exponents permitted by the secular equation (4.37). They are produced by integrals (4.35). Their explicit calculation can be obtained from four basic integrals:

$$\begin{aligned} I_c &\equiv \int_{-d/2}^{d/2} \frac{e^{-q|x-x'|}}{2q}\cos k_x x' dx' \\ &= \frac{\cos k_x x}{k^2} - \frac{e^{-qd/2}}{qk^2}\cosh qx\, f_c \end{aligned} \tag{4.43}$$

$$\begin{aligned} I_s &\equiv \int_{-d/2}^{d/2} \frac{e^{-q|x-x'|}}{2q}\sin k_x x' dx' \\ &= \frac{\sin k_x x}{k^2} - \frac{e^{-qd/2}}{qk^2}\sinh qx\, f_s \end{aligned} \tag{4.44}$$

$$\begin{aligned} I_{mc} &\equiv \int_{-d/2}^{d/2} \frac{e^{-q|x-x'|}}{2q}\cosh\lambda_m x' dx' \\ &= \frac{\cosh\lambda_m x}{q^2-\lambda_m^2} - \frac{e^{-qd/2}}{q\left(q^2-\lambda_m^2\right)}\cosh qx\, f_{mc}, (m=1,2) \end{aligned} \tag{4.45}$$

$$\begin{aligned} I_{sc} &\equiv \int_{-d/2}^{d/2} \frac{e^{-q|x-x'|}}{2q}\sinh\lambda_m x' dx' \\ &= \frac{\sinh\lambda_m x}{q^2-\lambda_m^2} - \frac{e^{-qd/2}}{q\left(q^2-\lambda_m^2\right)}\sinh qx\, f_{ms}, (m=1,2) \end{aligned} \tag{4.46}$$

where we defined

$$\begin{aligned} f_c &= q\cos\frac{k_x d}{2} - k_x \sin\frac{k_x d}{2} \\ f_s &= q\sin\frac{k_x d}{2} + k_x \cos\frac{k_x d}{2} \end{aligned} \tag{4.47}$$

$$\begin{aligned} f_{mc} &= q\cosh\frac{\lambda_m d}{2} + \lambda_m \sinh\frac{\lambda_m d}{2} \\ f_{ms} &= q\sinh\frac{\lambda_m d}{2} + \lambda_m \cosh\frac{\lambda_m d}{2}, (m=1,2) \end{aligned} \tag{4.48}$$

Employing these results, it is possible to calculate $\zeta_u(x)$ and $\zeta_v(x)$.

$$\zeta_u(x) = aI_c + bI_s + \sum_{m=1,2}(A_m I_{mc} + B_m I_{ms}) \tag{4.49}$$

$$\zeta_v(x) = cI_c + dI_s + \sum_{m=1,2}(C_m I_{mc} + D_m I_{ms}) \tag{4.50}$$

Thus, terms with $\zeta_u(x)$ and $\zeta_v(x)$ in eqs. (4.34) generate extra exponents $\cosh qx$ and $\sinh qx$ that is not conteined on the list of exponents allowed by eq. (4.37). They must vanish in two equations (4.34) at a proper choice of coefficients $a, b, c, d, A_1, B_1, C_1, D_1, A_2, B_2, C_2, D_2$.

The determinant of this system and all its main minors are identically equal to zero. Thus, this system does not determine quantization. Below we will show that, if the dispersion relation (4.38) is satisfied (on the mass shell in the terminology of field theory), only six variables, for example a, b, A_1, B_1, A_2, B_2 are independent, whereas six others are their linear combinations. Determinant of system of resulting two equations is not identically equal to zero. The condition of turning it to zero determines the quantized values of k_x. With this purpose we return to the derivation of the secular equation (4.37) from equations for Bogoliubov transformation functions (4.34) plugging in the latter equations $u_{\mathbf{q}}(x) = a\cos k_x x + b\sin k_x x$ and $v_{\mathbf{q}}(x) = c\cos k_x x + d\sin k_x x$ (we use truncated equations (4.41,4.42) using the same argument about small amplitudes of evenescent waves). Assuming that the excessive evanescent waves are removed, equations (4.34) result in

a system of 4 linear homogeneous equations for coefficients a, b, c, d. The matrix of this system reads:

$$\begin{pmatrix} \omega - \mathcal{A} & 0 & -\mathcal{B} & \mathcal{C} \\ 0 & \omega - \mathcal{A} & -\mathcal{C} & -\mathcal{B} \\ \mathcal{B} & \mathcal{C} & \omega + \mathcal{A} & 0 \\ -\mathcal{C} & \mathcal{B} & 0 & \omega + \mathcal{A} \end{pmatrix}, \tag{4.51}$$

We used abbreviated notations:

$$\begin{gathered} \mathcal{A} = \gamma \left(\mathcal{H} + MDk^2 + \frac{2\pi M\left(k_x^2 + k_y^2\right)}{k^2} \right) \\ \mathcal{B} = -2\pi\gamma M \frac{k_x^2 - k_y^2}{k^2} \\ \mathcal{C} = 4\pi\gamma M \frac{k_x k_y}{k^2} \end{gathered} \tag{4.52}$$

The determinant of this matrix is:

$$\mathcal{D} = \left(\omega^2 - \mathcal{A}^2 + \mathcal{B}^2 + \mathcal{C}^2\right)^2 \tag{4.53}$$

It turns into zero at $\omega = \sqrt{\mathcal{A}^2 - \mathcal{B}^2 - \mathcal{C}^2}$ that coincides with dispersion relation (4.38). Since the determinant has doubled zero, not only itself, but also its main minors turn into zero at the mass shell. It is why only two variables are independent. Matrix (4.51) implies the following relations between c, d and a, b:

$$c = -\frac{\mathcal{B}}{\omega + \mathcal{A}} a - \frac{\mathcal{C}}{\omega + \mathcal{A}} b;\ d = \frac{\mathcal{C}}{\omega + \mathcal{A}} a - \frac{\mathcal{B}}{\omega + \mathcal{A}} b \tag{4.54}$$

Again if we consider $u_{\mathbf{q}}(x) = A_m \cosh \lambda_m x + B_m \sinh \lambda_m x$ and $v_{\mathbf{q}}(x) = C_m \cosh \lambda_m x + D_m \sinh \lambda_m x$, using the same discussion above, we can get a system of 4 linear homogeneous

equations for coefficients A_1, B_1, C_1, D_1. The matrix of this system reads:

$$\begin{pmatrix} \omega - \mathcal{A}_m & 0 & -\mathcal{B}_m & \mathcal{C}_m \\ 0 & \omega - \mathcal{A}_m & \mathcal{C}_m & -\mathcal{B}_m \\ \mathcal{B}_m & \mathcal{C}_m & \omega + \mathcal{A}_m & 0 \\ \mathcal{C}_m & \mathcal{B}_m & 0 & \omega + \mathcal{A}_m \end{pmatrix}, \tag{4.55}$$

We used abbreviated notations:

$$\begin{aligned} \mathcal{A}_m &= \gamma \left(\mathcal{H} + MD\left(q^2 - \lambda_m^2\right) + \tfrac{2\pi M\left(k_y^2 - \lambda_m^2\right)}{q^2 - \lambda_m^2} \right) \\ \mathcal{B}_m &= 2\pi\gamma M \tfrac{\lambda_m^2 + k_y^2}{q^2 - \lambda_m^2} \\ \mathcal{C}_m &= 4\pi\gamma M \tfrac{\lambda_m k_y}{q^2 - \lambda_m^2} \end{aligned} \tag{4.56}$$

The determinant of this matrix is:

$$\mathcal{D}_m = \left(\omega^2 - \mathcal{A}_m^2 + \mathcal{B}_m^2 - \mathcal{C}_m^2\right)^2 \tag{4.57}$$

It turns into zero at $\omega = \sqrt{\mathcal{A}_m^2 - \mathcal{B}_m^2 + \mathcal{C}_m^2}$ that coincides with dispersion relation (4.38). Since the determinant has doubled zero, not only itself, but also its main minors turn into zero at the mass shell. It is why only two variables are independent. Matrix (4.3) implies the following relations between C_m, D_m and A_m, B_m:

$$\begin{aligned} C_m &= -\frac{\mathcal{B}_m}{\omega + \mathcal{A}_m} A_m - \frac{\mathcal{C}_m}{\omega + \mathcal{A}_m} B_m \\ D_m &= -\frac{\mathcal{C}_m}{\omega + \mathcal{A}_m} A_m - \frac{\mathcal{B}_m}{\omega + \mathcal{A}_m} B_m \end{aligned} \tag{4.58}$$

The condition of self-consistency is determined by any equation of the system (4.34). Taking the first equation and employing expressions of $u(x)$ and $v(x)$, nullifing the extra exponents $\cosh qx$ and $\sinh qx$, we arrive at the consistency conditions.

$$
\begin{aligned}
&\left(q_y^2-q^2\right)\left(\tfrac{f_c}{k^2}a+\textstyle\sum_{m=1,2}\tfrac{f_{mc}}{q^2-\lambda_m^2}A_m\right)\\
&+\left(q_y^2+q^2\right)\left(\tfrac{f_c}{k^2}c+\textstyle\sum_{m=1,2}\tfrac{f_{mc}}{q^2-\lambda_m^2}C_m\right)\\
&-2q_yq\left(\tfrac{f_s}{k^2}d+\textstyle\sum_{m=1,2}\tfrac{f_{ms}}{q^2-\lambda_m^2}D_m\right)=0\\
&\left(q_y^2-q^2\right)\left(\tfrac{f_s}{k^2}b+\textstyle\sum_{m=1,2}\tfrac{f_{ms}}{q^2-\lambda_m^2}B_m\right)\\
&+\left(q_y^2+q^2\right)\left(\tfrac{f_s}{k^2}d+\textstyle\sum_{m=1,2}\tfrac{f_{ms}}{q^2-\lambda_m^2}D_m\right)\\
&-2q_yq\left(\tfrac{f_c}{k^2}c+\textstyle\sum_{m=1,2}\tfrac{f_{mc}}{q^2-\lambda_m^2}C_m\right)=0
\end{aligned}
$$

For the boundary condition $\frac{d}{dx}u(x)\big|_{x=\pm\frac{d}{2}}=0$, $\frac{d}{dx}v(x)\big|_{x=\pm\frac{d}{2}}=0$ Thus we get a system of 6 linear homogeneous equations for coefficients a,b,A_1,B_1,A_2,B_2. $\mathbf{A}=(a,b,A_1,B_1,A_2,B_2)^T$, $\mathbf{C}\cdot\mathbf{A}=0$ .The matrix $\mathbf{C}$ of this system reads:

$$
\begin{pmatrix}
\frac{\mathcal{M}}{k^2} & \frac{\mathcal{P}}{k^2(\omega+\mathcal{A})} & \frac{\mathcal{M}_1}{q^2-\lambda_1^2} & \frac{\mathcal{P}_1}{\left(q^2-\lambda_1^2\right)(\omega+\mathcal{A}_1)} & \frac{\mathcal{M}_2}{q^2-\lambda_2^2} & \frac{\mathcal{P}_2}{\left(q^2-\lambda_2^2\right)(\omega+\mathcal{A}_2)}\\
\frac{\mathcal{Q}}{k^2(\omega+\mathcal{A})} & \frac{\mathcal{N}}{k^2} & \frac{\mathcal{Q}_1}{\left(q^2-\lambda_1^2\right)(\omega+\mathcal{A}_1)} & \frac{\mathcal{N}_1}{q^2-\lambda_1^2} & \frac{\mathcal{Q}_2}{\left(q^2-\lambda_2^2\right)(\omega+\mathcal{A}_2)} & \frac{\mathcal{N}_2}{q^2-\lambda_2^2}\\
0 & k_x\cos\alpha & 0 & \lambda_1\cosh\beta_1 & 0 & \lambda_2\cosh\beta_2\\
-k_x\sin\alpha & 0 & \lambda_1\sinh\beta_1 & 0 & \lambda_2\sinh\beta_2 & 0\\
\frac{\mathcal{C}}{\omega+\mathcal{A}}k_x\cos\alpha & -\frac{\mathcal{B}}{\omega+\mathcal{A}}k_x\cos\alpha & -\frac{\mathcal{C}_1}{\omega+\mathcal{A}_1}\lambda_1\cosh\beta_1 & -\frac{\mathcal{B}_1}{\omega+\mathcal{A}_1}\lambda_1\cosh\beta_1 & -\frac{\mathcal{C}_2}{\omega+\mathcal{A}_2}\lambda_2\cosh\beta_2 & -\frac{\mathcal{B}_2}{\omega+\mathcal{A}_2}\lambda_2\cosh\beta_2\\
\frac{\mathcal{B}}{\omega+\mathcal{A}}k_x\sin\alpha & \frac{\mathcal{C}}{\omega+\mathcal{A}}k_x\sin\alpha & -\frac{\mathcal{B}_1}{\omega+\mathcal{A}_1}\lambda_1\sinh\beta_1 & -\frac{\mathcal{C}_1}{\omega+\mathcal{A}_1}\lambda_1\sinh\beta_1 & -\frac{\mathcal{B}_2}{\omega+\mathcal{A}_2}\lambda_2\sinh\beta_2 & -\frac{\mathcal{C}_2}{\omega+\mathcal{A}_2}\lambda_2\sinh\beta_2
\end{pmatrix}
$$

where

$$
\begin{aligned}
\mathcal{P} &= -f_c\left(q_y^2+q^2\right)\mathcal{C}+2q_yqf_s\mathcal{B}\\
\mathcal{P}_m &= -f_{mc}\left(q_y^2+q^2\right)\mathcal{C}_m+2q_yqf_{ms}\mathcal{B}_m\\
\mathcal{Q} &= f_s\left(q_y^2+q^2\right)\mathcal{C}+2q_yqf_c\mathcal{B}\\
\mathcal{Q}_m &= -f_{ms}\left(q_y^2+q^2\right)\mathcal{C}_m+2q_yqf_{mc}\mathcal{B}_m\\
\mathcal{M} &= \left[\left(q_y^2-q^2\right)-\left(q_y^2+q^2\right)\frac{\mathcal{B}}{\omega+\mathcal{A}}\right]f_c-2q_yqf_s\frac{\mathcal{C}}{\omega+\mathcal{A}}\\
\mathcal{M}_m &= \left[\left(q_y^2-q^2\right)-\left(q_y^2+q^2\right)\frac{\mathcal{B}_m}{\omega+\mathcal{A}_m}\right]f_{mc}+2q_yqf_{ms}\frac{\mathcal{C}_m}{\omega+\mathcal{A}_m}\\
\mathcal{N} &= \left[\left(q_y^2-q^2\right)-\left(q_y^2+q^2\right)\frac{\mathcal{B}}{\omega+\mathcal{A}}\right]f_s+2q_yqf_c\frac{\mathcal{C}}{\omega+\mathcal{A}}\\
\mathcal{N}_m &= \left[\left(q_y^2-q^2\right)-\left(q_y^2+q^2\right)\frac{\mathcal{B}_m}{\omega+\mathcal{A}_m}\right]f_{ms}+2q_yqf_{mc}\frac{\mathcal{C}_m}{\omega+\mathcal{A}_m}\\
\alpha &= \frac{k_xd}{2}\\
\beta_m &= \frac{\lambda_md}{2}(m=1,2)
\end{aligned}
$$

Equations $\mathbf{C}\cdot\mathbf{A}=0$ have non-zero solutions if and only if $\det\mathbf{C}=0$. Then we can get the quantized k_x and energy spectrum, this is the same result with chapter 3.

4.4 With interactions

Previously we considered only quadratic (in amplitudes) part of the Hamiltonian. Here we take into account higher order contributions, i.e. we consider interaction between magnons. In particular we will take into account terms up to 4th order. Let's recall the Hamiltonian in amplitudes:

$$H_{ex}=\frac{\gamma D}{2}\int\left[\gamma\left(\nabla\left(|\psi|^2\right)\right)^2+\left|\nabla\left(\psi\sqrt{2M-\gamma|\psi|^2}\right)\right|^2\right]dV, \tag{4.59}$$

$$H_z=\gamma\mathcal{H}\int|\psi|^2\,dV, \tag{4.60}$$

$$H_d = \frac{1}{2}\iint \left[\left(M-\gamma\left|\psi\right|^2\right)\partial_z + \frac{1}{2}\sqrt{\gamma\left(2M-\gamma\left|\psi\right|^2\right)}\left(\psi\partial_- + \psi^*\partial_+\right)\right]$$
$$\left[\left(M-\gamma\left|\psi'\right|^2\right)\partial'_z + \frac{1}{2}\sqrt{\gamma\left(2M-\gamma\left|\psi'\right|^2\right)}\left(\psi'\partial'_- + \psi'^*\partial'_+\right)\right]\frac{dVdV'}{\left|\mathbf{r}-\mathbf{r}'\right|}. \tag{4.61}$$

where $\psi \equiv \psi(\mathbf{r})$, $\psi' \equiv \psi(\mathbf{r}')$, and $\partial_\pm \equiv \partial_x \pm i\partial_y;\ \partial'_\pm \equiv \partial_{x'} \pm i\partial_{y'}$.

For the exchange energy:

$$H_{ex} = \frac{\gamma D}{2}\int\left[\gamma\left(\nabla\left(\left|\psi\right|^2\right)\right)^2 + \left|\nabla\left(\psi\sqrt{2M-\gamma\left|\psi\right|^2}\right)\right|^2\right]dV$$
$$= \frac{\gamma D}{2}\int\left[\gamma\left(\nabla\left(\left|\psi\right|^2\right)\right)^2 + \left|\sqrt{2M-\gamma\left|\psi\right|^2}\nabla\psi - \frac{\gamma\psi\nabla\left(\left|\psi\right|^2\right)}{2\sqrt{2M-\gamma\left|\psi\right|^2}}\right|^2\right]dV$$
$$= \frac{\gamma D}{2}\int\left[\gamma\left(\nabla\left(\left|\psi\right|^2\right)\right)^2 + (2M-\gamma\left|\psi\right|^2)|\nabla\psi|^2 - \frac{\gamma\left(\nabla\left(\left|\psi\right|^2\right)\right)^2}{2} + \frac{\gamma^2|\psi|^2\left(\nabla\left(\left|\psi\right|^2\right)\right)^2}{4(2M-\gamma\left|\psi\right|^2)}\right]dV$$
$$= \frac{\gamma D}{2}\int\left[2M|\nabla\psi|^2 - \gamma\left|\psi\right|^2|\nabla\psi|^2 + \frac{\gamma}{2}\left(\nabla\left(\left|\psi\right|^2\right)\right)^2 + \frac{\gamma^2|\psi|^2\left(\nabla\left(\left|\psi\right|^2\right)\right)^2}{4(2M-\gamma\left|\psi\right|^2)}\right]dV. \tag{4.62}$$

The first term is the quadratic contribution we considered earlier, the second and third terms are of 4th order, and the last term is of at least 6th order.

The Zeeman energy contains only up to quadratic terms.

For the dipolar energy:

$$
\begin{aligned}
H_d &= \frac{1}{2}\iint \left[\left(M-\gamma\left|\psi\right|^2\right)\partial_z + \frac{1}{2}\sqrt{\gamma\left(2M-\gamma\left|\psi\right|^2\right)}\left(\psi\partial_- + \psi^*\partial_+\right)\right] \\
&\left[\left(M-\gamma\left|\psi'\right|^2\right)\partial'_z + \frac{1}{2}\sqrt{\gamma\left(2M-\gamma\left|\psi'\right|^2\right)}\left(\psi'\partial'_- + \psi'^*\partial'_+\right)\right]\frac{dVdV'}{\left|\mathbf{r}-\mathbf{r}'\right|} \\
&= \frac{1}{2}\iint \left[\left(M-\gamma\left|\psi\right|^2\right)\left(M-\gamma\left|\psi'\right|^2\right)\partial_z\partial'_z\right. \\
&+\frac{\gamma}{4}\sqrt{\left(2M-\gamma\left|\psi\right|^2\right)\left(2M-\gamma\left|\psi'\right|^2\right)}\left(\psi\partial_- + \psi^*\partial_+\right)\left(\psi'\partial'_- + \psi'^*\partial'_+\right) \\
&\left.+\ \left(M-\gamma\left|\psi\right|^2\right)\sqrt{\gamma\left(2M-\gamma\left|\psi'\right|^2\right)}\partial_z\left(\psi'\partial'_- + \psi'^*\partial'_+\right)\right]\frac{dVdV'}{\left|\mathbf{r}-\mathbf{r}'\right|} \\
&= \frac{1}{2}\iint \left[\left(M-\gamma\left|\psi\right|^2\right)\left(M-\gamma\left|\psi'\right|^2\right)\partial_z\partial'_z\right. \\
&+\frac{\gamma M}{2}\left(1-\frac{\gamma}{2M}\left|\psi\right|^2\right)\left(\psi\partial_- + \psi^*\partial_+\right)\left(\psi'\partial'_- + \psi'^*\partial'_+\right) \\
&\left.+M\sqrt{2\gamma M}\left(1-\frac{\gamma}{M}\left|\psi\right|^2-\frac{\gamma}{4M}\left|\psi'\right|^2\right)\partial_z\left(\psi'\partial'_- + \psi'^*\partial'_+\right)+O(\psi^5)\right]\frac{dVdV'}{\left|\mathbf{r}-\mathbf{r}'\right|}.
\end{aligned}
\tag{4.63}
$$

Note that the third term is of odd order of the amplitudes, and so does not conserve the number of magnons. These terms are responsible for attenuation of spin waves. If we consider only interactions between condensed magnons, then due to conservation of momentum only the even order terms will contribute.

4.4.1 3rd order terms

Let's first write out the 3rd order terms of the Hamiltonian, which comes solely from the dipolar part.

$$
H_{d3} = -\frac{\gamma\sqrt{2\gamma M}}{2}\iint\left(\left|\psi\right|^2+\frac{1}{4}\left|\psi'\right|^2\right)\partial_z\left(\psi'\partial'_- + \psi'^*\partial'_+\right)\frac{dVdV'}{\left|\mathbf{r}-\mathbf{r}'\right|}. \tag{4.64}
$$

Like before, we define the Fourier transformation with respect to in-plane variables y and z:

$$
\psi\left(\mathbf{r}\right) = \sum_{\mathbf{q}}\chi_{\mathbf{q}}\left(x\right)\frac{e^{i\mathbf{q}\mathbf{r}}}{\sqrt{A}}. \tag{4.65}
$$

where $\mathbf{q} = q_y\hat{y} + q_z\hat{z}$. We also make use of the expression

$$\frac{1}{|\mathbf{r}-\mathbf{r}'|} = \frac{4\pi}{A}\sum_{\mathbf{q}} e^{i\mathbf{q}(\mathbf{r}-\mathbf{r}')} G_q\left(x-x'\right),$$
$$G_q\left(x\right) = \frac{e^{-q|x|}}{2q}. \tag{4.66}$$

Plugging the 2D-Fourier transformation into the 3rd order Hamiltonian, and using the above expression of $1/\left|\mathbf{r}-\mathbf{r}'\right|$, we get:

$$\begin{aligned}
H_{d3} &= -\frac{2\pi\gamma\sqrt{2\gamma M}}{A^{\frac{5}{2}}}\iint\sum_{\mathbf{q}_1,\mathbf{q}_2,\mathbf{q}_3,\mathbf{q}}\left(\chi_{\mathbf{q}_1}\chi^*_{\mathbf{q}_2}e^{i(\mathbf{q}_1-\mathbf{q}_2)\mathbf{r}} + \frac{1}{4}\chi'_{\mathbf{q}_1}\chi'^*_{\mathbf{q}_2}e^{i(\mathbf{q}_1-\mathbf{q}_2)\mathbf{r}'}\right)\\
&\times iq_z\left[\chi'_{\mathbf{q}_3}\left(d_{x'}-q_y\right)+\chi'^*_{-\mathbf{q}_3}\left(d_{x'}+q_y\right)\right]e^{i\mathbf{q}_3\mathbf{r}'}e^{i\mathbf{q}(\mathbf{r}-\mathbf{r}')}G_q(x-x')dVdV'\\
&= -\frac{2\pi\gamma\sqrt{2\gamma M}}{\sqrt{A}}\iint\sum_{\mathbf{q}_1,\mathbf{q}_2,\mathbf{q}_3,\mathbf{q}}\left(\chi_{\mathbf{q}_1}\chi^*_{\mathbf{q}_2}\delta_{\mathbf{q}_1-\mathbf{q}_2+\mathbf{q}}\delta_{\mathbf{q}_3-\mathbf{q}} + \frac{1}{4}\chi'_{\mathbf{q}_1}\chi'^*_{\mathbf{q}_2}\delta_{\mathbf{q}}\delta_{\mathbf{q}_1-\mathbf{q}_2+\mathbf{q}_3-\mathbf{q}}\right)\\
&\times iq_z\left[\chi'_{\mathbf{q}_3}\left(d_{x'}-q_y\right)+\chi'^*_{-\mathbf{q}_3}\left(d_{x'}+q_y\right)\right]G_q(x-x')dxdx'.
\end{aligned}\tag{4.67}$$

In the second term, the delta function gives $\mathbf{q}=0$. The factor $q_z\left[\chi'_{\mathbf{q}_3}\left(d_{x'}-q_y\right)+\chi'^*_{-\mathbf{q}_3}\left(d_{x'}+q_y\right)\right]$ is $\sim q^2$ at small q, while $G_q(x-x')$ is $\sim 1/q$, so this term should be zero. We then have

$$\begin{aligned}
H_{d3} &= -\frac{2\pi\gamma\sqrt{2\gamma M}}{\sqrt{A}}\iint\sum_{\mathbf{q}_1,\mathbf{q}_2,\mathbf{q}_3,\mathbf{q}}\chi_{\mathbf{q}_1}\chi^*_{\mathbf{q}_2}\delta_{\mathbf{q}_1-\mathbf{q}_2+\mathbf{q}}\delta_{\mathbf{q}_3-\mathbf{q}}\\
&\times iq_z\left[\chi'_{\mathbf{q}_3}\left(d_{x'}-q_y\right)+\chi'^*_{-\mathbf{q}_3}\left(d_{x'}+q_y\right)\right]G_q(x-x')dxdx'\\
&= -\frac{2\pi\gamma\sqrt{2\gamma M}}{\sqrt{A}}\iint\sum_{\mathbf{q}_1,\mathbf{q}_2,\mathbf{q}_3}\chi_{\mathbf{q}_1}\chi^*_{\mathbf{q}_2}\delta_{\mathbf{q}_1-\mathbf{q}_2+\mathbf{q}_3}\\
&\times iq_{3z}\left[\chi'_{\mathbf{q}_3}\left(d_{x'}-q_{3y}\right)+\chi'^*_{-\mathbf{q}_3}\left(d_{x'}+q_{3y}\right)\right]G_{q_3}(x-x')dxdx'.
\end{aligned}\tag{4.68}$$

Next we should put in Bogoliubov transformed functions, which is obtained when diagonalizing the quadratic Hamiltonian. It reads:

$$\chi_{\mathbf{q}}(x)=\sum_{n}\left(u_{\mathbf{q}n}^{*}(x)\,\eta_{\mathbf{q}n}-v_{-\mathbf{q}n}(x)\,\eta_{-\mathbf{q}n}^{*}\right)\equiv f_{\mathbf{q}}(x)+g_{-\mathbf{q}}^{*}(x), \tag{4.69}$$

where we defined

$$f_{\mathbf{q}}(x)=\sum_{n}u_{\mathbf{q}n}^{*}(x)\,\eta_{\mathbf{q}n},\quad g_{\mathbf{q}}(x)=-\sum_{n}v_{\mathbf{q}n}^{*}(x)\,\eta_{\mathbf{q}n} \tag{4.70}$$

Also let's recall the condition:

$$\sum_{n}\left(u_{\mathbf{q}n}^{*}(x)\,u_{\mathbf{q}n}(x')-v_{-\mathbf{q}n}(x)\,v_{-\mathbf{q}n}^{*}(x')\right)=\delta(x-x'). \tag{4.71}$$

Then

$$\begin{aligned}
H_{d3}&=-\frac{2\pi\gamma\sqrt{2\gamma M}}{\sqrt{A}}\iint\sum_{\mathbf{q}_1,\mathbf{q}_2,\mathbf{q}_3}(f_{\mathbf{q}_1}+g_{-\mathbf{q}_1}^{*})(f_{\mathbf{q}_2}^{*}+g_{-\mathbf{q}_2})\delta_{\mathbf{q}_1-\mathbf{q}_2+\mathbf{q}_3}\\
&\times iq_{3z}\left[(f_{\mathbf{q}_3}'+g_{-\mathbf{q}_3}'^{*})(d_{x'}-q_{3y})+(f_{-\mathbf{q}_3}'^{*}+g_{\mathbf{q}_3}')(d_{x'}+q_{3y})\right]G_{q_3}(x-x')dxdx'\\
&=-\frac{2\pi\gamma\sqrt{2\gamma M}}{\sqrt{A}}\iint\sum_{n_1,n_2,n_3}\sum_{\mathbf{q}_1,\mathbf{q}_2,\mathbf{q}_3}\delta_{\mathbf{q}_1-\mathbf{q}_2+\mathbf{q}_3}\\
&\times(u_{\mathbf{q}_1n_1}^{*}\eta_{\mathbf{q}_1n_1}-v_{-\mathbf{q}_1n_1}\eta_{-\mathbf{q}_1n_1}^{*})(u_{\mathbf{q}_2n_2}\eta_{\mathbf{q}_2n_2}^{*}-v_{-\mathbf{q}_2n_2}^{*}\eta_{-\mathbf{q}_2n_2})\\
&\times iq_{3z}\left[(u_{\mathbf{q}_3n_3}'^{*}\eta_{\mathbf{q}_3n_3}-v_{-\mathbf{q}_3n_3}'\eta_{-\mathbf{q}_3n_3}^{*})(d_{x'}-q_{3y})+(u_{-\mathbf{q}_3n_3}'\eta_{-\mathbf{q}_3n_3}^{*}-v_{\mathbf{q}_3n_3}'^{*}\eta_{\mathbf{q}_3n_3})(d_{x'}+q_{3y})\right]\\
&\times G_{q_3}(x-x')dxdx'\\
&=-\frac{2\pi\gamma\sqrt{2\gamma M}}{\sqrt{A}}\iint\sum_{n_1,n_2,n_3}\sum_{\mathbf{q}_1,\mathbf{q}_2,\mathbf{q}_3}\delta_{\mathbf{q}_1-\mathbf{q}_2+\mathbf{q}_3}\\
&\times(u_{\mathbf{q}_1n_1}^{*}\eta_{\mathbf{q}_1n_1}-v_{-\mathbf{q}_1n_1}\eta_{-\mathbf{q}_1n_1}^{*})(u_{\mathbf{q}_2n_2}\eta_{\mathbf{q}_2n_2}^{*}-v_{-\mathbf{q}_2n_2}^{*}\eta_{-\mathbf{q}_2n_2})\\
&\times iq_{3z}\left\{\left[u_{\mathbf{q}_3n_3}'^{*}(d_{x'}-q_{3y})-v_{\mathbf{q}_3n_3}'^{*}(d_{x'}+q_{3y})\right]\eta_{\mathbf{q}_3n_3}+\left[u_{-\mathbf{q}_3n_3}'(d_{x'}+q_{3y})-v_{-\mathbf{q}_3n_3}'(d_{x'}-q_{3y})\right]\eta_{-\mathbf{q}_3n_3}^{*}\right\}\\
&\times G_{q_3}(x-x')dxdx'.
\end{aligned} \tag{4.72}$$

Writing contributions to each term with different factors of η separately, we get:

$$
\begin{aligned}
H_{d3} = & -\frac{2\pi\gamma\sqrt{2\gamma M}}{\sqrt{A}} \sum_{n_1,n_2,n_3} \sum_{\mathbf{q}_1,\mathbf{q}_2,\mathbf{q}_3} \delta_{\mathbf{q}_1-\mathbf{q}_2+\mathbf{q}_3} \\
& \times \big[\big(I_{d3,---} \eta_{\mathbf{q}_1 n_1} \eta_{-\mathbf{q}_2 n_2} \eta_{\mathbf{q}_3 n_3} + I_{d3,--+} \eta_{\mathbf{q}_1 n_1} \eta_{-\mathbf{q}_2 n_2} \eta^*_{-\mathbf{q}_3 n_3} \\
& + I_{d3,+--} \eta^*_{-\mathbf{q}_1 n_1} \eta_{-\mathbf{q}_2 n_2} \eta_{\mathbf{q}_3 n_3} + I_{d3,-+-} \eta_{\mathbf{q}_1 n_1} \eta^*_{\mathbf{q}_2 n_2} \eta_{\mathbf{q}_3 n_3} \big) + c.c. \big] ,
\end{aligned} \tag{4.73}
$$

where the $I_{d3,\pm\pm\pm}$ are integrals over x and x' (a subscript $+$ or $-$ in ith place corresponds to the function with subscript i being η^* or η, respectively):

$$
\begin{aligned}
I_{d3,---} &= -iq_{3z} \iint u^*_{\mathbf{q}_1 n_1} v^*_{-\mathbf{q}_2 n_2} \left[u'^*_{\mathbf{q}_3 n_3} (d_{x'} - q_{3y}) - v'^*_{\mathbf{q}_3 n_3} (d_{x'} + q_{3y}) \right] G_{q_3}(x - x') dx dx', \\
I_{d3,--+} &= -iq_{3z} \iint u^*_{\mathbf{q}_1 n_1} v^*_{-\mathbf{q}_2 n_2} \left[u'_{-\mathbf{q}_3 n_3} (d_{x'} + q_{3y}) - v'_{-\mathbf{q}_3 n_3} (d_{x'} - q_{3y}) \right] G_{q_3}(x - x') dx dx', \\
I_{d3,+--} &= iq_{3z} \iint v_{-\mathbf{q}_1 n_1} v^*_{-\mathbf{q}_2 n_2} \left[u'^*_{\mathbf{q}_3 n_3} (d_{x'} - q_{3y}) - v'^*_{\mathbf{q}_3 n_3} (d_{x'} + q_{3y}) \right] G_{q_3}(x - x') dx dx', \\
I_{d3,-+-} &= iq_{3z} \iint u^*_{\mathbf{q}_1 n_1} u_{\mathbf{q}_2 n_2} \left[u'^*_{\mathbf{q}_3 n_3} (d_{x'} - q_{3y}) - v'^*_{\mathbf{q}_3 n_3} (d_{x'} + q_{3y}) \right] G_{q_3}(x - x') dx dx'.
\end{aligned} \tag{4.74}
$$

In obtaining (4.73) we have used the fact that some terms (e.g. the term with $\eta^*_{-\mathbf{q}_1 n_1} \eta^*_{\mathbf{q}_2 n_2} \eta^*_{-\mathbf{q}_3 n_3}$) can be expressed as complex conjugates of others (e.g. the term with $\eta_{\mathbf{q}_1 n_1} \eta_{-\mathbf{q}_2 n_2} \eta_{\mathbf{q}_3 n_3}$) by sending the summation indices $\mathbf{q}_1 \leftrightarrow \mathbf{q}_2$ and $\mathbf{q}_3 \to -\mathbf{q}_3$ simultaneously. (Later we will use this kind of connections between terms when calculating 4th order terms.) Note also that the three terms involving one complex conjugated function in (4.73) can also be combined if we rename the indices.

With (4.73) we could in principle calculate the rate of a corresponding process by using Fermi's golden rule, and further write out the kinetic equation of magnon numbers and calculate the attenuation time due to 3rd order processes.

let us calculate the decay time for this process. for the decay time:

$$
W_{k,k'} = \frac{2\pi}{\hbar} n_i \delta \left(\varepsilon(k) - \varepsilon(k') \right) | \langle k | U | k' \rangle |^2 \tag{4.75}
$$

where n_i is the number of impurities per unit volume.

$$| \langle k| U |k'\rangle | = \int dr \psi^*_{nk'}(r) U(r) \psi_{nk}(r) \tag{4.76}$$

and the Bloch functions are taken to be normalized so that

$$\int_{cell} dr |\psi_{nk}(r)|^2 = v_{cell} \tag{4.77}$$

The kinetic equation under the 3-magnon process can be written as follows:

$$\frac{dn_{k,n_1}}{dt} = \sum_{n_2,n_3} \sum_{q} W(k,q,n_1,n_2,n_3)[n(k+q,n_3) \tag{4.78}$$
$$(n(k,n_1)+1)(n(q,n_2)+1) - (n(k+q,n_3)+1)n(k,n_1)n(q,n_2)]$$

where

$$W(k,q,n_1,n_2,n_3) = \frac{2\pi}{\hbar} |I|^2 \delta(\omega_{k+q}(n_3) - \omega_k(n_1) - \omega_q(n_2)) \tag{4.79}$$

Then

$$\frac{1}{\tau_k} = \sum_q W(k,q,n_1,n_2,n_3)(n^0_q - n^0_{k+q}) \tag{4.80}$$

Assuming that

$$u = a \cos \frac{\pi x}{d}$$
$$v = c \cos \frac{\pi x}{d}$$

we have

$$
\begin{aligned}
I_1 &= -\frac{ia_1c_2dq_{3z}e^{-dq_3}\left(-2a_3q_{3y}e^{dq_3}\left(2d^4q_3^4+8\pi^2d^2q_3^2+3\pi^4\right)+6\pi^4a_3q_{3y}-3\pi^4c_3\left(e^{2dq_3}-1\right)\left(q_3+q_{3y}\right)\right)}{3q_3^2\left(\pi d^4q_3^4+5\pi^3d^2q_3^2+4\pi^5\right)}\\
I_2 &= -\frac{2ia_1c_2dq_{3z}\left(3\pi^4\sinh(dq_3)(q_{3y}(a_3+c_3)-c_3q_3)+a_3q_{3y}\left(2d^4q_3^4+8\pi^2d^2q_3^2-3\pi^4\cosh(dq_3)+3\pi^4\right)\right)}{3q_3^2\left(\pi d^4q_3^4+5\pi^3d^2q_3^2+4\pi^5\right)}\\
I_3 &= \frac{ic_1c_2dq_{3z}e^{-dq_3}\left(-2a_3q_{3y}e^{dq_3}\left(2d^4q_3^4+8\pi^2d^2q_3^2+3\pi^4\right)+6\pi^4a_3q_{3y}-3\pi^4c_3\left(e^{2dq_3}-1\right)\left(q_3+q_{3y}\right)\right)}{3q_3^2\left(\pi d^4q_3^4+5\pi^3d^2q_3^2+4\pi^5\right)}\\
I_4 &= \frac{ia_1a_2dq_{3z}e^{-dq_3}\left(-2a_3q_{3y}e^{dq_3}\left(2d^4q_3^4+8\pi^2d^2q_3^2+3\pi^4\right)+6\pi^4a_3q_{3y}-3\pi^4c_3\left(e^{2dq_3}-1\right)\left(q_3+q_{3y}\right)\right)}{3q_3^2\left(\pi d^4q_3^4+5\pi^3d^2q_3^2+4\pi^5\right)}
\end{aligned}
$$

Meanwhile we have

$$a=\pm\sqrt{\frac{2}{d[1-\frac{\mathcal{B}^2}{(\omega+\mathcal{A})^2}]}}, \tag{4.81}$$

$$c=\mp\frac{\mathcal{B}}{\omega+\mathcal{A}}\sqrt{\frac{2}{d[1-\frac{\mathcal{B}^2}{(\omega+\mathcal{A})^2}]}}, \tag{4.82}$$

for the case $d=5\mu m$, H=600 Oe, we get the decay time for the condensates of magnons $\tau=10^{-4515}s$ due to three magnon process.. Our result shows that the three magnon processes are not important in determining the relaxation rate. It is much smaller than that provided by magnon-phonon interaction.

4.4.2 4th order terms

Now let's consider the 4th order terms of the Hamiltonian, which read:

$$H_4=H_{ex4}+H_{d4}, \tag{4.83}$$

$$H_{ex4}=\frac{\gamma^2D}{2}\int\left[-\left|\psi\right|^2\left|\nabla\psi\right|^2+\frac{1}{2}\left(\nabla\left(\left|\psi\right|^2\right)\right)^2\right]dV, \tag{4.84}$$

$$H_{d4}=\frac{\gamma^2}{2}\iint\left[\left|\psi\right|^2\left|\psi'\right|^2\partial_z\partial'_z-\frac{1}{4}\left|\psi\right|^2\left(\psi\partial_-+\psi^*\partial_+\right)\left(\psi'\partial'_-+\psi'^*\partial'_+\right)\right]\frac{dVdV'}{|\mathbf{r}-\mathbf{r}'|}. \tag{4.85}$$

Plugging the 2D-Fourier transformation

$$\psi(\mathbf{r}) = \sum_{\mathbf{q}} \chi_{\mathbf{q}}(x) \frac{e^{i\mathbf{q}\mathbf{r}}}{\sqrt{A}}, \tag{4.86}$$

into the 4th order exchange Hamiltonian, we get:

$$\begin{aligned}
H_{ex4} &= \frac{\gamma^2 D}{2A^2} \int \sum_{\mathbf{q}_1,\mathbf{q}_2,\mathbf{q}_3,\mathbf{q}_4} \Big[-\chi_{\mathbf{q}_1}\chi^*_{\mathbf{q}_2} \left(d_x\chi_{\mathbf{q}_3} d_x\chi^*_{\mathbf{q}_4} + \mathbf{q}_3\mathbf{q}_4\chi_{\mathbf{q}_3}\chi^*_{\mathbf{q}_4} \right) \\
&+ \frac{1}{2} d_x(\chi_{\mathbf{q}_1}\chi^*_{\mathbf{q}_2}) d_x(\chi_{\mathbf{q}_3}\chi^*_{\mathbf{q}_4}) - \frac{1}{2}(\mathbf{q}_1 - \mathbf{q}_2)(\mathbf{q}_3 - \mathbf{q}_4)\chi_{\mathbf{q}_1}\chi^*_{\mathbf{q}_2}\chi_{\mathbf{q}_3}\chi^*_{\mathbf{q}_4} \Big] e^{i(\mathbf{q}_1 - \mathbf{q}_2 + \mathbf{q}_3 - \mathbf{q}_4)\mathbf{r}} dV \\
&= \frac{\gamma^2 D}{2A} \int \sum_{\mathbf{q}_1,\mathbf{q}_2,\mathbf{q}_3,\mathbf{q}_4} \Big[-\chi_{\mathbf{q}_1}\chi^*_{\mathbf{q}_2} \left(d_x\chi_{\mathbf{q}_3} d_x\chi^*_{\mathbf{q}_4} + \mathbf{q}_3\mathbf{q}_4\chi_{\mathbf{q}_3}\chi^*_{\mathbf{q}_4} \right) \\
&+ \frac{1}{2} d_x(\chi_{\mathbf{q}_1}\chi^*_{\mathbf{q}_2}) d_x(\chi_{\mathbf{q}_3}\chi^*_{\mathbf{q}_4}) - \frac{1}{2}(\mathbf{q}_1 - \mathbf{q}_2)(\mathbf{q}_3 - \mathbf{q}_4)\chi_{\mathbf{q}_1}\chi^*_{\mathbf{q}_2}\chi_{\mathbf{q}_3}\chi^*_{\mathbf{q}_4} \Big] \delta_{\mathbf{q}_1 - \mathbf{q}_2 + \mathbf{q}_3 - \mathbf{q}_4} dx \\
&= \frac{\gamma^2 D}{4A} \int \sum_{\mathbf{q}_1,\mathbf{q}_2,\mathbf{q}_3,\mathbf{q}_4} \Big[\chi^*_{\mathbf{q}_2}\chi^*_{\mathbf{q}_4} d_x\chi_{\mathbf{q}_1} d_x\chi_{\mathbf{q}_3} + \chi_{\mathbf{q}_1}\chi_{\mathbf{q}_3} d_x\chi^*_{\mathbf{q}_2} d_x\chi^*_{\mathbf{q}_4} \\
&+ (\mathbf{q}_1^2 + \mathbf{q}_2^2)\chi_{\mathbf{q}_1}\chi^*_{\mathbf{q}_2}\chi_{\mathbf{q}_3}\chi^*_{\mathbf{q}_4} - 4\mathbf{q}_1\mathbf{q}_2\chi_{\mathbf{q}_1}\chi^*_{\mathbf{q}_2}\chi_{\mathbf{q}_3}\chi^*_{\mathbf{q}_4} \Big] \delta_{\mathbf{q}_1 - \mathbf{q}_2 + \mathbf{q}_3 - \mathbf{q}_4} dx
\end{aligned} \tag{4.87}$$

Note that in obtaining this expression we used the symmetries between indices.

For the 4th order dipolar Hamiltonian, we have

$$\begin{aligned}
H_{d4} &= \frac{2\pi\gamma^2}{A^3} \iint \sum_{\mathbf{q}_1,\mathbf{q}_2,\mathbf{q}_3,\mathbf{q}_4,\mathbf{q}} \Big\{ q_z^2 \chi_{\mathbf{q}_1}\chi^*_{\mathbf{q}_2}\chi'_{\mathbf{q}_3}\chi'^*_{\mathbf{q}_4} e^{i[(\mathbf{q}_1 - \mathbf{q}_2)\mathbf{r} + (\mathbf{q}_3 - \mathbf{q}_4)\mathbf{r}' + \mathbf{q}(\mathbf{r} - \mathbf{r}')]} \\
&- \frac{1}{4}\chi_{\mathbf{q}_1}\chi^*_{\mathbf{q}_2} \left[\chi_{\mathbf{q}_3}(d_x + q_y) + \chi^*_{-\mathbf{q}_3}(d_x - q_y) \right] \left[\chi'_{\mathbf{q}_4}(d_{x'} - q_y) + \chi'^*_{-\mathbf{q}_4}(d_{x'} + q_y) \right] \\
&\times e^{i[(\mathbf{q}_1 - \mathbf{q}_2)\mathbf{r} + \mathbf{q}_3\mathbf{r} + \mathbf{q}_4\mathbf{r}' + \mathbf{q}(\mathbf{r} - \mathbf{r}')]} \Big\} G_q(x - x') dV dV' \\
&= \frac{2\pi\gamma^2}{A} \iint \sum_{\mathbf{q}_1,\mathbf{q}_2,\mathbf{q}_3,\mathbf{q}_4,\mathbf{q}} \big\{ q_z^2 \chi_{\mathbf{q}_1}\chi^*_{\mathbf{q}_2}\chi'_{\mathbf{q}_3}\chi'^*_{\mathbf{q}_4} \delta_{\mathbf{q}_1 - \mathbf{q}_2 + \mathbf{q}} \delta_{\mathbf{q}_3 - \mathbf{q}_4 - \mathbf{q}} \\
&- \frac{1}{4}\chi_{\mathbf{q}_1}\chi^*_{\mathbf{q}_2} \left[\chi_{\mathbf{q}_3}(d_x + q_y) + \chi^*_{-\mathbf{q}_3}(d_x - q_y) \right] \left[\chi'_{\mathbf{q}_4}(d_{x'} - q_y) + \chi'^*_{-\mathbf{q}_4}(d_{x'} + q_y) \right] \\
&\times \delta_{\mathbf{q}_1 - \mathbf{q}_2 + \mathbf{q}_3 + \mathbf{q}} \delta_{\mathbf{q}_4 - \mathbf{q}} \big\} G_q(x - x') dx dx'.
\end{aligned} \tag{4.88}$$

In all 4th order terms, the second term in the dipolar Hamiltonian is the only one that do not

conserve magnon numbers.

4.4.2.1 For condensates

We are most interested to magnons in the two condensates, which momenta are $\pm\mathbf{Q} = \pm Q\hat{z}$. To consider interaction among the condensed magnons, we will single out in the Hamiltonian the terms in which every χ has argument $\pm\mathbf{Q}$. Note that conservation of momentum need to be satisfied (namely, the Kronecker delta functions should have zero arguments). We have for the exchange part:

$$\begin{aligned} H_{ex4}^{cond} &= \frac{\gamma^2 D}{2A}\int dx \chi_{\mathbf{Q}}\chi^*_{\mathbf{Q}}\chi_{\mathbf{Q}}\chi^*_{\mathbf{Q}}\left(-Q^2\right) + \frac{\gamma^2 D}{2A}\int dx \chi_{\mathbf{Q}}\chi^*_{\mathbf{Q}}\chi_{-\mathbf{Q}}\chi^*_{-\mathbf{Q}}\left(4Q^2\right) \\ &+ \frac{\gamma^2 D}{2A}\int dx \chi_{-\mathbf{Q}}\chi^*_{-\mathbf{Q}}\chi_{-\mathbf{Q}}\chi^*_{-\mathbf{Q}}\left(-Q^2\right) \\ &+ \frac{\gamma^2 D}{4A}\int dx \chi^*_{\mathbf{Q}}\chi^*_{\mathbf{Q}}d_x\chi_{\mathbf{Q}}d_x\chi_{\mathbf{Q}} + \frac{\gamma^2 D}{4A}\int dx \chi_{\mathbf{Q}}\chi_{\mathbf{Q}}d_x\chi^*_{\mathbf{Q}}d_x\chi^*_{\mathbf{Q}} \\ &+ \frac{\gamma^2 D}{A}\int dx \chi^*_{\mathbf{Q}}\chi^*_{-\mathbf{Q}}d_x\chi_{\mathbf{Q}}d_x\chi_{-\mathbf{Q}} + \frac{\gamma^2 D}{A}\int dx \chi_{\mathbf{Q}}\chi_{-\mathbf{Q}}d_x\chi^*_{\mathbf{Q}}d_x\chi^*_{-\mathbf{Q}} \\ &+ \frac{\gamma^2 D}{4A}\int dx \chi^*_{-\mathbf{Q}}\chi^*_{-\mathbf{Q}}d_x\chi_{-\mathbf{Q}}d_x\chi_{-\mathbf{Q}} + \frac{\gamma^2 D}{4A}\int dx \chi_{-\mathbf{Q}}\chi_{-\mathbf{Q}}d_x\chi^*_{-\mathbf{Q}}d_x\chi^*_{-\mathbf{Q}} \end{aligned} \tag{4.89}$$

and for the dipolar part: Note that

$$d_x d_{x'} G_Q(x-x') = -d_x^2 G_Q(x-x') = \delta(x-x') - Q^2 G_Q(x-x'). \tag{4.90}$$

$$
\begin{aligned}
H_{d4}^{cond} &= \frac{8\pi\gamma^2}{A}\iint dxdx' Q^2 \chi_{\mathbf{Q}}\chi^*_{-\mathbf{Q}}\chi'_{-\mathbf{Q}}\chi'^*_{\mathbf{Q}} G_{2Q}(x-x') \\
&+ \frac{8\pi\gamma^2}{A}\iint dxdx' Q^2 \chi_{-\mathbf{Q}}\chi^*_{\mathbf{Q}}\chi'_{\mathbf{Q}}\chi'^*_{-\mathbf{Q}} G_{2Q}(x-x') \\
&- \frac{\pi\gamma^2}{2A}\iint dxdx' \chi_{\mathbf{Q}}\chi^*_{\mathbf{Q}}\left[\chi_{\mathbf{Q}}+\chi^*_{-\mathbf{Q}}\right]\left[\chi'_{-\mathbf{Q}}+\chi'^*_{\mathbf{Q}}\right]\left[\delta(x-x')-Q^2G_Q(x-x')\right] \\
&- \frac{\pi\gamma^2}{2A}\iint dxdx' \chi_{\mathbf{Q}}\chi^*_{\mathbf{Q}}\left[\chi_{-\mathbf{Q}}+\chi^*_{\mathbf{Q}}\right]\left[\chi'_{\mathbf{Q}}+\chi'^*_{-\mathbf{Q}}\right]\left[\delta(x-x')-Q^2G_Q(x-x')\right] \\
&- \frac{\pi\gamma^2}{2A}\iint dxdx' \chi_{\mathbf{Q}}\chi^*_{-\mathbf{Q}}\left[\chi_{-\mathbf{Q}}+\chi^*_{\mathbf{Q}}\right]\left[\chi'_{-\mathbf{Q}}+\chi'^*_{\mathbf{Q}}\right]\left[\delta(x-x')-Q^2G_Q(x-x')\right] \\
&- \frac{\pi\gamma^2}{2A}\iint dxdx' \chi_{-\mathbf{Q}}\chi^*_{\mathbf{Q}}\left[\chi_{\mathbf{Q}}+\chi^*_{-\mathbf{Q}}\right]\left[\chi'_{\mathbf{Q}}+\chi'^*_{-\mathbf{Q}}\right]\left[\delta(x-x')-Q^2G_Q(x-x')\right] \\
&- \frac{\pi\gamma^2}{2A}\iint dxdx' \chi_{-\mathbf{Q}}\chi^*_{-\mathbf{Q}}\left[\chi_{\mathbf{Q}}+\chi^*_{-\mathbf{Q}}\right]\left[\chi'_{-\mathbf{Q}}+\chi'^*_{\mathbf{Q}}\right]\left[\delta(x-x')-Q^2G_Q(x-x')\right] \\
&- \frac{\pi\gamma^2}{2A}\iint dxdx' \chi_{-\mathbf{Q}}\chi^*_{-\mathbf{Q}}\left[\chi_{-\mathbf{Q}}+\chi^*_{\mathbf{Q}}\right]\left[\chi'_{\mathbf{Q}}+\chi'^*_{-\mathbf{Q}}\right]\left[\delta(x-x')-Q^2G_Q(x-x')\right]
\end{aligned}
$$

Neglecting a common factor $\frac{\gamma^2}{Ad}$ and do transformation $\chi_{\mathbf{Q}} \to \sqrt{\frac{1}{d}}\chi_{\mathbf{Q}}$ and $\mathbf{r} \to \sqrt{\frac{MD}{H}}\mathbf{r}$. Then we have

$$
\begin{aligned}
H_{ex4}^{cond} &= \frac{2\pi}{d\chi}\int dx \chi_{\mathbf{Q}}\chi^*_{\mathbf{Q}}\chi_{\mathbf{Q}}\chi^*_{\mathbf{Q}}\left(-Q^2\right) + \frac{2\pi}{d\chi}\int dx \chi_{\mathbf{Q}}\chi^*_{\mathbf{Q}}\chi_{-\mathbf{Q}}\chi^*_{-\mathbf{Q}}\left(4Q^2\right) \\
&+ \frac{2\pi}{d\chi}\int dx \chi_{-\mathbf{Q}}\chi^*_{-\mathbf{Q}}\chi_{-\mathbf{Q}}\chi^*_{-\mathbf{Q}}\left(-Q^2\right) \\
&+ \frac{\pi}{d\chi}\int dx \chi^*_{\mathbf{Q}}\chi^*_{\mathbf{Q}} d_x\chi_{\mathbf{Q}} d_x\chi_{\mathbf{Q}} + \frac{\pi}{d\chi}\int dx \chi_{\mathbf{Q}}\chi_{\mathbf{Q}} d_x\chi^*_{\mathbf{Q}} d_x\chi^*_{\mathbf{Q}} \\
&+ \frac{4\pi}{d\chi}\int dx \chi^*_{\mathbf{Q}}\chi^*_{-\mathbf{Q}} d_x\chi_{\mathbf{Q}} d_x\chi_{-\mathbf{Q}} + \frac{4\pi}{d\chi}\int dx \chi_{\mathbf{Q}}\chi_{-\mathbf{Q}} d_x\chi^*_{\mathbf{Q}} d_x\chi^*_{-\mathbf{Q}} \\
&+ \frac{\pi}{d\chi}\int dx \chi^*_{-\mathbf{Q}}\chi^*_{-\mathbf{Q}} d_x\chi_{-\mathbf{Q}} d_x\chi_{-\mathbf{Q}} + \frac{\pi}{d\chi}\int dx \chi_{-\mathbf{Q}}\chi_{-\mathbf{Q}} d_x\chi^*_{-\mathbf{Q}} d_x\chi^*_{-\mathbf{Q}}
\end{aligned} \tag{4.91}
$$

$$
\begin{aligned}
H_{d4}^{cond} &= \frac{8\pi}{d}\iint dxdx' Q^2 \chi_{\mathbf{Q}}\chi^*_{-\mathbf{Q}}\chi'_{-\mathbf{Q}}\chi'^*_{\mathbf{Q}} G_{2Q}(x-x') \\
&+ \frac{8\pi}{d}\iint dxdx' Q^2 \chi_{-\mathbf{Q}}\chi^*_{\mathbf{Q}}\chi'_{\mathbf{Q}}\chi'^*_{-\mathbf{Q}} G_{2Q}(x-x') \\
&- \frac{\pi}{2d}\iint dxdx' \chi_{\mathbf{Q}}\chi^*_{\mathbf{Q}}\left[\chi_{\mathbf{Q}}+\chi^*_{-\mathbf{Q}}\right]\left[\chi'_{-\mathbf{Q}}+\chi'^*_{\mathbf{Q}}\right]\left[\delta(x-x')-Q^2G_Q(x-x')\right] \\
&- \frac{\pi}{2d}\iint dxdx' \chi_{\mathbf{Q}}\chi^*_{\mathbf{Q}}\left[\chi_{-\mathbf{Q}}+\chi^*_{\mathbf{Q}}\right]\left[\chi'_{\mathbf{Q}}+\chi'^*_{-\mathbf{Q}}\right]\left[\delta(x-x')-Q^2G_Q(x-x')\right] \\
&- \frac{\pi}{2d}\iint dxdx' \chi_{\mathbf{Q}}\chi^*_{-\mathbf{Q}}\left[\chi_{-\mathbf{Q}}+\chi^*_{\mathbf{Q}}\right]\left[\chi'_{-\mathbf{Q}}+\chi'^*_{\mathbf{Q}}\right]\left[\delta(x-x')-Q^2G_Q(x-x')\right] \\
&- \frac{\pi}{2d}\iint dxdx' \chi_{-\mathbf{Q}}\chi^*_{\mathbf{Q}}\left[\chi_{\mathbf{Q}}+\chi^*_{-\mathbf{Q}}\right]\left[\chi'_{\mathbf{Q}}+\chi'^*_{-\mathbf{Q}}\right]\left[\delta(x-x')-Q^2G_Q(x-x')\right] \\
&- \frac{\pi}{2d}\iint dxdx' \chi_{-\mathbf{Q}}\chi^*_{-\mathbf{Q}}\left[\chi_{\mathbf{Q}}+\chi^*_{-\mathbf{Q}}\right]\left[\chi'_{-\mathbf{Q}}+\chi'^*_{\mathbf{Q}}\right]\left[\delta(x-x')-Q^2G_Q(x-x')\right] \\
&- \frac{\pi}{2d}\iint dxdx' \chi_{-\mathbf{Q}}\chi^*_{-\mathbf{Q}}\left[\chi_{-\mathbf{Q}}+\chi^*_{\mathbf{Q}}\right]\left[\chi'_{\mathbf{Q}}+\chi'^*_{-\mathbf{Q}}\right]\left[\delta(x-x')-Q^2G_Q(x-x')\right]
\end{aligned}
$$

In terms of Bogoliubov transformed functions, the 4th order interactions for condensed magnons will be in the form of a sum of products of terms in 4th order of $\eta_{\pm\mathbf{Q}n}$ and $\eta^*_{\pm\mathbf{Q}n}$ which coefficients depend on integration of functions of u and v over spacial coordinates. But the condensed magnons are at the bottom of spectrum which has $n = 0$. So in later considerations we will keep only the terms with $\eta_{\pm\mathbf{Q}0}$ and $\eta^*_{\pm\mathbf{Q}0}$.

We also note that the condensed magnons has $k_y = 0$, in which case the modes are either even or odd. Since condensate is the lowest branch with $n = 0$, the corresponding modes are even, so that

$$u_{\mathbf{q}}(x) = a\cos k_x x + \sum_{m=1,2} A_m \cosh\lambda_m x, \tag{4.92}$$

$$v_{\mathbf{q}}(x) = c\cos k_x x + \sum_{m=1,2} C_m \cosh\lambda_m x. \tag{4.93}$$

Relation between a and c is determined by the normalization condition , and relation between a, A_1, A_2 can be determined by the kernel of the matrix $\mathcal{C}_Q$ For the condensed magnons, we have:

$$\chi_{\pm\mathbf{Q}}(x) = u^*_{\pm\mathbf{Q}}(x)\,\eta_{\pm\mathbf{Q}0} - v_{\mp\mathbf{Q}0}(x)\,\eta^*_{\mp\mathbf{Q}0}. \tag{4.94}$$

In the later discussions on condensed magnons, we are going to drop the subscript 0 for the a, c amplitudes and for the η functions, with the understanding that they are at $n = 0$. We also note that the a, c coefficients are all real.

We now note that, due to the symmetry between the two condensates, the a, b, c, d coefficients for at $\pm\mathbf{Q}$ are the same, e.g. $a_{\mathbf{Q}} = a_{-\mathbf{Q}}$. Thus, later we will drop the subscript of the a, c coefficients, with the understanding that they are at wavevectors $\pm\mathbf{Q}$.

With these simplification of notations, we have:

$$\begin{aligned}
\chi_{\pm\mathbf{Q}} &= u\eta_{\pm\mathbf{Q}} - v\eta^*_{\mp\mathbf{Q}} \\
&= \left(a\cos k_x x + \sum_{m=1,2} A_m \cosh \lambda_m x \right) \eta_{\pm\mathbf{Q}} \\
&- \left(c\cos k_x x + \sum_{m=1,2} C_m \cosh \lambda_m x \right) \eta^*_{\mp\mathbf{Q}}
\end{aligned} \tag{4.95}$$

We now write the 4th order Hamiltonian in the form:

$$\begin{aligned}
H^{cond} &= A(|\eta_{\mathbf{Q}}|^4 + |\eta_{-\mathbf{Q}}|^4) + 2B|\eta_{\mathbf{Q}}|^2|\eta_{-\mathbf{Q}}|^2 \\
&+ C(|\eta_{\mathbf{Q}}|^2 + |\eta_{-\mathbf{Q}}|^2)(\eta_{\mathbf{Q}}\eta_{-\mathbf{Q}} + c.c.) + D(\eta^2_{\mathbf{Q}}\eta^2_{-\mathbf{Q}} + c.c.).
\end{aligned} \tag{4.96}$$

The ground state of the condensates depends on the criterion papameter: $\Delta = A - B + |C| - D$. When $\Delta < 0$, corresponds to an asymmetric state. When $\Delta > 0$, corresponds to an symmetric state. The state diagram is shown in Fig.4.1. Our phase diagram is different from the previous result [5], especially that at usual experimental conditions, there is no existence for the symmetric phase.

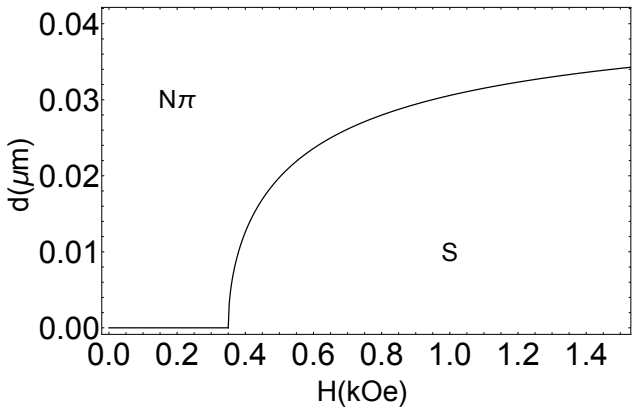

(a)

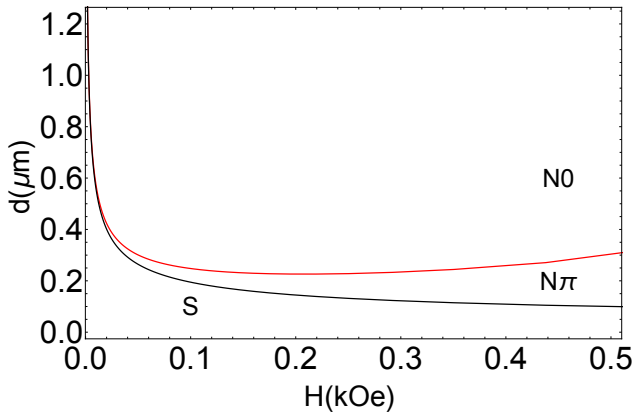

(b)

Figure 4.1: The state diagram in the $d - H$ plane. S, $N0$ and $N\pi$ correspond to the symmetric state, the non-symmetric 0 state and the non-symmetric π state, respectively. (a) Amplitude representation method. (b) Phase diagram that is modified from [5].

5. SUMMARY AND CONCLUSIONS

In this work, we first review the Bose-Einstein condensation and the magnons.

In Chapter 3, a new version of the asymptotically exact theory of the spectrum and transverse distribution of magnetization in long-wave magnons is presented. we have found many features of the solution that were not found earlier. We considered the group of symmetry for solutions that allow their classification. We studied not the only property of thick, but also thin films, most important for their possible technological applications. We also studied quantization of transverse motion for ultrathin limit and have discovered that there is a big gap in the spectrum in this limit and only the lowest mode has the transverse wave vector and frequency that do not depend on thickness. We also use this theory to show that the effective magnon repulsion can be associated with the influence of additional dipolar magnetic fields appearing in response to any local increase of the condensate density. We conclude that the origin of this stability is the effective repulsive magnon-magnon interaction having the magneto-dipolar nature.

In Chapter 4, we develop a classical representation for the Landau-Lifshitz equation. we calculated the relaxation rate of condensed magnons in the ferromagnetic YIG film with a finite thickness. We also calculated the 4th order magnon-magnon interactions in the condensate of a film of YIG, including magnon non-conserving term responsible for the coherence of two condensates.

In reality the thermodynamic approach becomes invalid. It states that the phase with smaller energy wins. Thermodynamic approach is valid if the lifetime is much longer than the relaxation time. This is definitely correct for relaxation of the magnons in one minimum, but not for inter-minima relaxation. Each such process leads to change of the total moment by $2Q$. it can proceed only due to Compton process with participation of thermal magnons. They will compensate the non-conservation of momentum. However, this process probably is not shorter than the lifetime. So, what we expect is that, because the process of pumping is symmetric, the stationary state will be much closer to symmetric than it is obtained by simple thermodynamic approach. The previous calculations give us the starting place for this new development.

REFERENCES

[1] A. Kreisel, F. Sauli, L. Bartosch, and P. Kopietz, "Microscopic spin-wave theory for yttrium-iron garnet films," *The European Physical Journal B*, vol. 71, no. 1, p. 59, 2009.

[2] A. A. Serga, C. W. Sandweg, V. I. Vasyuchka, M. B. Jungfleisch, B. Hillebrands, A. Kreisel, P. Kopietz, and M. P. Kostylev, "Brillouin light scattering spectroscopy of parametrically excited dipole-exchange magnons," *Phys. Rev. B*, vol. 86, p. 134403, 2012.

[3] V. E. Demidov, O. Dzyapko, S. O. Demokritov, G. A. Melkov, and A. N. Slavin, "Observation of spontaneous coherence in bose-einstein condensate of magnons," *Phys. Rev. Lett.*, vol. 100, p. 047205, 2008.

[4] J. Lim, J. T. W. Bang, J. A. Kreisel, C. T. A. Hoffmann, and J. Ketterson, "Study of micron scale dispersion of spin waves in Yttrium Iron Garnet film," *Abstract of presentation at March APS Meeting 2018, Los Angeles*, 2018.

[5] F. Li, W. M. Saslow, and V. L. Pokrovsky, "Phase diagram for magnon condensate in yttrium iron garnet film," *Scientific Reports*, vol. 3, p. 1372, 2013.

[6] R. W. Damon and J. Eshbach, "Magnetostatic modes of a ferromagnet slab," *Journal of Physics and Chemistry of Solids*, vol. 19, no. 3-4, pp. 308–320, 1961.

[7] V. Gann, "Nonuniform resonance in a ferromagnetic plate," *Soviet Physics Solid State, USSR*, vol. 8, no. 11, p. 2537, 1967.

[8] R. De Wames and T. Wolfram, "Dipole-exchange spin waves in ferromagnetic films," *Journal of Applied Physics*, vol. 41, no. 3, pp. 987–993, 1970.

[9] T. Wolfram and R. De Wames, "Macroscopic and microscopic theories of dipole-exchange spin waves in thin films: Case of the missing surface states," *Physical Review Letters*, vol. 24, no. 26, p. 1489, 1970.

[10] R. Arias, "Spin-wave modes of ferromagnetic films," *Physical Review B*, vol. 94, no. 13, p. 134408, 2016.

[11] B. Kalinikos, "Excitation of propagating spin waves in ferromagnetic films," in *IEE Proceedings H (Microwaves, Optics and Antennas)*, vol. 127, pp. 4–10, IET, 1980.

[12] B. Kalinikos and A. Slavin, "Theory of dipole-exchange spin wave spectrum for ferromagnetic films with mixed exchange boundary conditions," *Journal of Physics C: Solid State Physics*, vol. 19, no. 35, p. 7013, 1986.

[13] S. M. Rezende, "Theory of coherence in bose-einstein condensation phenomena in a microwave-driven interacting magnon gas," *Physical Review B*, vol. 79, no. 17, p. 174411, 2009.

[14] E. Sonin, "Spin superfluidity and spin waves in yig films," *Physical Review B*, vol. 95, no. 14, p. 144432, 2017.

[15] Y. Sun, Z. Wang, and L. Lu, "Magnetic insulator-based spintronics: Spin pumping, magnetic proximity, spin hall, and spin seebeck effects on yttrium iron garnet thin films," in *Metallic Spintronic Devices*, pp. 171–220, CRC Press, 2014.

[16] R. Duine, A. Brataas, S. A. Bender, and Y. Tserkovnyak, "Spintronics and magnon bose-einstein condensation," *arXiv preprint arXiv:1505.01329*, 2015.

[17] C. Sun, T. Nattermann, and V. L. Pokrovsky, "Bose–einstein condensation and superfluidity of magnons in yttrium iron garnet films," *Journal of Physics D: Applied Physics*, vol. 50, no. 14, p. 143002, 2017.

[18] I. Tupitsyn, P. Stamp, and A. Burin, "Stability of bose-einstein condensates of hot magnons in yttrium iron garnet films," *Physical Review Letters*, vol. 100, no. 25, p. 257202, 2008.

[19] G. Li, C. Sun, T. Nattermann, and V. L. Pokrovsky, "Long-wave magnons in a ferromagnetic film," *Phys. Rev. B*, vol. 98, p. 014436, 2018.

[20] I. V. Borisenko, B. Divinskiy, V. E. Demidov, G. Li, T. Nattermann, V. L. Pokrovsky, and S. O. Demokritov, "Direct evidence of spatial stability of Bose-Einstein condensate of magnons," *Nature Communications*, vol. 11, no. 1, p. 1691, 2020.

[21] A. Einstein, "Quantentheorie des einatomigen idealen gases," *Prussian Academy of Sciences*, pp. 261–267, 1924.

[22] P. Kapitza, "Viscosity of liquid helium below the λ-point," *Nature*, vol. 141, no. 3558, p. 74, 1938.

[23] J. Allen and A. Misener, "Flow of liquid helium ii," *Nature*, vol. 141, no. 3558, p. 75, 1938.

[24] F. London, "On the bose-einstein condensation," *Physical Review*, vol. 54, no. 11, p. 947, 1938.

[25] M. H. Anderson, J. R. Ensher, M. R. Matthews, C. E. Wieman, and E. A. Cornell, "Observation of bose-einstein condensation in a dilute atomic vapor," *Science*, vol. 269, no. 5221, pp. 198–201, 1995.

[26] K. B. Davis, M.-O. Mewes, M. R. Andrews, N. Van Druten, D. Durfee, D. Kurn, and W. Ketterle, "Bose-einstein condensation in a gas of sodium atoms," *Physical Review Letters*, vol. 75, no. 22, p. 3969, 1995.

[27] S. Demokritov, V. Demidov, O. Dzyapko, G. Melkov, A. , B. Hillebrands, and A. Slavin, "Bose–einstein condensation of quasi-equilibrium magnons at room temperature under pumping," *Nature*, vol. 443, no. 7110, p. 430, 2006.

[28] J. Kasprzak, M. Richard, S. Kundermann, A. Baas, P. Jeambrun, J. Keeling, F. Marchetti, M. Szymańska, R. Andre, J. Staehli, *et al.*, "Bose–einstein condensation of exciton polaritons," *Nature*, vol. 443, no. 7110, p. 409, 2006.

[29] J. Klaers, J. Schmitt, F. Vewinger, and M. Weitz, "Bose–einstein condensation of photons in an optical microcavity," *Nature*, vol. 468, no. 7323, p. 545, 2010.

[30] F. Bloch, "Zur theorie des ferromagnetismus," *Zeitschrift für Physik*, vol. 61, no. 3-4, pp. 206–219, 1930.

[31] P. Nowik-Boltyk, O. Dzyapko, V. Demidov, N. Berloff, and S. Demokritov, "Spatially non-uniform ground state and quantized vortices in a two-component bose-einstein condensate of magnons," *Scientific Reports*, vol. 2, p. 482, 2012.

[32] D. A. Bozhko, A. A. Serga, P. Clausen, V. I. Vasyuchka, F. Heussner, G. A. Melkov, A. Pomyalov, V. S. L'vov, and B. Hillebrands, "Supercurrent in a room-temperature bose–einstein magnon condensate," *Nature Physics*, vol. 12, no. 11, p. 1057, 2016.

[33] A. Rückriegel, P. Kopietz, D. A. Bozhko, A. A. Serga, and B. Hillebrands, "Magnetoelastic modes and lifetime of magnons in thin yttrium iron garnet films," *Phys. Rev. B*, vol. 89, p. 184413, 2014.

[34] J. Holanda, D. S. Maior, A. Azevedo, and S. M. Rezende, "Detecting the phonon spin in magnon–phonon conversion experiments," *Nature Physics*, vol. 14, no. 5, pp. 500–506, 2018.

[35] V. E. Demidov, O. Dzyapko, S. O. Demokritov, G. A. Melkov, and A. N. Slavin, "Thermalization of a parametrically driven magnon gas leading to bose-einstein condensation," *Phys. Rev. Lett.*, vol. 99, p. 037205, 2007.

[36] V. E. Demidov, O. Dzyapko, M. Buchmeier, T. Stockhoff, G. Schmitz, G. A. Melkov, and S. O. Demokritov, "Magnon kinetics and bose-einstein condensation studied in phase space," *Phys. Rev. Lett.*, vol. 101, p. 257201, 2008.

[37] A. A. Serga, V. S. Tiberkevich, C. W. Sandweg, V. I. Vasyuchka, D. A. Bozhko, A. V. Chumak, T. Neumann, B. Obry, G. A. Melkov, A. N. Slavin, and B. Hillebrands, "Bose–Einstein condensation in an ultra-hot gas of pumped magnons," *Nature Communications*, vol. 5, no. 1, p. 3452, 2014.

[38] C. Sun, T. Nattermann, and V. L. Pokrovsky, "Unconventional superfluidity in yttrium iron garnet films," *Physical Review Letters*, vol. 116, no. 25, p. 257205, 2016.

[39] O. Dzyapko, P. Nowik-Boltyk, B. Koene, V. E. Demidov, J. Jersch, A. Kirilyuk, T. Rasing, and S. O. Demokritov, "High-resolution magneto-optical kerr-effect spectroscopy of magnon bose-einstein condensate," *IEEE Magnetics Letters*, vol. 7, pp. 1–5, 2016.

[40] V. Tiberkevich, I. V. Borisenko, P. Nowik-Boltyk, V. E. Demidov, A. B. Rinkevich, S. O. Demokritov, and A. N. Slavin, "Excitation of coherent second sound waves in a dense magnon gas," *Scientific Reports*, vol. 9, no. 1, p. 9063, 2019.

[41] D. A. Bozhko, A. J. E. Kreil, H. Y. Musiienko-Shmarova, A. A. Serga, A. Pomyalov, V. S. L'vov, and B. Hillebrands, "Bogoliubov waves and distant transport of magnon condensate at room temperature," *Nature Communications*, vol. 10, no. 1, p. 2460, 2019.

[42] F. Dalfovo, S. Giorgini, L. P. Pitaevskii, and S. Stringari, "Theory of bose-einstein condensation in trapped gases," *Rev. Mod. Phys.*, vol. 71, pp. 463–512, Apr 1999.

[43] L. Pitaevskii and S. Stringari, *Bose-Einstein Condensation*. Clarendon Press, 2003.

[44] Y. Kagan, A. E. Muryshev, and G. V. Shlyapnikov, "Collapse and bose-einstein condensation in a trapped bose gas with negative scattering length," *Phys. Rev. Lett.*, vol. 81, pp. 933–937, Aug 1998.

[45] E. A. Donley, N. R. Claussen, S. L. Cornish, J. L. Roberts, E. A. Cornell, and C. E. Wieman, "Dynamics of collapsing and exploding Bose–Einstein condensates," *Nature*, vol. 412, no. 6844, pp. 295–299, 2001.

[46] B. I. Ivanov and A. M. Kosevich, "Bound states of a large nuber of magnons in three-dimensional ferromagnet (magnons drops)," *JETP Lett.*, vol. 24, pp. 454–458, 1977.

[47] V. S. L'vov, *Wave Turbulence Under Parametric Excitation*. Springer, New York, 1994.

[48] M. G. Cottam, *Linear and Nonlinear Spin Waves in Magnetic Films and Superlattices*. World Scientific, 1994.

[49] A. G. Gurevich and G. A. Melkov, *Magnetization Oscillations and Waves*. CRC, 1996.

[50] K. N. G. . S. A. N. Kalinikos, B. A., "Observation of spin-wave solitons in ferromagnetic films," *Sov. Phys. JETP Lett.*, vol. 38, p. 413, 1983.

[51] M. Chen, M. A. Tsankov, J. M. Nash, and C. E. Patton, "Backward-volume-wave microwave-envelope solitons in yttrium iron garnet films," *Phys. Rev. B*, vol. 49, pp. 12773–12790, May 1994.

[52] S. Demokritov, B. Hillebrands, and A. Slavin, "Brillouin light scattering studies of confined spin waves: linear and nonlinear confinement," *Physics Reports*, vol. 348, no. 6, pp. 441 – 489, 2001.

[53] D. Backes, F. Macià, S. Bonetti, R. Kukreja, H. Ohldag, and A. D. Kent, "Direct observation of a localized magnetic soliton in a spin-transfer nanocontact," *Phys. Rev. Lett.*, vol. 115, p. 127205, Sep 2015.

[54] S. Chung, Q. T. Le, M. Ahlberg, A. A. Awad, M. Weigand, I. Bykova, R. Khymyn, M. Dvornik, H. Mazraati, A. Houshang, S. Jiang, T. N. A. Nguyen, E. Goering, G. Schütz, J. Gräfe, and J. Åkerman, "Direct observation of zhang-li torque expansion of magnetic droplet solitons," *Phys. Rev. Lett.*, vol. 120, p. 217204, May 2018.

[55] B. N. G. . D. S. O. Salman, H., *Universal Themes of Bose-Einstein Condensation*. Cambridge University Press, 2017.

[56] B. I. V. D. V. E. . D. S. O. Nowik-Boltyk, P., "Magnon laser," *Ukran. J. Phys.*, vol. 64, p. 938, 2019.

APPENDIX A

ANALYSIS OF SECULAR EQUATION

Secular equation for a magnon solution in a ferromagnetic film is a cubic equation for the variable $z \equiv k^2 = k_\parallel^2 + k_x^2$ that reads as follows:

$$P(z) \equiv z^3 + (2+\chi)\, z^2 + \left(1 + \chi - \omega^2 - \chi k_z^2\right) z - \chi k_z^2 = 0 \tag{A.1}$$

The product of three roots is equal to $\chi k_z^2 > 0$ and their sum is equal to $-(2+\chi) < 0$. Since coefficients of the polynomial $P(z)$ are real, its roots are either all three real or one of them is real and two others are complex conjugated. In the first case one root is positive and two others are negative. In the second case, since the product of two complex conjugated roots is positive the remaining root is also positive. In both cases one root $z_1 \equiv k_1^2$ is positive. We will show that due to physical limitations, two other roots are negative and the opportunity of two complex conjugated roots is not realized.

Indeed, the two other roots z_2 and z_3 are expressed in terms of positive root z_1 as follows (see eq. (3.23)):

$$z_{2,3} = -1 - \frac{\chi + z_1}{2} \pm \sqrt{\left(1 + \frac{\chi + z_1}{2}\right)^2 - \frac{\chi k_z^2}{z_1}} \tag{A.2}$$

The roots $z_{2,3}$ are complex with non-zero imaginary part if the expression under square root is negative. It happens if the following inequality is satisfied:

$$\frac{\chi k_z^2}{z_1} > \left(1 + \frac{\chi + z_1}{2}\right)^2 \tag{A.3}$$

However, at this condition the square of frequency $\omega^2 = (1+z_1)(1+z_1+\chi-\frac{\chi k_z^2}{z_1})$ becomes negative. It is physically forbidden. Thus, the positivity of ω^2 excludes the opportunity of complex roots.

The same requirement of positivity ω^2 gives a lower boundary for the value z_1:

$$z_1 > \sqrt{\left(\frac{1+\chi}{2}\right)^2 + \chi k_z^2} - \frac{1+\chi}{2} \tag{A.4}$$

APPENDIX B

MOTION OF SPECTRAL MINIMA IN A THICK FILM

The dependence of frequency on wave vector is determined by equation (3.13) of the main text. For the reader's convenience we reproduce it:

$$\omega^2 = \left(1 + k^2\right)\left(1 + k^2 + \chi - \chi\frac{k_z^2}{k^2}\right) \tag{B.1}$$

Here $k^2 = k_\parallel^2 + k_x^2$, where k_x is a positive quantized transverse component of wave vector. Generally to find minimum of frequency for a given mode with fixed quantum numbers and direction of propagation, it is necessary to take in account the dependence of quantized k_x on $k_\parallel$. This dependence can be neglected in thick films with $d \gg 1$. Indeed according to the main text, quantized values of k_x are equal to $k_{x,\nu,n} = \frac{2\pi n}{d} + \mu_{\nu,n}$. Here $\mu_{\nu,n} = \frac{2}{d}\arctan f_{\nu,n}\left(k_\parallel\right)$, where $f_{\nu,n}\left(k_\parallel\right)$ is a smooth function. According to this definition, $\mu_{\nu,n}$ varies in the limits $\left(-\frac{\pi}{d}, \frac{\pi}{d}\right)$ when $k_\parallel$ changes at least by $1/\sqrt{d}$. Therefore, the derivative $\frac{dk_x}{dk_\parallel} \lesssim \frac{1}{\sqrt{d}} \ll 1$ and the values $k_\parallel$ and k_x can be considered as independent. In this approximation the value of parallel wave vector $k_{\parallel 0}$ at which frequency has minimum can be found from equation:

$$\frac{\partial\omega^2}{\partial\left(k_\parallel^2\right)} = 2k^2 + 2 + \chi\sin^2\theta - \frac{\chi k_x^2\cos^2\theta}{k^4} = 0 \tag{B.2}$$

At small k_x i.e. at $n \ll d/2\pi$, the value k^2 satisfying eq. (B.2) is also small and equal to

$$k_0^2 \approx k_{\parallel 0}^2 \approx \sqrt{\frac{\chi}{2 + \chi\sin^2\theta}}k_x\cos\theta \tag{B.3}$$

It is however much larger than k_x^2. The value of frequency in minimum is $\omega_{min} \approx \sqrt{1 + \chi\sin^2\theta}$. The equation for k_0^2 valid in the range of larger k_x comparable with 1 can be found by the following

scaling transformation:

$$k_0^2 = \frac{2+\chi\sin^2\theta}{2} w\left(\xi\right);\ \xi = \frac{4\chi k_x^2\cos^2\theta}{\left(2+\chi\sin^2\theta\right)^3}, \tag{B.4}$$

where function $w\left(\xi\right)$ obeys cubic equation:

$$w^3 + w^2 = \xi \tag{B.5}$$

At small ξ, this equation gives the result (B.3). This equation shows that at small k_x, the wave vector corresponding to minimal frequency $k_{\|0}$ grows with k_x. To study the motion of minimum in a broader interval of k_x it is useful to look at the derivative $\frac{dk_{\|0}^2}{d(k_x^2)}$. According to eq. (B.2), it can be expressed as follows:

$$\frac{dk_{\|0}^2}{d(k_x^2)} = -\frac{\frac{\partial^2\omega^2}{\partial\left(k_\|^2\right)\partial(k_x^2)}}{\frac{\partial^2\omega^2}{\left(\partial\left(k_\|^2\right)\right)^2}} \tag{B.6}$$

From this equation it follows that maximal value of $k_{\|0}$ can be found from equation:

$$\frac{\partial^2\omega^2}{\partial\left(k_\|^2\right)\partial\left(k_x^2\right)} = 2 - \chi\frac{\cos^2\theta}{k^4} + 2\chi\frac{k_x^2\cos^2\theta}{k^6} = 0 \tag{B.7}$$

It is cubic equation for k^2. It must be solved together with equation of frequency minimum (B.2). Eliminating k_x^2 from these two equations, we arrive at a closed equation for k^2:

$$6k^6 + 2\left(2+\chi\sin^2\theta\right)k^4 - \chi\cos^2\theta k^2 = 0 \tag{B.8}$$

Dividing this equation by $k^2 \neq 0$, we obtain a quadratic equation for k^2, whose solution reads:

$$k_m^2 = \frac{\sqrt{\left(2+\chi\sin^2\theta\right)^2 + 6\chi\cos^2\theta} - \left(2+\chi\sin^2\theta\right)}{6} \tag{B.9}$$

The value of k_x^2 corresponding to maximal value of $k_{\|0}$ can be found by eliminating k^6 from eqs. (B.2,B.8). It reads:

$$\left(k_x^2\right)_m = \frac{1}{3\chi\cos^2\theta}\left[\left(2+\chi\sin^2\theta\right)k_m^4 + \chi\cos^2\theta k_m^2\right] \tag{B.10}$$

The maximal value of $k_{\|0}^2$ is equal to

$$\left(k_{\|0}^2\right)_{\max} = k_m^2 - \left(k_x^2\right)_m = \frac{2}{3}k_m^2 - \frac{\left(2+\chi\sin^2\theta\right)k_m^4}{3\chi\cos^2\theta}$$

At further increase of k_x, the position of minimum $k_{\|0}$ decreases and finally becomes zero. At this point, $k^2 = k_x^2$ and eq. (B.2) turns into quadratic equation for k_x^2. Its solution reads:

$$\left(k_x^2\right)_f = \frac{\sqrt{\left(2+\chi\sin^2\theta\right)^2 + 8\chi\cos^2\theta} - \left(2+\chi\sin^2\theta\right)}{4}$$

At this value of k_x, minimum merges with a local maximum at $k_\| = 0$. At larger values of k_x, the only minimum of frequency is at $k_\| = 0$.

APPENDIX C

SPECTRUM OF MAGNONS PROPAGATING PERPENDICULARLY TO MAGNETIZATION

The consistency method used in this article requires to nullify all contributions of evanescent waves of the type $e^{\pm k_{\|}x}$ or $\cosh k_{\|}x$ and $\sinh k_{\|}x$ arguing that such functions are not solutions of the 6-th order differential equation for magnetization following from equations of motion. This method fails in the case of spin wave propagating perpendicularly to the magnetization, i.e. for $k_z = 0$. Indeed, in this case one of solutions of secular equation (A.1) is $k^2 = 0$. For this root $k_x = \pm ik_{\|}$. It means that $e^{\pm k_{\|}x}$ are solutions of the 6-th order differential equation. Therefore, our method of solution must be modified for this special case. In this appendix we present a modified method solving the problem of perpendicularly propagating magnons. In their article [**?**] Wolfram and de Wames considered the spectrum of perpendicularly propagating magnons, but did not establish its quantization.

When one of solutions of the secular equation (A.1) is $z = 0$, two others can be easily found. They are:

$$z_1 \equiv k_1^2 = k_{1x}^2 + k_y^2;\ z_2 \equiv k_2^2 = -2 - \chi - z_1 \tag{C.1}$$

General solution for $k_z = 0$ reads:

$$\begin{aligned} \mathbf{m}(x) &= \sum_{j=1}^{2} (\mathbf{a}_j \cos k_{jx}x + \mathbf{b}_j \sin k_{jx}x) \\ &+ \mathbf{p}\cosh k_y x + \mathbf{q}\sinh k_y x, \end{aligned} \tag{C.2}$$

where $\mathbf{a}_j, \mathbf{b}_j, \mathbf{p}, \mathbf{q}$ are constant 2-component vectors; $k_{2x} = i\sqrt{2 + \chi + k_1^2 + k_y^2}$. Differential equations for $\mathbf{m}(x)$ following from eqs. (3.8, 3.10) of the main text give the same relation between

amplitudes $\mathbf{a}_j$ and $\mathbf{b}_j$ as for general case (compare with eq. (3.16):

$$\mathbf{b}_j = \Lambda_j \mathbf{a}_j;\ \Lambda_j = \frac{1}{B_j} \begin{pmatrix} \omega & -A_{jy} \\ A_{jx} & -\omega \end{pmatrix}; \tag{C.3}$$

where $A_{jy} = 1 + k_j^2 + \frac{\chi k_y^2}{k_j^2}$; $A_{jx} = 1 + k_j^2 + \frac{\chi k_{jx}^2}{k_j^2}$ and $B_j = \frac{\chi k_{jx} k_y}{k_j^2}$. A new relation follows from the same differential equations for vectors $\mathbf{p}$ and $\mathbf{q}$:

$$\mathbf{q} = -\sigma_1 \mathbf{p} \tag{C.4}$$

Here $\sigma_1 = \begin{pmatrix} 0 & 1 \\ 1 & 0 \end{pmatrix}$ is the first Pauli matrix. Thus, only six amplitudes, namely components of 2-component vectors $\mathbf{a}_j$ $(j = 1, 2)$ and $\mathbf{p}$ are independent.

The 4 EBC equations are only slightly modified in comparison to the case of $\theta \neq \pi/2$:

$$\begin{cases} \sum_{j=1}^{2} k_{jx} \mathbf{a}_j \sin \frac{k_{jx} d}{2} - k_y \mathbf{p} \sinh \frac{k_y d}{2} = 0 \\ \sum_{j=1}^{2} k_{jx} \mathbf{b}_j \cos \frac{k_{jx} d}{2} + k_y \mathbf{q} \cosh \frac{k_y d}{2} = 0 \end{cases} \tag{C.5}$$

But the CE equation are different from those at $\theta \neq \pi/2$ in two respects. First, not only integral terms in the linearized LLE equations generate evanescent waves $\cosh k_y x$, $\sinh k_y x$, but they also enter in the solution (C.2). Second, the integral terms for these evanescent waves are singular. Indeed, the basic integrals that enter $\eta_{x,y}$ for such waves are:

$$\begin{aligned} &\int_{-\frac{d}{2}}^{\frac{d}{2}} \frac{e^{-|k_y(x-x')|} \cosh k_y x'}{2|k_y|} dx' \\ = \ & \frac{\cosh k_y x \left(1 - e^{-|k_y| d} + |k_y| \, d\right)}{4k_y^2} - \frac{x \sinh k_y x}{2k_y} \end{aligned} \tag{C.6}$$

$$\begin{aligned}
&\int_{-\frac{d}{2}}^{\frac{d}{2}} \frac{e^{-|k_y(x-x')|}\sinh k_y x'}{2|k_y|}dx' \\
&= \frac{\sinh k_y x\left(1+e^{-|k_y|d}+|k_y|\,d\right)}{4k_y^2} - \frac{x\cosh k_y x}{2k_y}
\end{aligned} \tag{C.7}$$

Singular terms $x\sinh k_y x$, $x\cosh k_y x$ in the magnetic potential $\phi = d_x\eta_x + k_y\eta_y$ vanish as a consequence of $\mathbf{q}-\mathbf{p}$ relation (C.4). The same relation implies that terms with components of $\mathbf{p}$ and $\mathbf{q}$ do not contribute to the volume magnetic charge $d_x m_x + k_y m_y$. However, magnetic field is created not only by volume charge, but also by surface charge equal to $\mp m_x\left(\pm\frac{d}{2}\right)$. The contribution of the same terms to the magnetic potential in some inner point reads (we omit its dependence on longitudinal coordinate and time $\cos\left(k_y y-\omega t\right)$):

$$\begin{aligned}
&\phi_{\mathbf{pq}}(x) \\
&= 4\pi G\left(x-\frac{d}{2}\right)\left(p_x\cosh\frac{k_y d}{2}+q_x\sinh\frac{k_y d}{2}\right) \\
&- 4\pi G\left(x+\frac{d}{2}\right)\left(p_x\cosh\frac{k_y d}{2}-q_x\sinh\frac{k_y d}{2}\right)
\end{aligned} \tag{C.8}$$

where $G(x)=\frac{\exp(-|k_y x|)}{2|k_y|}$ is the Green function of the Helmholtz equation. After some simplification the potential $\phi_{\mathbf{pq}}(x)$ takes a form:

$$\begin{aligned}
\phi_{\mathbf{pq}}(x) &= 4\pi\frac{e^{-\frac{|k_y|d}{2}}}{|k_y|}p_x\cosh\frac{k_y d}{2}\cosh k_y x \\
&+ 4\pi\frac{e^{-\frac{|k_y|d}{2}}}{|k_y|}q_x\sinh\frac{k_y d}{2}\sinh k_y x
\end{aligned} \tag{C.9}$$

Returning to the integral form of equations of motion (3.11), extracting from them terms propor-

tional to $\cosh k_y x$ and $\sinh k_y x$ and nullifying them, we arrive at two equations:

$$\begin{aligned} & \chi e^{-\frac{|k_y|d}{2}} \frac{k_y}{|k_y|} \left[q_x \sinh \frac{k_y d}{2} + k_y \sum_{j=1}^{2} \frac{1}{k_j^2} \left(a_{jy} f_{jc} + b_{jx} f_{js} \right) \right] \\ + \quad & \omega p_x - p_y = 0 \\ - \quad & \chi e^{-\frac{|k_y|d}{2}} \frac{k_y}{|k_y|} \left[p_x \cosh \frac{k_y d}{2} + k_y \sum_{j=1}^{2} \frac{1}{k_j^2} \left(a_{jx} f_{jc} + b_{jy} f_{js} \right) \right] \\ - \quad & p_x + \omega p_y = 0 \end{aligned} \tag{C.10}$$

4 equations of EBC and 2 CE form a system of 6 equations for 6 independent amplitudes. The determinant of this system must be zero for their solvability. This condition determines the quantization of wave vectors k_{1x} and frequency. Numerical calculation with this determinant can be performed in general case. The results are shown in several figures in the main text. In the case of thick film $d \gg 1$, $1/d \ll k_y \ll d$ and $n \ll d$, the calculation is simplified since $|\mathbf{a}_2|$ occurs much less than $|\mathbf{a}_1|$ and can be neglected in eqs. (C.10). Another two equations are obtained by elimination of $\mathbf{a}_2$ from 4 equations (C.5).